

Feedback between Shrub Encroachment and Microclimate
in the Southwestern United States

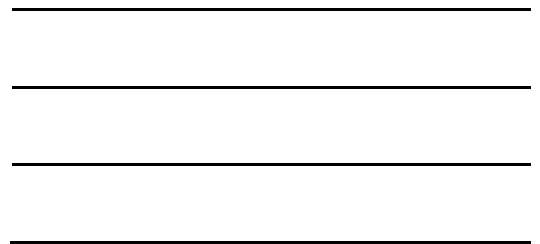
Yufei He
Sichuan, China

Bachelor of Science, Peking University, 2005
Master of Science, Peking University, 2008

A Dissertation presented to the Graduate Faculty
of the University of Virginia in Candidacy for the Degree of
Doctor of Philosophy

Department of Environmental Sciences

University of Virginia
May, 2014



ABSTRACT

Shrub encroachment is a world-wide ecological phenomenon which is associated with abrupt transition from grassland to shrubland. Such a change of vegetation cover has the potential of impacting the local and regional climate and may contribute to further shift in vegetation cover in many ecosystems. It has been recently proposed that such a vegetation-microclimate feedback may exist in the southwestern U.S. deserts, in which a cold sensitive shrub species, *Larrea tridentata*, could be favored by the feedback. This dissertation uses both observational and numerical modeling approaches to investigate the interaction between shrub encroachment and microclimate in the northern Chihuahuan desert, and to assess the role of the vegetation-microclimate feedback in favoring further shrub encroachment. In particular, field observations reveal that the shrubland has a significantly higher nighttime temperature (of about 2K on average) than the adjacent grassland, demonstrating the effect of different vegetation covers on local microclimate. Such a temperature difference only extends to a low height level (<20m above ground), which establishes itself shortly after sunset and then persists throughout the night. The observed warmer nocturnal condition over the shrubland is interpreted as the consequence of the increased bare soil fraction caused by shrub encroachment: the less insulated ground surface enhances the diurnal soil heating and the nocturnal release of longwave radiation, which results in a higher nighttime temperature. Such a shrub-induced warming is found to be overall important, because it is comparable to a regional climate warming over a timescale of one century. To better understand the underlying mechanisms, both an idealized single column configuration and an idealized two-dimensional configuration of the Weather Research and Forecast (WRF) model coupled

with the Noah land surface model are used to simulate the land-surface interactions which result in the observed temperature difference. It is found that the green vegetation fraction is the key parameter that drives the temperature difference, based on the sensitivity tests of various parameterizations. Then, with the knowledge learnt from the idealized simulations, three-dimensional realistic simulations using the WRF model with multiple grassland and/or shrubland vegetation cover scenarios are carried out to investigate the role of the vegetation-microclimate feedback in promoting the shrub encroachment. The simulation results show that the effect of feedback could result in a microclimate condition that is generally more favorable for the survival of juvenile shrubs. This can induce bi-stability to the shrubland-grassland system in extreme cold winters, and contribute to further the shrub encroachment.

ACKNOWLEDGEMENTS

First of all, I would like to express my sincere thanks to my co-advisors: Paolo D’Odorico and Stephan De Wekker. They provided me the extraordinary opportunity of working on such an interesting and interdisciplinary topic. I truly appreciate their guidance, inspiration, encouragement, support, and help during the six years of my Ph.D. life. It has been a great pleasure for me to work with them. I would also like to thank my other dissertation committee members, Howard Epstein and Zhi-Yun Li, for their helpful comments and counsel towards the dissertation and defense.

Thanks to the people who have contributed to this work. I want to thank the professors, Jose Fuentes from the Pennsylvania State University, Scott Collins and Marcy Litvak from the University of New Mexico, who participated the project and provided data and advice. I would also like to thank all the field assistants who helped me with the field work; special thanks go to Abi Bhattachan, Stephen Chan, Bin Chen, and Leo Stoscheck. I, too, would like to acknowledge the personnel at the Sevilleta Long-Term Ecological Research site who have provided supports for this project.

This work is mainly funded by the National Science Foundation DEB-0743678 and DEB-0620482 to the University of New Mexico for Long-Term Ecological Research. The Department of Environmental Sciences at the University of Virginia also supported me with graduate assistantships, fellowships and the Exploratory Research Award.

I am grateful for my fellow graduate students, especially those in the D’Odorico Group and the De Wekker Group, and the professors and staffs in the Department of Environmental Sciences, for their help throughout these years of study and work. I also

thank my friends in Charlottesville for the wonderful memories they have given me in this small town.

I would like to express my deepest gratitude to my family. I owe tremendous thanks to my beloved husband, Bin, who has always loved me, trusted me and encouraged me. Meeting and marrying him is the best thing happened to my life. Bin is the one who tells me “you can do it” every time when I feel frustrated or uncertain, and is also the one I can bother anytime to discuss issues on IDL programming, research ideas, and presentation of science results. I thank my daughter, Yulan, for the ultimate sunshine she has been bringing to my life and for the time we spent together at the wilderness of Sevilleta when I was expecting. I also thank my soon-to-be-born son, Yuhan, whose kicks have accompanied me during the whole process of dissertation writing and kept me awake into many late-nights. Lastly, I am deeply grateful for my parents for their always love and support throughout my whole life.

Table of Contents

| | |
|---|---------------|
| ABSTRACT | I |
| ACKNOWLEDGEMENTS | III |
| LIST OF FIGURES | VII |
| LIST OF TABLES | XIII |
| CHAPTER 1 INTRODUCTION | - 1 - |
| SHRUB ENCROACHMENT | - 1 - |
| INTERACTIONS BETWEEN VEGETATION COVER AND CLIMATE | - 4 - |
| POSITIVE FEEDBACK BETWEEN SHRUB ENCROACHMENT AND MICROCLIMATE IN SOUTHWESTERN U.S. | - 5 - |
| RESEARCH OBJECTIVES AND APPROACHES | - 7 - |
| STUDY SITE DESCRIPTION..... | - 8 - |
| CHAPTER 2 ON THE IMPACT OF SHRUB ENCROACHMENT ON MICROCLIMATE CONDITIONS IN THE NORTHERN CHIHUAHUAN DESERT | - 11 - |
| 2.1 INTRODUCTION | - 11 - |
| 2.2 METHODS..... | - 14 - |
| 2.2.1 <i>Study Site</i> | - 14 - |
| 2.2.2 <i>Surface aerodynamic characteristics</i> | - 16 - |
| 2.2.3 <i>Surface emissivity and albedo</i> | - 17 - |
| 2.2.4 <i>Atmospheric stability</i> | - 19 - |
| 2.3 RESULTS | - 19 - |
| 2.3.1 <i>Observations</i> | - 19 - |
| 2.3.2 <i>Energy budget model</i> | - 24 - |
| 2.4 DISCUSSION | - 28 - |
| ACKNOWLEDGEMENTS | - 33 - |
| CHAPTER 3 COUPLED LAND-ATMOSPHERE MODELING OF THE EFFECTS OF SHRUB ENCROACHMENT ON NIGHTTIME TEMPERATURES | - 34 - |
| 3.1 INTRODUCTION | - 34 - |
| 3.2 METHOD | - 36 - |
| 3.2.1 <i>Numerical Model Description</i> | - 36 - |
| 3.2.2 <i>Model setup</i> | - 37 - |
| 3.3 RESULTS AND DISCUSSION..... | - 40 - |
| 3.3.1 <i>Baseline simulation</i> | - 40 - |
| 3.3.2 <i>Sensitivity to vegetation parameters</i> | - 44 - |
| 3.3.3 <i>Sensitivity to initialization profiles</i> | - 50 - |
| 3.3.4 <i>Sensitivity to the daytime warming period</i> | - 51 - |
| 3.4 SUMMARY | - 53 - |
| ACKNOWLEDGEMENTS | - 55 - |
| CHAPTER 4 CONTRASTING NOCTURNAL TEMPERATURE PROFILES IN ADJACENT SHRUBLAND AND GRASSLAND | - 56 - |

| | |
|--|----------------|
| 4.1 INTRODUCTION | - 56 - |
| 4.2 METHODS..... | - 58 - |
| 4.2.1 <i>Study Site and Tethered Sounding Measurements</i> | - 58 - |
| 4.2.2 <i>Model setup</i> | - 59 - |
| 4.2.3 <i>Cumulative temperature difference</i> | - 61 - |
| 4.3 RESULTS AND DISCUSSION..... | - 62 - |
| 4.3.1 <i>Observed nocturnal boundary layer profiles</i> | - 62 - |
| 4.3.2 <i>Simulated nocturnal boundary layer profiles</i> | - 68 - |
| 4.3 SUMMARY AND CONCLUSION..... | - 74 - |
| CHAPTER 5 THE RELATIVE IMPORTANCE OF CLIMATE CHANGE AND SHRUB ENCROACHMENT ON NOCTURNAL WARMING IN THE SOUTHWESTERN U.S. | - 77 - |
| 5.1 INTRODUCTION | - 77 - |
| 5.2 METHODS..... | - 79 - |
| 5.3 RESULTS | - 82 - |
| 5.3.1 <i>Winter minimum temperature change caused by shrub encroachment</i> | - 82 - |
| 5.3.2 <i>Historical minimum winter temperature change</i> | - 83 - |
| 5.3.3 <i>Future minimum winter temperature change from regional climate simulations</i> | - 86 - |
| 5.4 DISCUSSION | - 86 - |
| ACKNOWLEDGEMENTS | - 90 - |
| CHAPTER 6 THE ROLE OF VEGETATION-MICROCLIMATE FEEDBACK IN PROMOTING SHRUB ENCROACHMENT IN THE NORTHERN CHIHUAHUAN DESERT..... | - 92 - |
| 6.1 INTRODUCTION | - 92 - |
| 6.2 METHODS..... | - 95 - |
| 6.2.1 <i>Numerical model setup</i> | - 95 - |
| 6.2.2 <i>Experiment design: Vegetation distribution scenarios</i> | - 99 - |
| 6.2.3 <i>Model validation data</i> | - 100 - |
| 6.2.4 <i>Mortality probability of creosotebush juveniles and cold stress indices</i> ... | - 101 - |
| 6.3 RESULTS AND DISCUSSION | - 103 - |
| 6.3.1 <i>Minimum temperatures with single vegetation cover</i> | - 103 - |
| 6.3.2 <i>Cold mortality to juvenile shrub with single vegetation cover</i> | - 106 - |
| 6.3.3 <i>Cold stress to juvenile shrub with combination of shrubland and grassland covers</i> | - 111 - |
| 6.4 SUMMARY | - 115 - |
| CHAPTER 7 SUMMARY AND CONCLUSION | - 117 - |
| REFERENCES..... | - 123 - |

LIST OF FIGURES

Figure 1.1 Positive feedbacks contributing to shrub encroachment at different scales.
This dissertation focuses on the feedback loop between shrub encroachment and microclimate (brown circle). Adopted from (D’Odorico et al., 2010). - 6 -

Figure 1.2 Locations of the SNWR and the Rio Grande in New Mexico (upper left panel), observational sites in the SNWR that are used in this study (bottom left panel) and the view of the grassland, ecotone and shrubland (right panel). Dot, plus, and cross symbols mark the three flux towers, the two long-term meteorological towers, and the two sounding locations, respectively. - 9 -

Figure 2.1 Night time temperature comparison between shrubland and grassland, for the whole year and (inset) in the winter months only. Analysis based on Jul 2007 to Jun 2008 half hourly points (Nov 2007 to Feb 2008 data in the inset). The nighttime air temperature in the shrubland is significantly higher than in the grassland ($p < 0.0001$ both for the t-test of the whole year and of the winter months). For 72% of the time (or 79% of the time if only winter months are considered) the shrubland has warmer near-surface conditions than the grassland. - 20 -

Figure 2.2 Monthly mean and standard deviation of temperature differences between the two vegetation covers in the winter months (Nov 2007 to Feb 2008). - 21 -

Figure 2.3 Monthly mean and standard deviation of maximum daily nighttime temperature differences between the two vegetation covers. - 22 -

Figure 2.4 (a) Relationship between nighttime temperature differences and Richardson number under stable conditions, and (b) relationship between night time temperature differences and wind speed for the whole year (Jul 2007 to Jun 2008) and winter months (Nov 2007 to Feb 2008). - 22 -

Figure 2.5 Schematic representation of the one-dimensional energy budget model. The parameters are explained in text. - 25 -

Figure 2.6 Comparison of the observed temperature differences between shrubland and grassland (solid line connecting solid circles) with the results of a one-dimensional energy budget model (solid line) in a selected sample case (the clear-sky calm winter night between 16 and 17 Dec 2007). Sensitivity test with respect to longwave radiation emitted by the ground surface is shown with dashed line (i.e., the same ground longwave radiation is used for the two vegetation covers. See text). Each dotted line shows the result of a sensitivity test with respect to the other components of the energy balance, including (1) sensible heat fluxes, (2) ground heat fluxes, (3) measured upwelling and (4) downwelling longwave radiation. - 27 -

Figure 2.7 Comparison between cumulated ground heat fluxes measured between 1 Nov and 31 Dec, 2007 at the shrubland and grassland sites. Inset: Mean and standard deviation of ground heat fluxes over shrubland and grassland in clear days in the same period. At each site, ground heat flux values were calculated as weighted averages of the values measured at vegetated and unvegetated micro-sites using the fractional land cover reported for each site. - 29 -

Figure 2.8 Mean and standard deviation of ground heat fluxes under bare soil and vegetation cover, in the shrubland (a) and the grassland (b) in clear winter days (Nov 2007 to Feb 2008). - 31 -

Figure 3.1: Mean and standard deviation of temperature differences between shrubland and grassland of Seville National Wildlife Refuge in December 2007 to February 2008. - 35 -

Figure 3.2 Simulated time series of (a) air temperature at 2m height, skin temperature, soil temperature of the 10cm depth layer below ground in the adjacent shrubland ('s') and grassland ('g'); (b) air temperature differences at 2m height between the shrubland and grassland; and (c) the net radiation (Rnet), sensible heat (H) and ground heat fluxes (G) of both land covers. - 41 -

Figure 3.3 Observed time series of net radiation (Rnet), sensible heat (H) and ground heat fluxes (G) over shrubland ('s') and grassland ('g'). Fluxes are the average of 16 selected clear days with small wind speed in the time period from November 2007 to January 2008. - 41 -

Figure 3.4 (a) Simulated mean residual wind speed in the lowest 50 m and averaged over 11 grid points across the shrubland-grassland boundary. Residual wind speed is defined here as the difference between the simulated wind speed and the ambient geostrophic wind (1m/s, the initial wind speed). Positive values indicate a residual wind component blowing from shrubland to grassland (shrub breeze), while negative values indicate a grass breeze. (b) Simulated mean temperature difference between shrubland and grassland in the lowest 50m. - 42 -

Figure 3.5 Sensitivity of the air temperature differences, averaged from 0000 to 0600 LT, between the shrubland and the grassland to (a) green vegetation fraction, (b) albedo, (c) emissivity and (d) roughness length. Positive values indicate higher air temperatures at 2m above ground in shrubland than in grassland. Zero difference is indicated by the black dashed line. The black triangle corresponds to the default values of the vegetation parameters for December in Noah LSM, and the black dot corresponds to the values of the vegetation parameters used in this study. - 46 -

Figure 3.6 Air temperature differences, averaged from 0000 to 0600 LT, between shrubland and grassland for different combinations of changes in vegetation parameters from those used in the baseline simulation (see also black dots in Figure 3.5 and Table 3.1) to those used in default setup of Noah LSM for December (see also triangle markers in Figure 3.5 and Table 3.1). The black dot indicates the temperature difference in the baseline simulation. The changed vegetation parameters are labeled as A for albedo, E for emissivity, R for roughness length, and G for green vegetation fraction. For example, GA indicates the temperature difference between shrubland and grassland in a simulation where the green vegetation factor and albedo are changed from values in the baseline simulation to the default values in Noah LSM. - 47 -

Figure 3.7 (a) Differences in air temperature between shrubland and grassland and (b) the simulated air temperature in grassland for five simulations with different initialization times. The black dots in (a) correspond to mean temperature differences over 12 hours starting from the establishment of higher temperatures in the shrubland than in grassland. - 50 -

Figure 4.1 Profiles of temperature differences between shrubland and grassland (thin dash-dot lines) observed in 2008 (left) and 2011 (right). Filled circles and error bars show mean and standard deviation of temperatures in 5-m height bins..... - 63 -

Figure 4.2 Temporal evolution of temperature profiles in adjacent shrubland (“s”) and grassland (“g”) measured in the night of 16 November 2011..... - 64 -

Figure 4.3 Observed cumulative temperature differences (CTD) from surface to 60m in adjacent shrubland (“s”) and grassland (“g”). CTD is calculated relative to the sounding in shrubland at the beginning of each nighttime period (see text). - 66 -

Figure 4.4 The initialization (1700 LT) and simulated temperature profiles over shrubland (“s”) and grassland (“g”) at the different times during the night of 16 November 2011 using the QNSE PBL scheme. - 68 -

Figure 4.5 Simulated cumulative temperature differences (CTD) from surface to 60m in shrubland (“s”) and grassland (“g”) using three PBL schemes (YSU, QNSE, and UW). CTD is calculated relative to the initial profile at 1700 LT. - 70 -

Figure 4.6 Schematic nighttime temperature profiles (upper figure) in shrubland (black line) and grassland (grey line), and near-surface air temperature differences between shrubland and grassland (bottom figure) in clear and calm wind conditions. A is around sunset, B is right after the establishment of the air temperature difference between shrubland and grassland, and C is some time later during the night. - 75 -

Figure 5.1 Locations of the SNWR (light grey shaded area) in New Mexico, the shrubland (white x symbol) and grassland (white cross symbol) sites at SNWR, and Los Lunas

(black square symbol) and Socorro (black circle symbol) USHCN stations located along the Rio Grande (grey line) valley. Also shown are the areas of PRISM grid cells encompassing the McKenzie Flats (dark grey shaded area) and the SNWR (area indicated by the dashed line)..... - 79 -

Figure 5.2 box and whisker plot for differences of minimum temperatures between shrubland and grassland for 2007 to 2010. - 84 -

Figure 5.3 Historical minimum winter temperature for the grassland site and McKenzie Flats area at SNWR and at two UHSCN stations in central New Mexico. Shown are the observations from Sevilleta LTER at the deep well station (closed circles and corresponding solid grey trend line, data from 1990 to 2012), PRISM data for McKenzie Flats (open circles and corresponding solid black trend line, data from 1896 to 2012). Data from the two USHCN stations are shown as trend lines for Los Lunas (dash-dot line) and for Socorro (dashed line, data from 1894-2013). - 84 -

Figure 6.1 Domain setting (A), and vegetation distribution and isoheights within the 3rd (innermost) domain (B). The three domains (black solid thick lines) are centered on the McKenzie flat area within the SNWR (light grey area). The Rio Grande in NM (dashed line) and the location of the Deep Well station in the grassland (black dot) are also shown. NM and the neighboring states are labeled and state boundaries are shown in light grey lines. In the zoomed-in figure (B), the white polygon is the target area used to investigate different vegetation distributions. The vegetation cover in the rest of the domain is from default settings based on USGS maps. The isoheights are shown with 100m interval, ranging from 1300m to 3100m. - 96 -

Figure 6.2 Mean daily minimum temperature in winter 2010-2011 (A, B and C) and winter 2011-2012 (D, E and F) obtained from simulations with the target area (enclosed by the black solid line) covered by grassland SV_G (A and D), shrubland SV_S (B and E) vegetation, and the difference between grassland and shrubland vegetation setting SV_G-SV_S (C and F). - 104 -

Figure 6.3 The simulated peak mortality probability (PMP, first row, A, B, C and D), cumulative mortality probability (CMP, second row, E, F, G and H), and total stress index (TSI, third row, I, J, K, L) calculated for winter 2010-2011 (first and second column, A, B, E, F, I and J) and winter 2011-2012 (third and fourth column, C, D, G, H, K and L) with grassland cover SV_G (first and third column, A, C, E, G, I and K) and shrubland cover SV_S (second and fourth column, B, D, F, H, J, and L) in the target area that enclosed by the think solid line. - 107 -

Figure 6.4 The simulated cumulative mortality probability (CMP) of winter 2010-2011 without the three extreme cold days (and nights) calculated with grassland cover SV_G (A) and shrubland cover SV_S (B) in the target area that enclosed by the think solid line. - 110 -

Figure 6.5 The simulated peak mortality probability (PMP, first row, A, B, C, D, E and F), cumulative mortality probability (CMP, second row, G, H, I, J, K and L), and total stress index (TSI, third row, M, N, O, P, Q and R) for winter 2010-2011 using different vegetation distributions with grassland in the north and shrubland in the southern in the target area (enclosed by the black solid line). The west to east straight black solid line within the target indicates the shrubland-grassland boundary. The following positions of this boundary are considered: GS_S10 (first column, A, G and M); GS_CURR (first column, B, H and N); GS_N5 (first column, C, I and O); GS_N10 (first column, D, J and P); GS_N20 (first column, E, K and Q); GS_N25 (first column, F, L and R). - 112 -

LIST OF TABLES

Table 2.1 Information on vegetation cover, aerodynamic parameters, albedo and emissivity for the shrubland and grassland sites..... - 16 -

Table 2.2 The nighttime energy components for shrubland, grassland, and the difference between shrubland and grassland, reported as the average over winter months (Nov 2007 to Feb 2008). Constraint 1 conditions are defined as when temperature differences over the two land covers are equal to or larger than 2 oC. Constraint 2 only concerns the measurements from sunset to 2000 LST. - 23 -

Table 3.1 Noah LSM default vegetation parameter settings, observations from Sevilleta National Wildlife Refuge in northern Chihuahuan desert, and the vegetation parameters used in this study. - 39 -

Table 3.2 Comparison of the observed and simulated energy components in shrubland and grassland during clear winter conditions. “s” indicates that the energy component in absolute value is larger in shrubland than in grassland, while “g” indicates the opposite. - 42 -

Table 4.1 The mean and maximum absolute differences in temperature ($|\Delta T|$) of the lowest 10 levels (about 100m) from 1800 to 0600 LT, the difference in 2m temperature (ΔT_2) and CTD (ΔCTD) at 0000 LT between a simulation with a particular vegetation setting (S, or I1, or I2) and a simulation with grassland (G). For vegetation parameters, gvff is green vegetation fraction; z0 is roughness length; “other” stands for all parameters other than green vegetation fraction, roughness length, albedo and emissivity. A check mark (“✓”) in the “parameter” boxes indicates that a vegetation parameter was changed relative to the vegetation setting for grassland. - 73 -

Table 5.1 The average increase in the minimum winter temperature over a 70-year period from current (1969-1999 or 1969-2000, depending on the model combinations) to future (2039-2069 or 2039-2070) using the output of 11 AOGCM

and RCM combinations from NARCCAP. These temperature changes are calculated using temperature values obtained as means of the 4 grid points closest to the encroaching front at SNWR. - 85 -

Table 5.2 Comparison between the increase in minimum winter temperature due to shrub encroachment and the estimated historical and future regional warming trend at the SNWR. The corresponding years indicate the number of years for climate change to cause a warming effect of the same magnitude as the increase in temperature induced by shrub encroachment. - 87 -

Table 6.1 The vegetation distribution scenarios used in this study. - 99 -

Table 6.2 Comparison between simulated mean winter daily minimum temperature in the grid points corresponding to the location of the Deep Well and the Five Points stations, and the observed mean daily minimum temperature in these two stations. - 103 -

CHAPTER 1

INTRODUCTION

Shrub encroachment

Shrub encroachment is an ecological phenomenon associated with the increase in density, cover and biomass of woody shrub species at the expense of former grasslands. Shrub encroachment has been occurring in all continents except Antarctica (Ravi et al., 2009). In the case of the Southwestern U.S. deserts, the dramatic transition from perennial grassland to mesquite (*Prosopis glandulosa*) or creosotebush (*Larrea tridentata*) dominated shrubland has been documented since the mid 19th century (Buffington and Herbel, 1965; Gibbens et al., 2005). It has been argued the introduction of cattle and the associated overgrazing of arid and semiarid rangelands likely caused the early stages of this vegetation cover transition (Grover and Musick, 1990; Archer et al., 1995a; Van Auken, 2009). The subsequent encroachment of shrubs into the grassland has been explained as the result of interactions between biotic and abiotic processes (Archer, 1990), which are associated with drivers such as increased atmospheric carbon dioxide concentration (Polley et al., 1992; Polley, 1997), climate warming (Pockman and Sperry, 1997), shift in precipitation regime (Brown et al., 1997), overgrazing, and fire management (Archer et al., 1995a). However, no single factor has conclusively been proved to be the only driver either regionally or globally. Multiple processes seem to interact and promote this change in vegetation composition (ALAN K Knapp et al., 2008; Van Auken, 2000).

Although the impacts of shrub encroachment may differ from region to region (Eldridge et al., 2011), in the southwestern U.S. (and many other regions), the

encroachment of creosotebush results in the modification of land surface properties, in particular, in an increase in the bare soil fraction. Once the shrub successfully establishes, its spatial distribution tends to be patched because overlap of the neighboring root systems is not favored (Brisson and Reynolds, 1994). With deep root systems which can have the access to ground water (Gibbens and Lenz, 2001) and low soil nitrogen requirements (Van Auken, 2000), creosotebush may take advantage over grass species in areas with limited resource availability. As a result, a spatial heterogeneity of biomass and an overall increase in bare soil fraction have often been observed associated with shrub encroachment (Gillette and Pitchford, 2004; Huenneke et al., 2002). By virtue of its capability to cause land degradation and loss of ecosystem services, shrub encroachment has both ecological and economic relevance if we consider its impact on biogeochemical cycles (Hibbard et al., 2001), hydrological processes (Huxman et al., 2005), soil nutrient loss (Schlesinger et al., 1990), and decreasing rangeland productivity (Geist and Lambin, 2004).

North America has a long history of widespread shrub encroachment. In 2001 it was estimated that in the U.S. about 335 million hectares of non-forest land had been affected by shrub encroachment, mostly in the arid and semi-arid western states (Pacala et al., 2001). The rate of shrub encroachment varies from site to site (Gibbens et al., 2005) and from time to time (Goslee et al., 2003). However, an assessment of the transition rate from grassland to shrubland is often rare and poorly documented. A unique example is the Jornada Basin in the Chihuahuan desert, where the change in vegetation over a long period of time has been studied using historical survey data, aerial photography and high-resolution imagery. (Goslee et al., 2003) showed that the shrub

cover and patch density increased from the 1930s to the 1970s and then stabilized thereafter, and the shrub patches were extremely persistent over time. (Laliberte et al., 2004) found that shrub cover increased by one order of magnitude and the grass cover decreased by one order of magnitude from 1937 to 2003. (Gibbens et al., 2005) carried out a study of the vegetation change over this region, which covered the largest area and the longest time period to date. It showed that the region changed from mostly fair or good grass cover with large shrub-free areas in the mid 1800s to a shrub-dominated cover by the end of 20th century: more than three quarters of the area is dominated by shrub species.

The abrupt character of the grassland to shrubland transition observed in many regions around the world (Anderies et al., 2002; Okin et al., 2009; Van Langevelde et al., 2003) suggests that the ecosystem in the transition zone may exhibit bi-stable dynamics (Noy-Meir, 1975; Walker et al., 1981; Westoby et al., 1989) with two alternative states (i.e., grass-dominated or shrub-dominated landscape). External environmental drivers can often interact with positive feedbacks and induce the shift between these two stable states (Wilson and Agnew, 1992). Some examples include the feedback between vegetation and fire (Anderies et al., 2002; Ravi et al., 2009) as well as the feedbacks between vegetation and soil erosion (Schlesinger et al., 1990; Okin et al., 2009), which were proposed to positively contribute to the abrupt transition from grassland to shrubland. However, whether and how shrub encroachment in drylands interacts with the local climate has often been overlooked.

Is shrub encroachment solely a result of climate warming or also a contributor to changes in microclimate conditions? My dissertation will address this question by

studying the impacts of shrub encroachment on microclimate and assessing its role in vegetation change in southwestern U.S. desert grasslands. In the following sections I will firstly give a brief introduction to the vegetation climate interactions, and then I will outline my research objectives and the approaches used to address them.

Interactions between vegetation cover and climate

Interactions between vegetation cover and climate have been well studied for a number of ecosystems (Bonan, 2002). Vegetation cover affects the exchange of mass and energy between the land surface and the atmosphere and therefore modifies the near surface microclimate conditions (Bonan, 1997; Pielke et al., 1998; Foley et al., 2003). On the other hand, the distribution of vegetation at global and regional scales can also be controlled by climate related factors, including temperature and water (Stephenson, 1990; Bachelet et al., 2001; Dullinger et al., 2004). For example, nighttime warming is found to be correlated with the decrease in dominant herbaceous species and increase in forbs in semi-arid shortgrass prairie (Alward et al., 1999). In the case of the southwestern U.S. deserts, some studies have shown how differences in vegetation cover, i.e., between shrub-dominated and grass-dominated areas, may cause local-scale differences in soil moisture, evapotranspiration, sensible heat fluxes and other energy fluxes (Dugas et al., 1996; Bhark and Small, 2003; Kurc and Small, 2004, 2007). Numerical model simulations suggested that vegetation change due to shrub encroachment could modify the land surface properties, alter the distribution of sensible and latent heat, and affect the near-surface temperature (Beltrán-Przekurat et al., 2008). In addition, some observations found that creosotebush-dominated shrubland has a higher nighttime minimum temperature than adjacent grassland (Hayden, 1998; Carre, 2005).

Although drought was found to cause regional mortality of woody plants in the southwestern U.S. (Breshears et al., 2005), in this region the two dominant shrub species, mesquite and creosotebush, are well adapted to seasonal droughts (Reynolds et al., 1999). Conversely, the freezing temperature is a limiting factor that affects the northern distribution of creosotebush while drought can increase its cold tolerance (Pockman and Sperry, 1997; Martínez-Vilalta and Pockman, 2002; Medeiros and Pockman, 2011). Therefore, further shrub encroachment could be favored by the predicted warmer and drier climate in the southwestern U.S. (Seager et al., 2007; Solomon et al., 2009).

Positive feedback between shrub encroachment and microclimate in Southwestern U.S.

As noted above, the two-way interactions between creosotebush and climate parameters, especially the surface temperature in the southwestern deserts of the U.S., suggest that a vegetation-microclimate feedback may sustain the shift from grassland to shrubland. Similar feedback mechanisms have been found to be effective in several other ecosystems, such as the boreal woodyland-tundra (Epstein et al., 2004) and the alpine forest-meadow (Körner, 1998) transitions. These feedbacks may promote further grassland-to-woodland transitions. Here I demonstrate how shrub encroachment is able to induce a warmer nocturnal microclimate ((He et al., 2010); therefore, I propose that a positive feedback between creosotebush and nighttime temperatures facilitates further shrub encroachment in the southwestern U.S. desert (D'Odorico et al., 2010; see also Figure 1.1).

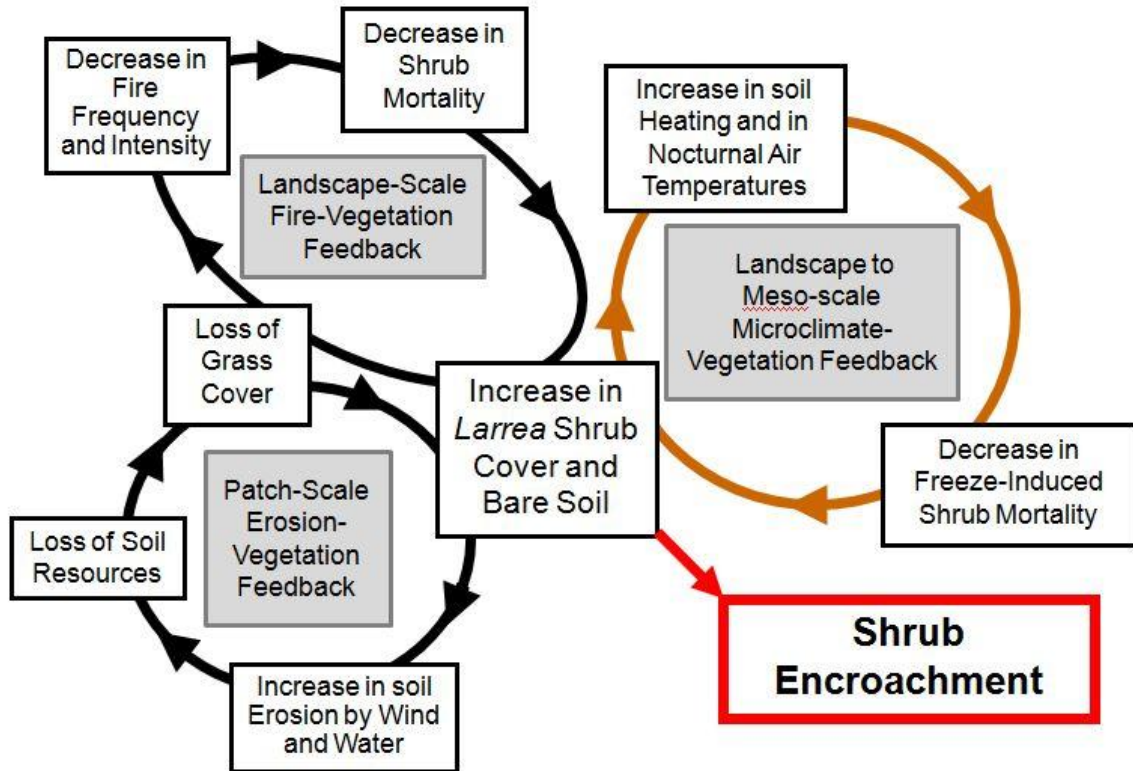


Figure 1.1 Positive feedbacks contributing to shrub encroachment at different scales. This dissertation focuses on the feedback loop between shrub encroachment and microclimate (brown circle). Adopted from (D’Odorico et al., 2010).

Figure 1.1 illustrates such a feedback loop with the essential participating elements. First, shrub encroachment increases the bare soil fraction (Huenneke et al., 2002), which affects land-atmosphere interaction by enhancing soil heating and increasing the nighttime air temperature (He et al., 2010), see also Chapter 2). Consequently, the freeze-induced mortality decreases (Medeiros and Pockman, 2011), which may favor the continuing growth and survival of the shrubs, thereby further sustaining its establishment and northward expansion. As a result, this vegetation-microclimate feedback may induce bi-stability to the system and lead to abrupt vegetation transition in dryland ecosystems (D’Odorico et al., 2013), such as other feedbacks (e.g., (Schlesinger et al., 1990; Ravi et al., 2009)) reported in the region (Figure 1.1).

Research objectives and approaches

My dissertation aims to study the impacts of shrub encroachment on microclimate conditions. In particular, it tests the hypothesis that in the northern Chihuahuan desert creosote shrubs modify their microclimate to their own advantage by inducing a nocturnal warming effect that contributes to further shrub encroachment. To investigate the drivers and the effects of such a feedback, the following research activities are developed:

1. Analysis of observational data to study the surface temperature difference between shrubland and grassland, as well as differences in land surface properties and energy fluxes that cause the temperature difference (Chapter 2).
2. Use of a two-dimensional idealized grassland-shrubland configuration in an atmospheric mesoscale model to simulate the observed temperature difference; estimation of important vegetation parameters through sensitivity tests (Chapter 3).
3. Development of a tethered sounding experiment to investigate differences in the temperature profiles in the near-surface atmosphere; using a single column configuration of the atmospheric mesoscale model the evolution of the vertical temperature difference between shrubland and grassland throughout the night were better understood (Chapter 4).
4. Evaluating the relative importance of shrub-induced warming and the temperature increase associated with regional climate trends (Chapter 5).
5. Investigating the role of vegetation-microclimate feedback in promoting further shrub encroachment. A three-dimensional configuration of the atmospheric

mesoscale model is used with different vegetation distribution scenarios to assess the impact of vegetation cover on the winter minimum temperature in a region affected by shrub encroachment. (Chapter 6).

Study site description

This dissertation focuses on the encroachment front of creosotebush (*Larrea tridentata*) in the northern Chihuahuan desert. I use data from field sites located on the McKenzie Flats (34.34° N, 106.7° W, at about 1600m above mean sea level), to the east of the Rio Grande. The encroachment front and the field sites investigated in this dissertation are located within the Sevilleta national Wildlife Refuge (SNWR). Over the past century, the McKenzie Flats have undergone dramatic encroachment of creosotebush into desert grassland (Bhark and Small, 2003). The encroachment front in the SNWR is an ideal location to study differences in microclimate because in this zone both woody and herbaceous species exist in close distance, with little change in elevation and under the same regional climate conditions. In addition, the SNWR is at the northern limit of the creosotebush distribution (Pockman and Sperry, 1997). The mean annual temperature in the SNWR is 13.4°C. Most precipitation occurs from June to September (50%-70%) with a mean annual precipitation of 224 mm (Gosz et al., 1995). In January, the mean daily average/minimum temperature is 2.7/-4.9°C and the mean monthly precipitation is 8.0 mm (1989-2011).

Field measurements are taken in three different types of vegetation covers: shrubland, grassland, and shrubland-grassland transition zone (i.e., shrub encroachment front, or "ecotone"), respectively (Figure 1.2). The three sites are all on a flat terrain (elevation difference ~10m), located within about 4 km from the shrub encroachment

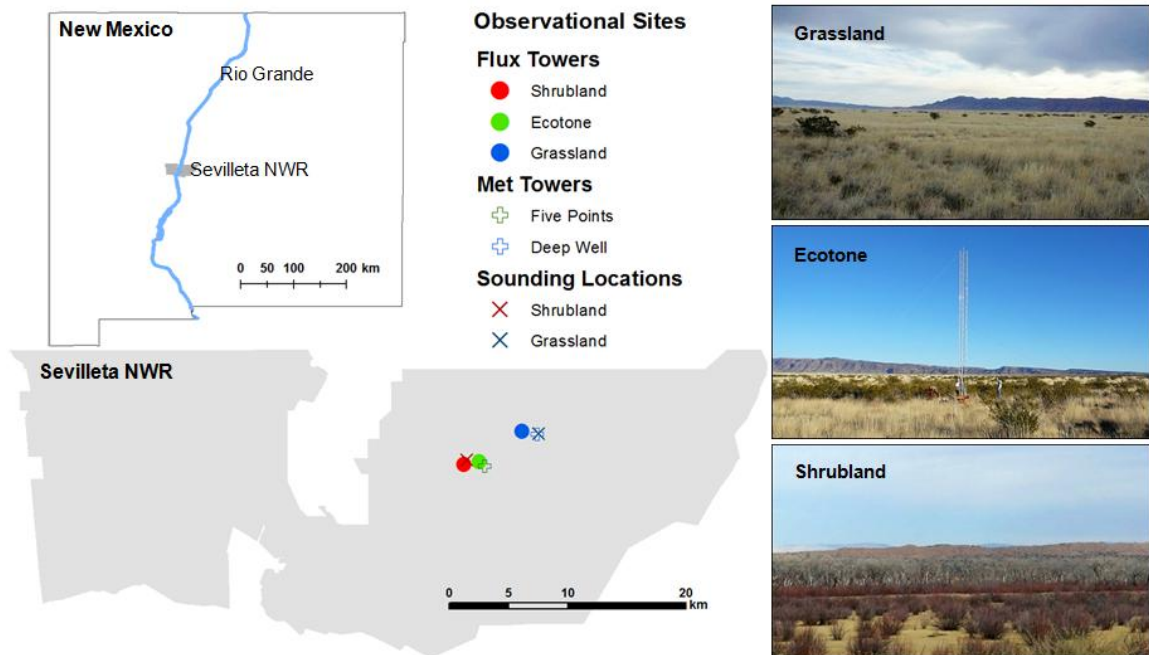


Figure 1.2 Locations of the SNWR and the Rio Grande in New Mexico (upper left panel), observational sites in the SNWR that are used in this study (bottom left panel) and the view of the grassland, ecotone and shrubland (right panel). Dot, plus, and cross symbols mark the three flux towers, the two long-term meteorological towers, and the two sounding locations, respectively.

front. The grassland site is dominated by relatively uniformly distributed C4 perennial grasses with about 60% vegetation cover and 40% bare soil, while in the shrubland larger portions of bare soil (70%) exist with a 30% shrub cover (Kurc and Small, 2004). A mixture of grass and shrub vegetation covers about 50% of the total area at the ecotone site, while the other half of the land surface is bare soil (D’Odorico et al., 2010).

Field measurements used in this study include observations at two identical flux towers located in the shrubland and the grassland (1999-present). Another flux tower was set up in the ecotone site in November 2008. Basic meteorological variables and energy fluxes are measured at all three fluxes towers. A network of temperature sensors that take near-ground temperature measurements over different vegetation/bare-soil

patches was deployed in November 2008 close to the three flux towers. In addition, two long-term meteorological towers maintained by the Sevilleta Long Term Ecological Research are present in the area (Figure 1.2).

CHAPTER 2

ON THE IMPACT OF SHRUB ENCROACHMENT ON MICROCLIMATE CONDITIONS IN THE NORTHERN CHIHUAHUAN DESERT¹

2.1 Introduction

Vegetation cover is known for its ability to influence the exchange of energy and water vapor between the land surface and the atmosphere (Bonan, 2002; Fraedrich et al., 1999). Vegetation affects the amount of solar irradiance that is reflected by the earth surface, the partitioning of net radiation into sensible and latent heat fluxes, the rate of precipitation recycling, the entrainment of dust and other aerosols into the atmosphere, and the partitioning of precipitation into soil moisture, evapotranspiration, and runoff (Charney, 1975; Eltahir and Bras, 1996; Foley et al., 2005; Rosenfeld et al., 2001; Villegas et al., 2010). Many studies have investigated and quantified the effects of land cover change on climate. Charney (1975) and (Charney et al., 1977) first discovered the link between changes in albedo and aridification in West Africa. Replacement of seasonal forests and grasslands with desert conditions has been associated with the reduction of evapotranspiration and precipitation in the Sahel region of Africa (Xue and Shukla, 1993) and in Mongolia (Xue, 1996). Other major land cover changes have been investigated for their potential impact on the regional climate (Bonan, 2002; Rotenberg and Yakir, 2010). For example, in the United States the replacement of temperate forests with croplands has been shown to modify climatic conditions through its impact on albedo, stomatal

¹ Published in Journal of Geophysical Research: **He, Y.**, D'Odorico P., De Wekker S. F. J., Fuentes J. D., Litvak M., 2010. On the impact of shrub encroachment on microclimate conditions in the northern Chihuahuan desert. Journal of Geophysical Research, 115, D21120, doi:10.1029/2009JD013529.

conductance, surface roughness, and root depth (Bonan, 1999, 1997). Similarly, tropical deforestation has been associated with major changes in regional temperature and rainfall regimes (Shukla et al., 1990), while the encroachment of boreal forest into regions historically dominated by tundra vegetation has been shown to lead to warming through important vegetation-albedo feedbacks (Foley et al., 1994).

Woody plant encroachment into grassland ecosystems has been happening in many regions around the world over the past several decades (Alan K. Knapp et al., 2008; Van Auken, 2000). Within the southwestern United States, this dramatic shift in plant community composition has been particularly well documented for the Sonoran and Chihuahuan deserts (Archer, 1989; Archer et al., 1988; Buffington and Herbel, 1965; Van Auken, 2009, 2000). Despite its global significance and its recognized impact on ecosystem function and services, this change in plant community composition has seldom been investigated with respect to its effect on near surface temperature. (Bhark and Small, 2003) investigated the effect of vegetation and shrub cover on soil moisture conditions; (Kurc and Small, 2007, 2004) studied soil moisture and evapotranspiration in adjacent grassland and shrubland, while (Dugas et al., 1996) examined the energy balance components over different grass and shrub species in the Chihuahuan desert. (Scott et al., 2006) investigated the impact of woody plant encroachment on energy, carbon and water vapor fluxes and found that, while woody plants can take up more carbon during the dry season because of the better use of groundwater, this effect may be offset by a larger soil respiration rate during the wet season. (Beltrán-Przekurat et al., 2008) used numerical simulations to show that changes in land cover from grass-dominated to shrub-dominated arid landscapes in the Chihuahuan desert cause an overall

decrease in sensible heat fluxes and a substantial increase in latent heat fluxes, thereby leading to a cooler and moister near-surface atmosphere during daytime. However, it is still unclear whether shrub encroachment has any impacts on nocturnal climatic conditions, and whether these effects have a feedback on vegetation dynamics. The two major shrub species in the Chihuahuan desert (i.e., *Larrea tridentata* and *Prosopis glandulosa*) are known for being sensitive to low nocturnal temperatures (Felker et al., 1982; Pockman and Sperry, 1997). Therefore, by changing the nocturnal temperature conditions, these shrub species may affect their own survival in this area.

The encroachment of mesquite (*Prosopis glandulosa*) and creosotebush (*Larrea tridentata*) in North-American deserts, has been explained as an effect of large scale drivers such as “climate warming” (Pockman and Sperry, 1997) or increased atmospheric carbon dioxide (CO₂) concentrations (Polley et al., 1992), and of local controls (e.g., grazing and fire management, (Archer et al., 1995b), which operate through important feedbacks between biotic and abiotic processes (Archer, 1994, 1990; Buffington and Herbel, 1965). We argue that in the case of *Larrea tridentata* one of the factors contributing to this shift in vegetation composition is the change in near surface microclimate conditions caused by the replacement of grass cover with woody vegetation. This dependence on microclimate conditions would be consistent with the observation that *Larrea* encroachment is sensitive to extreme negative temperatures (Pockman and Sperry, 1997). Thus, shrub establishment in relatively warm years could modify the surface energy balance and provide warmer nocturnal microclimate conditions thereby favoring the survival of *Larrea* during cold winters.

(Hayden, 1998) and (Carre, 2005) compared temperature measurements taken on two land covers in the northern Chihuahuan desert. They found that in the shrubland, the nighttime minimum temperatures were higher (by 4-6 °C) than in the adjacent grasslands. This warming effect is likely to enhance the chances of establishment and survival of these cold-sensitive shrub species. These results, which are in agreement with long-term temperature records from nearby areas in the Southwestern United States (Balling, 1988; Balling et al., 1998; Bryant et al., 1990; Small and Kurc, 2003), need to be validated by field observations capable of explaining the underlying processes. Therefore, the objective of this paper is to explain the difference of nighttime temperatures over grass-dominated and shrub-dominated areas and identify the salient processes causing the climatic differences observed between these two land covers. Understanding these processes will be necessary, for example, if we want to parameterize the effects of shrub encroachment on the near-surface atmosphere in climate models.

2.2 Methods

2.2.1 Study Site

To investigate the effect of shrub encroachment on near surface microclimatic conditions, we compared surface temperatures and energy fluxes at grassland and adjacent shrubland sites. To this end, we used data from the Sevilleta National Wildlife Refuge, located in the northern Chihuahuan Desert of the Rio Grande Valley, approximately 80 km south of Albuquerque, New Mexico. Because the Sevilleta National Wildlife Refuge shows a dramatic encroachment front of *Larrea tridentata* (creosotebush) shrubs into native desert grassland, it represents an ideal location to

investigate differences in surface energy flows associated with the two different land covers, both of which exist under the same regional climate conditions.

Concurrent measurements were made on two identical flux towers currently deployed over a *Larrea*-dominated shrubland and *Bouteloua*-dominated grassland as part of the Long Term Ecological Research (LTER) program. The grassland (34.3402°N, 106.6854°W) and shrubland (34.3338°N, 106.734010°W) tower sites are in the McKenzie Flats area of the Sevilleta National Wildlife Refuge. The distance between the towers is about 5 km, and the elevation difference is less than 10 m. The Sevilleta Refuge contains extensive semi-arid grassland dominated by C₄ perennial grasses (*Bouteloua gracilis*, *B. eriopoda*, *Sporobolus* spp., *Hilaria jamesii*, *Muhlenbergia* spp.) located on relatively level topography along the western edge of the Los Piños Mountains. In the grassland site the total vegetation cover (live plus litter) averages 60% with 40% bare soil, while in the shrubland site the average vegetation cover is 30% with 70% of bare soil (Kurc and Small, 2004).

Temperature, humidity (with HMP45C Vaisala temperature/ RH probe, 0.2-0.35 °C accuracy), and wind speed were measured (with CSAT3 sonic anemometer) at a height of 3 m above ground level since January 2007. The data we used here cover the period from July 2007 to June 2008. Turbulent energy fluxes were derived using the eddy covariance technique at 3m height above ground (CSAT3 sonic anemometer and LI-7500 open-path IRGA). The flux data represent 30-minute averages. In addition, measurements of radiation components (CNR1 4-way Kipp&Zonen net radiometer) and pressure (CS105 Vaisala PTB101B barometric) were taken at 3 m height above ground, while ground heat fluxes were measured in the ground at 5 cm depth (HFT3 REBS soil heat flux plates).

| Surface Characteristics | Shrubland | Grassland |
|--|-----------|-----------|
| Vegetation cover | 30% | 60% |
| Displacement height, d (m) | 0.3 | 0 |
| Roughness length, z_0 (m) | 0.04-0.06 | 0.03 |
| Winter albedo, α | 0.204 | 0.209 |
| Summer albedo, α | 0.201 | 0.184 |
| Winter emissivity, ε_{sfc} | | |
| All day | 0.963 | 0.964 |
| Daytime | 0.955 | 0.955 |
| Nighttime | 0.970 | 0.976 |
| Summer emissivity, ε_{sfc} | | |
| All day | 0.969 | 0.965 |
| Daytime | 0.962 | 0.961 |
| Nighttime | 0.983 | 0.986 |

Table 2.1 Information on vegetation cover, aerodynamic parameters, albedo and emissivity for the shrubland and grassland sites.

Days were considered to be “clear” when the ratio of daily incoming shortwave radiation to theoretically determined extraterrestrial solar radiation was greater than 64% (Whiteman et al., 1999). Nighttime was defined as those hours with zero incoming shortwave radiation. Wintertime was defined as the season from 1 November, 2007 to 29 February, 2008, while summertime included the months of May, June, July and August.

2.2.2 Surface aerodynamic characteristics

To explain the differences in surface energy flows between the two vegetation types, we determined the effect of landscape conditions on surface aerodynamic characteristics such as displacement height and roughness length for momentum sink. Using the logarithmic wind speed profile and the friction velocity (estimated from the momentum flux), the roughness length for momentum sink, z_0 , and the displacement height, d , were estimated following the procedure described by (Martano, 2000). As expected, both the

roughness length and the displacement height were larger in the shrubland than in the grassland (Table 2.1).

2.2.3 Surface emissivity and albedo

To investigate the processes governing the transfer of energy in the grassland or the shrubland site, we calculated surface emissivity and albedo. For the emissivity (ε_{sfc}) we used the Stefan-Boltzmann law, expressing the longwave radiation, LW_{sfc} , emitted by the ground surface as

$$LW_{sfc} = \varepsilon_{sfc} \sigma T_{sfc}^4 \quad (1)$$

where σ is the Stefan-Boltzmann constant and T_{sfc} is the ground surface temperature. Since T_{sfc} was not measured in this experiment, the aerodynamic method was employed to calculate T_{sfc} from measurements of sensible heat flux density (H). Using the Ohm's law analogy, over horizontal homogenous vegetation canopy, H can be expressed as a function of T_{sfc} and T_{air} . Solving for T_{sfc} , we obtain:

$$T_{sfc} = H \frac{R_H}{\rho c_p} + T_{air}, \quad (2)$$

where ρ is the density of air, c_p is the specific heat of air at constant pressure, and R_H is the resistance to heat transfer and consists of two components,

$$R_H = R_{bH} + R_{Aero}, \quad (3)$$

where R_{bH} is the bulk boundary layer resistance and R_{Aero} is the aerodynamic resistance.

R_{bH} is expressed in terms of atmospheric turbulence levels and the intrinsic characteristics of heat transfer (Wesely and Hicks, 1977),

$$R_{bH} = \frac{2}{\kappa u_*} \left(\frac{Sc}{Pr} \right)^{2/3}, \quad (4)$$

where $\kappa = 0.4$ is the von-Karman constant, u_* is the friction velocity, Pr is the Prandtl number (≈ 0.72) for air and Sc is the Schmidt number. The Schmidt number is calculated as the ratio of kinematic viscosity to mass diffusivity with temperature dependence (Campbell and Norman, 1998). The aerodynamic resistance R_{Aero} is a function of momentum transfer expressed as

$$R_{Aero} = \frac{\left[\ln \left(\frac{z-d}{z_0} \right) - \Psi_m \left(\frac{z-d}{L} \right) \right]}{\kappa u_*}, \quad (5)$$

where z is the height above the ground surface, $\Psi_m \left((z-d)/L \right)$ is the diabatic function (Businger et al., 1971; Dyer, 1974) expressed in terms of the Monin-Obukhov length (L). Therefore, with equations (1) to (5), using the observed upwelling longwave radiation as Lw_{sfc} , the emissivity is expressed as a function of air temperature and turbulence measurements as

$$\varepsilon_{sfc} = \frac{Lw_{sfc}}{\sigma \left[\left(\frac{u}{u_*^2} + \frac{2}{u_*} Sc^{2/3} \right) \frac{H}{\rho c_p} + T_{air} \right]^4}. \quad (6)$$

where u is the wind speed measured at the same height as T_{air} , u_* and H .

The surface albedo (α) was estimated to quantify the amount of solar energy absorbed by the surface in the presence of grass and shrub cover. The albedo was calculated by:

$$\alpha = \frac{K_{up}}{K_{dn}}, \quad (7)$$

where K_{up} and K_{dn} are the upwelling and downwelling shortwave radiation, respectively. These radiation components were measured by pyranometers at 3 m height. Only data from 0900 to 1600 LST (Local Standard Time) were used in the calculation of α to avoid the large uncertainties associated with low solar elevation angles. Values of emissivity and albedo are reported in Table 2.1.

2.2.4 Atmospheric stability

Different rates of surface cooling can occur due to differences in atmospheric stability. In this study the gradient Richardson number (R_i) was used to assess the impact of stability on rates of surface cooling. The gradient Richardson number represents the relative contribution of buoyancy and wind shear to the production/destruction of turbulence (Stull, 1988):

$$R_i = \frac{g}{\theta} \frac{\partial \theta}{\partial z} \frac{1}{\left(\frac{\partial u}{\partial z}\right)^2}, \quad (8)$$

where g is the gravitational acceleration and θ represents the potential temperature. The gradient Richardson number is related to the Monin-Obukhov length (L) through the Businger-Dyer formulas (Businger et al., 1971; Dyer, 1974); large positive values of R_i correspond to stable conditions with weak turbulent mixing.

2.3 Results

2.3.1 Observations

We analyzed near surface air temperatures to assess differences in minimum winter temperatures between the two land covers. Nighttime temperatures in the shrubland were

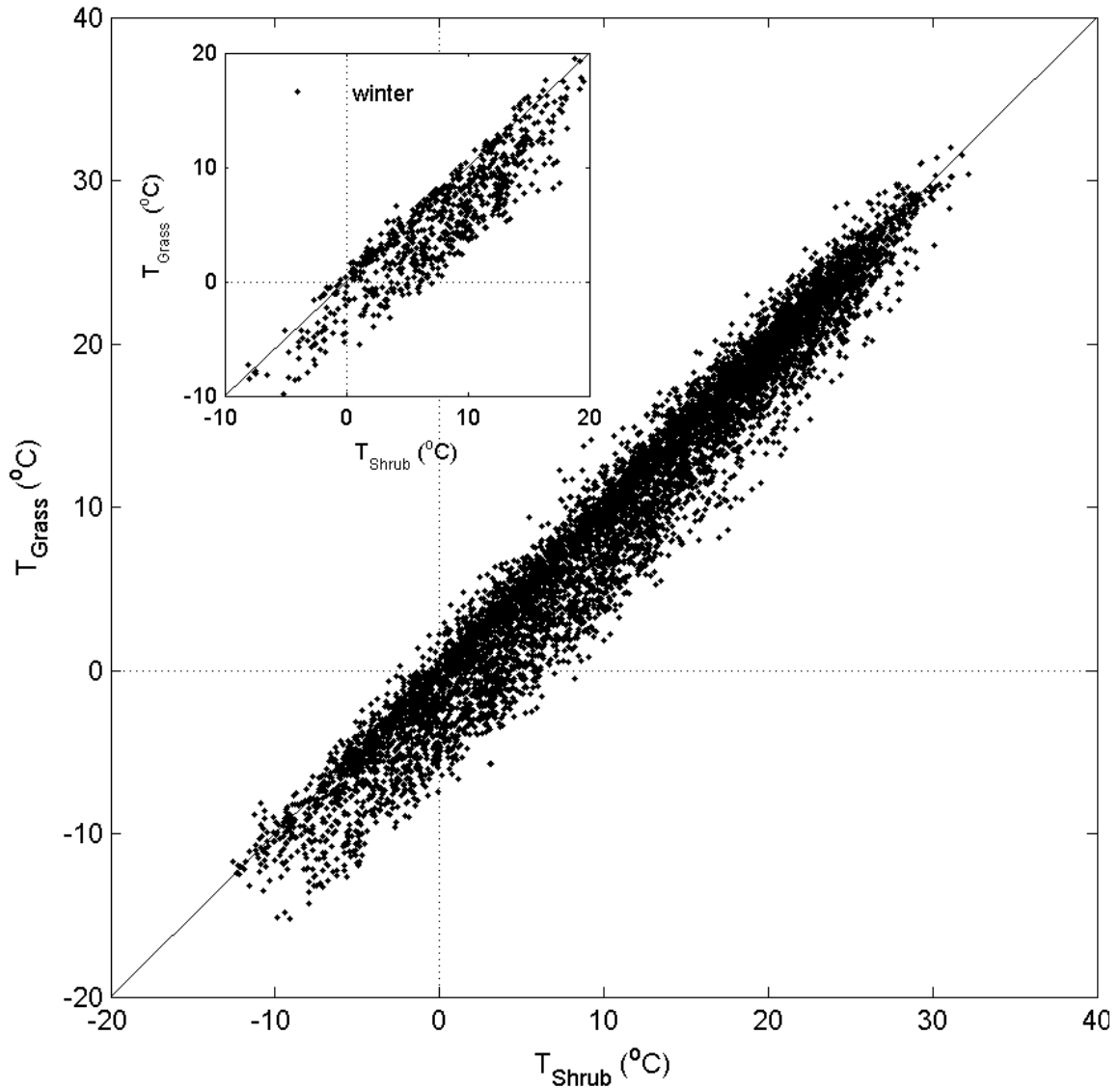


Figure 2.1 Night time temperature comparison between shrubland and grassland, for the whole year and (inset) in the winter months only. Analysis based on Jul 2007 to Jun 2008 half hourly points (Nov 2007 to Feb 2008 data in the inset). The nighttime air temperature in the shrubland is significantly higher than in the grassland ($p < 0.0001$ both for the t-test of the whole year and of the winter months). For 72% of the time (or 79% of the time if only winter months are considered) the shrubland has warmer near-surface conditions than the grassland.

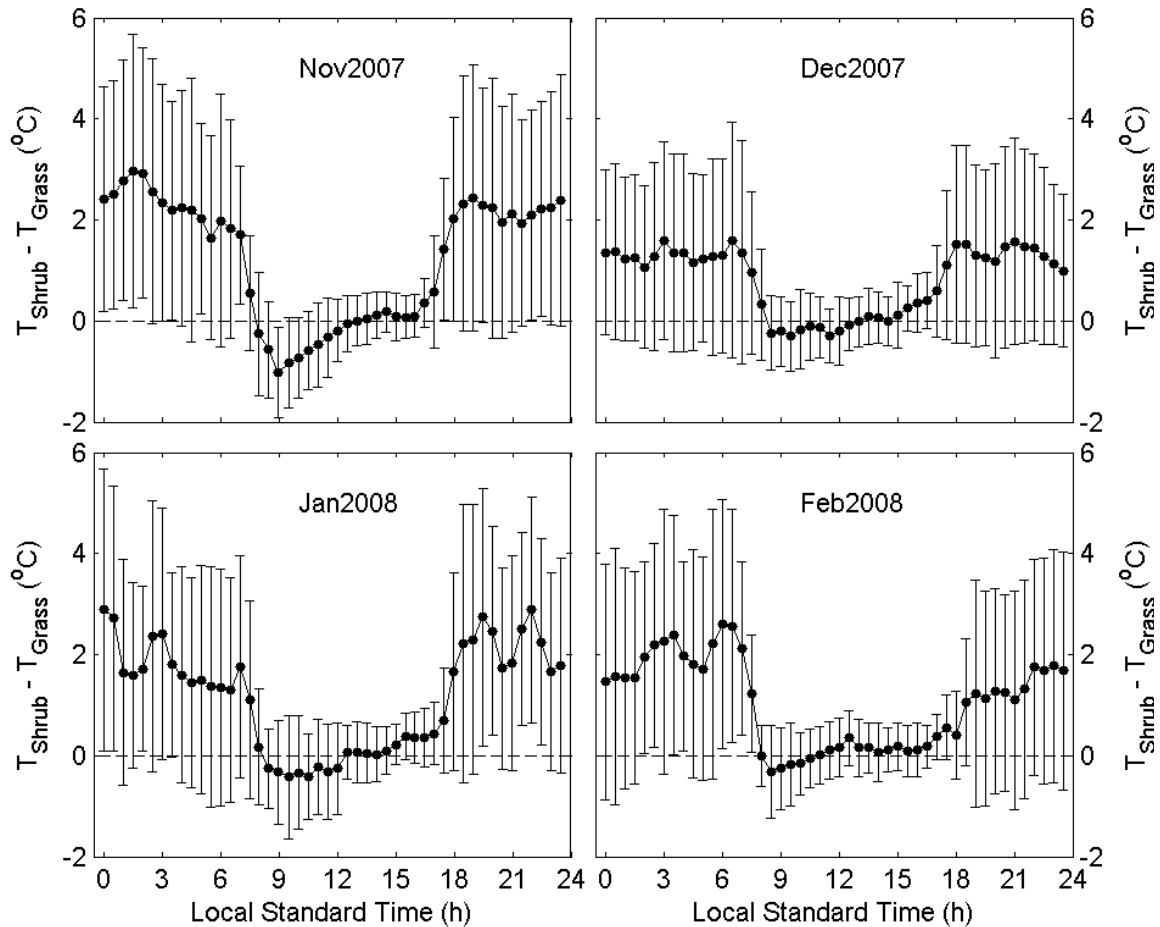


Figure 2.2 Monthly mean and standard deviation of temperature differences between the two vegetation covers in the winter months (Nov 2007 to Feb 2008).

higher than those in the grassland at most times (Figure 2.1). These differences were particularly strong in the winter months, when the mean nighttime air temperatures in the shrubland were on average about 2 °C higher than those in the grassland (Figure 2.2).

Temperature differences were established between 1700 and 1900 LST and were maintained throughout the night (Figure 2.2). Diurnal patterns of temperature differences between the shrubland and the grassland were similar throughout the year. Maximum nighttime differences between near surface air temperatures over the two land covers (Figure 2.3) ranged between 3 °C and 7 °C. The temperature differences between the shrubland and the grassland sites depended on near-surface stability (i.e., the Richardson

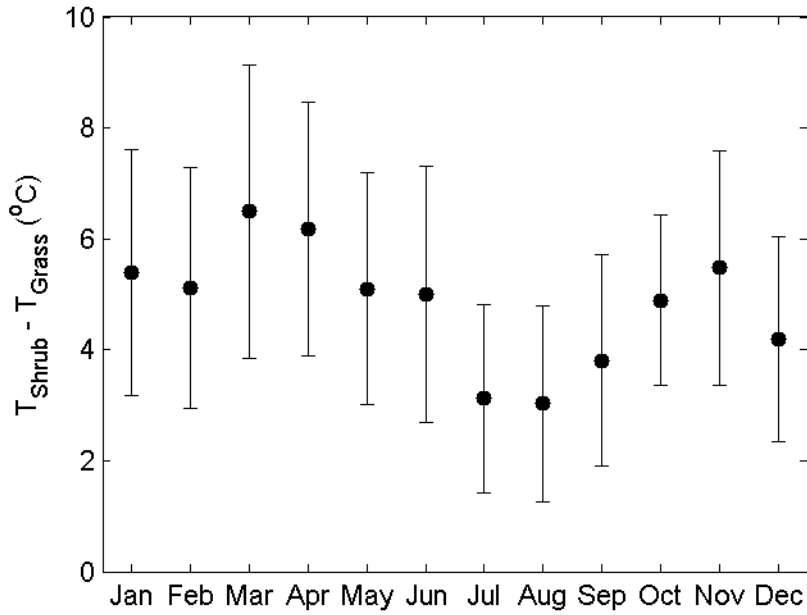


Figure 2.3 Monthly mean and standard deviation of maximum daily nighttime temperature differences between the two vegetation covers.

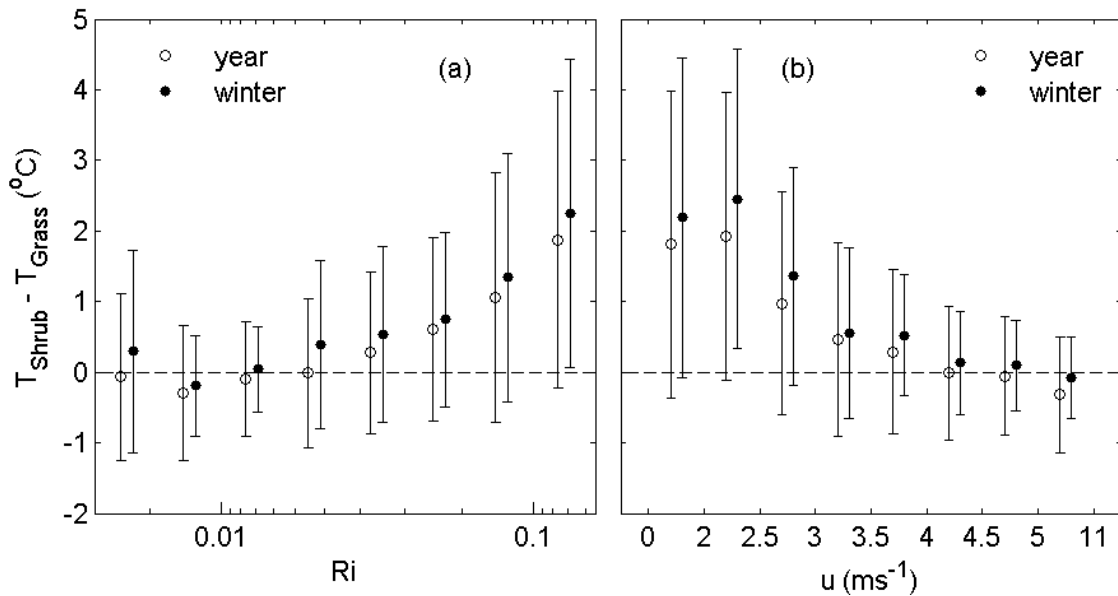


Figure 2.4 (a) Relationship between nighttime temperature differences and Richardson number under stable conditions, and (b) relationship between night time temperature differences and wind speed for the whole year (Jul 2007 to Jun 2008) and winter months (Nov 2007 to Feb 2008).

number, R_i) and wind speed (Figure 2.4). Temperature differences increased when the

| Energy Component | Constraint | Shrubland | Grassland | Difference |
|-----------------------------|------------|-----------|-----------|------------|
| $H(\text{Wm}^{-2})$ | 1 | -9.2 | -12.1 | 2.9 |
| | 2 | -19.6 | -22.1 | 2.5 |
| | no | -15.9 | -17.8 | 1.9 |
| $G(\text{Wm}^{-2})$ | 1 | -17.3 | -18.7 | 1.5 |
| | 2 | -9.0 | -8.5 | -0.5 |
| | no | -1.8 | -8.6 | 6.8 |
| $LW_{up} (\text{Wm}^{-2})$ | 1 | 316.7 | 307.5 | 9.2 |
| | 2 | 333.4 | 326.6 | 6.8 |
| | no | 335.7 | 331.7 | 4.0 |
| $LW_{dn} (\text{Wm}^{-2})$ | 1 | 247.8 | 246.9 | 1.0 |
| | 2 | 256.9 | 259.5 | -2.6 |
| | no | 245.3 | 249.0 | -3.7 |
| $LW_{net} (\text{Wm}^{-2})$ | 1 | -68.9 | -60.7 | -7.7 |
| | 2 | -76.5 | -67.1 | -8.6 |
| | no | -90.4 | -82.7 | -6.0 |

Table 2.2 The nighttime energy components for shrubland, grassland, and the difference between shrubland and grassland, reported as the average over winter months (Nov 2007 to Feb 2008). Constraint 1 conditions are defined as when temperature differences over the two land covers are equal to or larger than 2 oC. Constraint 2 only concerns the measurements from sunset to 2000 LST.

surface layer became more stable (i.e. for large values of R_i ; Figure 2.4a) or when the wind speed decreased (Figure 2.4b). Under these conditions, mixing was relatively weak so that the microclimate in the shrubland and the grassland was not strongly affected by air advected from the surrounding areas, but remained controlled mainly by local conditions (Geiger, 1965). Therefore, the shrubland and the grassland can create and maintain their own microclimate, particularly during calm nights. The overall implication of this analysis is that shrub encroachment leads to warmer near-ground nighttime conditions, especially in the winter season, when shrubs are able to maintain milder microclimate conditions. Warmer winter night conditions, in turn, may favor the survival of shrub species due to their lack of tolerance to freezing temperatures (Pockman and Sperry, 1997).

The differences in near-ground temperature between the two land covers can be explained by differences in energy fluxes and surface energy balance. The average values of each measured energy component, including sensible heat fluxes (H), ground heat fluxes (G), upwelling and downwelling longwave radiation (LW_{up} and LW_{dn} respectively) and the net longwave radiation (LW_{net}), are reported in Table 2.2 for the case of nocturnal wintertime conditions. To better relate surface energy fluxes to the differences in nocturnal temperature between the two land covers, we also constrained the analysis focusing in particular on (1) those nights in which shrubland temperatures exceeded by at least 2 °C those in the grassland (“Constraint 1”) and (2) the time period in which the nocturnal air temperature differences were established (i.e., between sunset and 2000 LST; “Constraint 2”). These results will be discussed in the section 2.4.

2.3.2 Energy budget model

To understand why nighttime temperature in the shrubland was higher than in the grassland and how differences in energy fluxes between the grassland and shrubland sites contributed to such temperature differences, we developed a one-dimensional energy budget model. The temporal variability of air temperature near the ground is driven by the surface energy budget. Assuming a negligible effect of horizontal advection during calm nights, the vertical energy transfer can be related to the temporal variability of the average air temperature within a near surface air layer of thickness z_a through the energy balance equation

$$\rho c_p z_a \frac{dT_{air}}{dt} = H + G + LW_{sfc} + LW_{dn} - LW_{up} - \varepsilon_{sfc} LW_{atm} + (1 - \varepsilon_{sfc}) LW_{atm}, \quad (9)$$

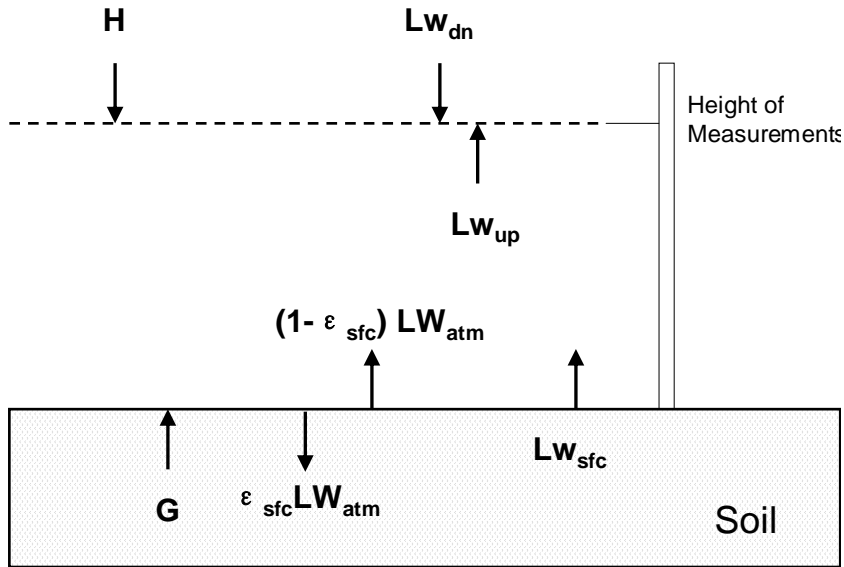


Figure 2.5 Schematic representation of the one-dimensional energy budget model. The parameters are explained in text.

which involves all the energy exchanges occurring at the upper and lower boundaries of the layer of air (Figure 2.5).

The term LW_{atm} is the downward longwave radiation emitted by the atmosphere. This radiation is partly absorbed by the ground ($\epsilon_{sfc} LW_{atm}$), and partly reflected to the atmosphere ($(1 - \epsilon_{sfc}) LW_{atm}$). LW_{atm} was estimated by the Stefan-Boltzmann law as a function of the air temperature and the emissivity of atmosphere (ϵ_{atm}). The other longwave radiation components in equation (9) include the longwave radiation emitted by the ground (LW_{sfc}), and the downwelling (LW_{dn}) and upwelling (LW_{up}) longwave radiation measured at 3m height (Figure 2.5).

The numerical integration of the energy balance equation (9) using energy flux measurements from the two sites allows us to calculate the average air temperature values within the near surface air layer. Six clear winter nights with calm wind and pronounced

temperature differences between grassland and shrubland sites were selected to test the model. To this end, we used values of ground surface emissivity calculated based on winter daytime measurements so that surface emissivity can be considered an independent quantity. The performance of this model is affected by errors associated with measurements and parameter estimation. Moreover we made the approximation of using the near ground air temperature to estimate the atmospheric longwave radiation LW_{atm} and we tested the model comparing the average temperature of a 3-m-thick air layer with values of air temperature measured at 3 m height. The emissivity of the atmosphere (ϵ_{atm}) was therefore the only parameter that can be varied in our model. This parameter was estimated so that air temperatures calculated with this energy budget model best fit those measured during the six selected clear-sky, calm winter nights. As a result, we found that $\epsilon_{atm}=0.88$.

Despite its approximated nature, this 1-D energy budget model reproduced the general pattern of temperature differences between shrubland and grassland observed in the experiment (Figure 2.6). Therefore, the energy budget model provides a process-based framework to explain the air temperature differences between the two land covers as an integrated effect of differences in all the energy fluxes.

In addition, this one-dimensional energy budget model allows us to examine the sensitivity of these temperature differences to different terms of the energy balance. To test this sensitivity, we replaced each energy flux component with the mean of values measured over the two land covers while keeping the other terms of the energy balance unchanged. As shown in Figure 2.6, differences in nocturnal air temperature are not very sensitive to changes in sensible heat fluxes, ground heat fluxes, measured upwelling or

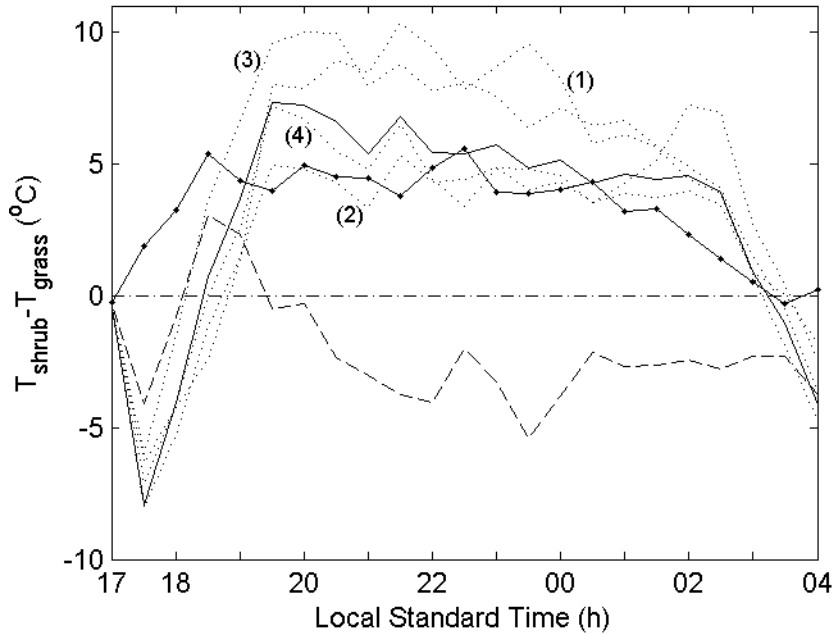


Figure 2.6 Comparison of the observed temperature differences between shrubland and grassland (solid line connecting solid circles) with the results of a one-dimensional energy budget model (solid line) in a selected sample case (the clear-sky calm winter night between 16 and 17 Dec 2007). Sensitivity test with respect to longwave radiation emitted by the ground surface is shown with dashed line (i.e., the same ground longwave radiation is used for the two vegetation covers. See text). Each dotted line shows the result of a sensitivity test with respect to the other components of the energy balance, including (1) sensible heat fluxes, (2) ground heat fluxes, (3) measured upwelling and (4) downwelling longwave radiation.

downwelling longwave radiation. In fact, changes in these energy components do not result in significant changes in the patterns of the calculated air temperature difference between the two land covers. Conversely, changes in ground surface temperature (hence in $L_{w_{sfc}}$) lead to a major change in the patterns of nighttime air temperatures over the two landcovers. Therefore, differences in ground longwave radiation between grassland and shrubland are the major contributor to the higher air temperatures observed at night in the

shrubland with respect to the grassland. This result is consistent with the mechanistic explanation of differences in nocturnal air temperature presented in the discussion.

2.4 Discussion

Diurnal surface temperature variation is controlled by factors involving the energy balance at the surface. The energy balance involves the net radiation, the ground heat flux, and the turbulent fluxes of latent and sensible heat. A detailed investigation of these factors is presented to explain the main processes underlying the nocturnal temperature difference between the shrubland and grassland. The net radiation is contributed by net longwave and shortwave radiation, which are affected by the albedo and emissivity of the ground surface. Differences in albedo between the shrubland and grassland were minor (Table 2.1) and did not cause relevant differences in the net radiation balance during daytime. At night, the shrubland lost more net longwave radiation than the grassland. The upwelling longwave radiation at night was larger in the shrubland than in the grassland in all the three cases reported in Table 2.2. Combining these results with the smaller average nighttime emissivity in the shrubland than in the grassland (Table 2.1), we can conclude that, compared to grassland, the shrubland not only had a higher nighttime air temperature but also a higher nighttime ground surface temperature.

The ground heat flux at each location was calculated as a weighted average of the values measured under the bare soil and vegetated microsites, using values of bare soil fractions typical of the two land covers (Table 2.1, shrubland: 70% bare soil, grassland: 40% bare soil, (Kurc and Small, 2004). Cumulative ground heat fluxes (i.e., the time integral of the ground heat fluxes throughout the day or night) were larger in absolute value in the shrubland than in the grassland. These differences became more pronounced

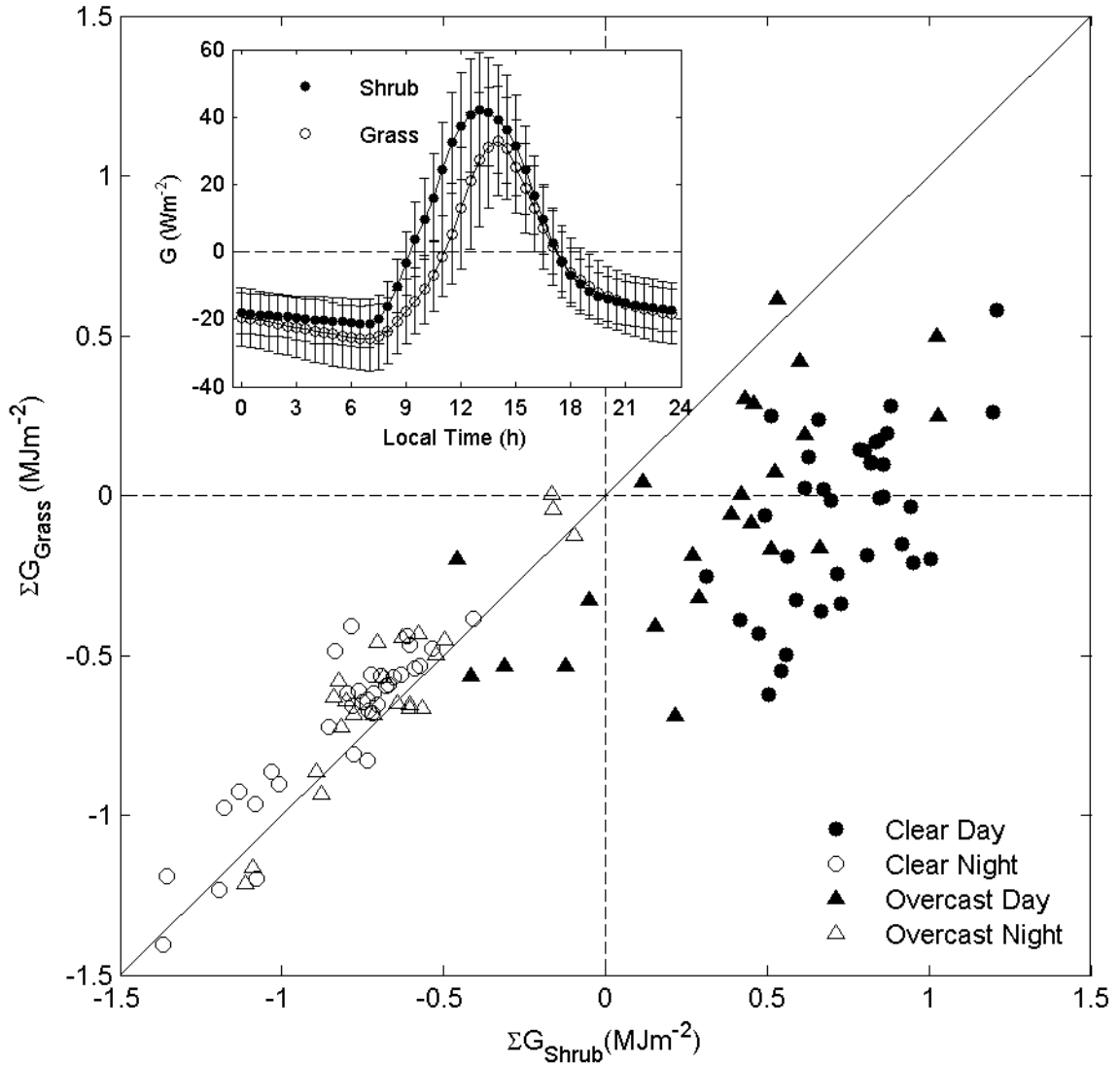


Figure 2.7 Comparison between cumulated ground heat fluxes measured between 1 Nov and 31 Dec, 2007 at the shrubland and grassland sites. Inset: Mean and standard deviation of ground heat fluxes over shrubland and grassland in clear days in the same period. At each site, ground heat flux values were calculated as weighted averages of the values measured at vegetated and unvegetated micro-sites using the fractional land cover reported for each site.

in clear sky conditions during the day (Figure 2.7), presumably because vegetation was less effective in causing the differences of received energy between shaded and non-shaded ground during cloudy days. To explain the differences in ground heat fluxes

between the two land covers, we looked at the ground heat fluxes from bare soil and vegetated microsites at the grassland and shrubland sites. We found that the diurnal ground heat fluxes in bare soil microsites were larger than those in microsites covered by either shrub or grass vegetation (Figure 2.8). Moreover, daytime ground heat fluxes were greater in the shrubland than in the grassland both in the bare soil (with 19.2 Wm^{-2} average difference for all clear winter days) and in the vegetated (with 9.2 Wm^{-2} average difference for all clear winter days) microsites. The greater ground heat fluxes observed at both sites in the bare soil microsites with respect to the adjacent vegetated soil plots (average difference of 24.4 Wm^{-2} for the shrubland and 14.4 Wm^{-2} for the grassland for all clear winter days) provide an explanation for the overall greater ground heat fluxes at the shrubland site (Figure 2.7), where a greater bare soil fraction existed. The different bare soil fractions existing in the two sites resulted in relatively large differences in ground heat fluxes between the two land covers corresponding with the observation and explanation by (Kurc and Small, 2004). At night, the differences in cumulative ground heat flux between shrubland and grassland were smaller than during daytime (on average -0.1 MJm^{-2} at night and 0.8 MJm^{-2} during day for all clear winter days, Figure 2.7), consistently with the smaller difference in nocturnal ground heat fluxes observed between bare soil and vegetation microsites at both locations (Figure 2.8).

Diurnal patterns of ground heat fluxes over the shrubland and the grassland showed a lag of about two hours between the daytime peaks in ground heat flux for the two land covers. In fact, in the shrubland the maximum ground heat flux occurred at 1300 LST, two hours earlier than in the grassland (Figure 2.7, insert). Thus, shrubland soils responded more quickly to daytime warming than grassland soils, due to the larger bare soil fraction

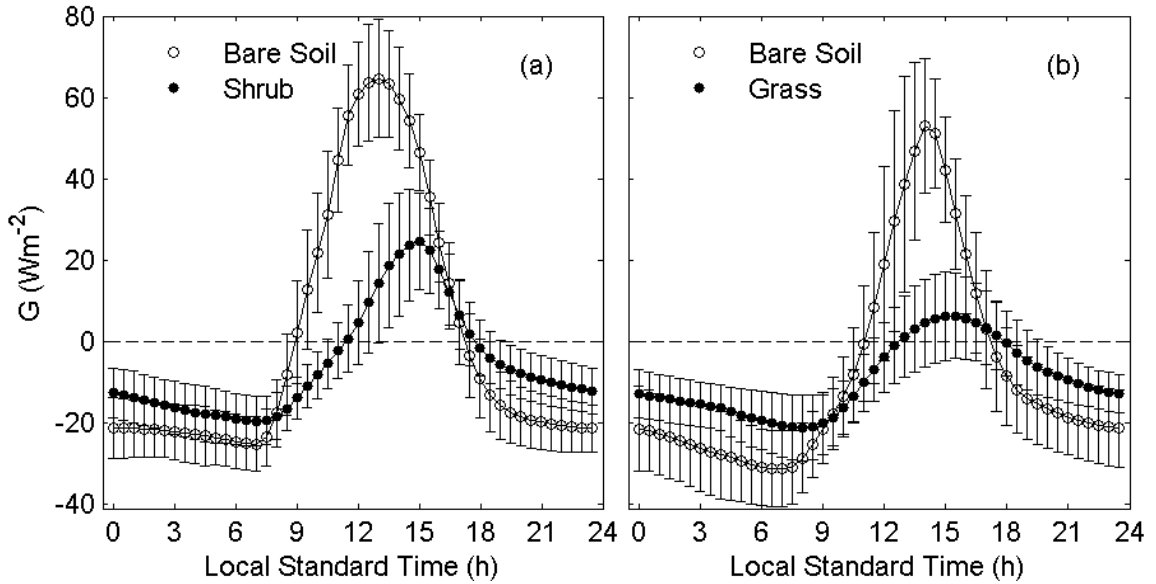


Figure 2.8 Mean and standard deviation of ground heat fluxes under bare soil and vegetation cover, in the shrubland (a) and the grassland (b) in clear winter days (Nov 2007 to Feb 2008).

in the shrubland and the lack of insulation of the ground surface by grass biomass. In fact, at the patch scale we found that a lag of about two hours exists between the peaks of ground heat fluxes measured in vegetated and bare soil microsites (Figure 2.8). The downward sensible heat fluxes were greater in absolute value ($>1.9 \text{ Wm}^{-2}$ on average) for the grassland than the shrubland (Table 2.2) consistently with the more rapid cooling of the air above the grassland.

In summary, on the basis of this analysis of radiation and energy fluxes, we can explain the emergence of nighttime temperature differences between the two land covers as follows. In the shrubland, where a larger fraction of bare soil typically exists, the soil surface is poorly insulated by vegetation. Thus, more energy was received by the underlying soil column during the day in the form of ground heat fluxes. Moreover, due to the limited insulation of the soil surface, soil heating occurred more rapidly in the

shrubland than in the grassland. This energy was then released at night in the form of longwave radiation. Because differences in ground surface emissivity between grassland and shrubland were negligible, the higher nocturnal longwave radiation emitted by the shrubland was due to differences in soil surface temperatures. Similar findings were reported for daytime conditions at the same shrubland and grassland research sites (Kurc and Small, 2004; Small and Kurc, 2003). Therefore, differences in bare soil fraction caused a differential diurnal heating of the soil in the two land covers. Thus, at night more energy was released from the ground in the shrubland than in the grassland, contributing – as indicated by simulations with the energy balance model - to the differential heating of the near surface air, thereby causing the observed differences in nocturnal air temperatures between shrubland and grassland. These differences were particularly strong during calm nights, and their persistence throughout the night was favored by the relatively stable boundary layer conditions.

The explanation of air temperature differences based on the different bare soil fractions existing on the two land cover is consistent with other observations from the Northern Chihuahuan Desert (Carre, 2005) and with similar findings from the Sonoran Desert, where differences in air temperature of about 4 °C were detected across the Mexico-United States border, and explained as a result of the higher bare soil fractions due to the heavy overgrazing on the Mexico side (Balling, 1988; Balling et al., 1998; Bryant et al., 1990). However, to our knowledge this effect of warming induced by an increase in bare soil had never been explained before in the context of its relation with shrub encroachment. Although warming may also have a positive effect on grass growth, in the case of *Larrea*-encroached landscapes the increase in minimum temperature

associated with grassland-to-shrubland conversion is likely to favor only the establishment of these freeze-sensitive shrub species, because grasses remain dormant during wintertime.

Acknowledgements

This research was supported by NSF-DEB 0743678 and the NSF-DEB 0620482 to the University of New Mexico for Long-term Ecological Research. We would like to thank the anonymous reviewers for their constructive comments which improved the manuscript.

CHAPTER 3

COUPLED LAND-ATMOSPHERE MODELING OF THE EFFECTS OF SHRUB ENCROACHMENT ON NIGHTTIME TEMPERATURES²

3.1 Introduction

Many semi-arid regions around the world have been experiencing a transition from grass to shrub dominance in recent times, a phenomenon also known as shrub encroachment (Alan K. Knapp et al., 2008; Van Auken, 2000). This change in plant community composition causes the loss of important ecosystem services, such as soil stabilization and rangeland grazing (Geist and Lambin, 2004; Schlesinger et al., 1990). Shrub encroachment is affecting regions of North and South America, Africa, Asia, and Australia (Archer, 1989; Cabral et al., 2003; Roques et al., 2001). As most changes in vegetation cover, the shift from grass to shrub dominance is expected to modify the land surface attributes and to alter the surface energy fluxes with important impacts on microclimate conditions (Bonan, 2002; Geiger, 1965). However, despite the widespread occurrence of shrub encroachment around the world, its impact on the local climate has remained poorly investigated.

Using data from the Northern Chihuahuan Desert, (Hayden, 1998) reported that the minimum temperature recorded at 1.5 m above a shrubland surface was about 4 K greater than that in an adjacent grassland. Recently, He et al. (2010) analyzed temperature records from a grass-shrub transition zone in the region and also showed that, on average,

² Published in Agricultural and Forest Meteorology : **He, Y.**, De Wekker, S.F.J., Fuentes, J.D., D'Odorico, P., 2011. Coupled land-atmosphere modeling of the effects of shrub encroachment on nighttime temperatures. *Agricultural and Forest Meteorology* 151, 1690–1697. doi:10.1016/j.agrformet.2011.07.005

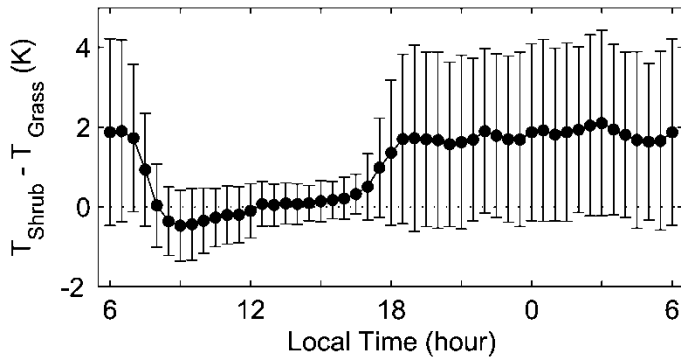


Figure 3.1: Mean and standard deviation of temperature differences between shrubland and grassland of Sevilleta National Wildlife Refuge in December 2007 to February 2008.

the nighttime air temperature observed in the shrubland is higher than in the grassland during winter. A temperature difference of about 2 K is mainly established around sunset and is then maintained throughout the night (Figure 3.1). Daytime temperature differences between shrubland and grassland are smaller in response to effective atmospheric mixing associated with high levels of turbulence. Using an energy balance model, He et al. (2010) concluded that the difference in nocturnal temperatures can be explained by differences in the amount of vegetation cover. The transition from grassland to shrubland reduces the vegetation cover, thereby increasing the amount of incoming radiation that is transformed into thermal energy and stored in the soil during daytime. At night, thermal energy is released at greater rates from soils occupied by shrubs, thereby inducing higher near-surface air temperatures in the shrubland than in the grassland, especially in wintertime. Because the encroached shrub species are prone to freezing-induced mortality, the increase in winter nighttime temperature favors their successful establishment (D’Odorico et al., 2010). This positive vegetation-microclimate feedback may facilitate a transition from grassland to shrubland, and sustain the shrub encroachment process.

Vegetation-climate interactions are typically investigated with global-scale climate models (Collins et al., 2006; Foley et al., 1998; Kiehl et al., 1998). However, to simulate vegetation-microclimate feedbacks at smaller scales, land-atmosphere interactions over sparse vegetation need to be accurately represented with coupled land-surface parameterization schemes typically used in regional climate models. To this end, we use an atmospheric mesoscale model to assess whether numerical simulations can realistically represent the observed differences in nocturnal temperature between shrubland and grassland. Through a sensitivity analysis with respect to soil and vegetation variables, we investigate the processes contributing to the observed temperature differences, and compare our findings to field observations and results from energy balance modeling presented in He et al. (2010).

3.2 Method

3.2.1 Numerical Model Description

In this study, we use the Weather Research and Forecasting model (Skamarock et al., 2008) coupled with the Noah Land Surface Model (Chen and Dudhia, 2001; Ek et al., 2003; Mahrt and Ek, 1984). This coupled modeling system has been shown to reliably simulate land-atmosphere interactions (Hong et al., 2009; James et al., 2009; LeMone et al., 2007). Noah LSM simulates the exchange and storage of heat and water, and the transfer of radiation between different layers both below and above ground, including soil, snow, vegetation and atmosphere. Energy fluxes are calculated between soil/snow layers and the atmosphere, with an additional component from the vegetation to the atmosphere for the latent heat flux. Heat fluxes in the soil are determined by the temperature gradient between soil layers and the thermal diffusivity of the soil. A soil

skin temperature is diagnosed based on the surface energy balance included in Noah LSM; the ground heat flux is the heat transfer from the top soil layer to the soil skin (i.e., the upper edge of the top soil layer), while the sensible heat flux is defined as the heat exchange from the soil skin to the atmosphere. Noah LSM uses a stability-dependent surface exchange coefficient to calculate the heat fluxes, and the temperature at 2 m above ground as a forcing variable, which are both obtained from the surface layer scheme in WRF (Eta surface layer scheme in this study, (Janjic, 2002, 1996). The latent heat flux is defined as the total evapotranspiration from snow, soil, and vegetation and is calculated using a Penman-based potential evaporation method (Mahrt and Ek, 1984), a multilayer soil model (Mahrt and Pan, 1984), and the canopy resistance (Chen et al., 1996).

3.2.2 Model setup

The 2-dimensional computational domain of the mesoscale model covers 480 km in the east-west direction, with a 1-km horizontal grid spacing and periodic boundary conditions. A domain size of 480 grid points ensures that the influence of the lateral boundaries in the region of interest (central portion of domain) is minimal. The model uses 65 vertical levels which extend from the height of the first level below 9 m does not result in differences in the simulation of near-surface (2-m) air temperature. WRF is a non-hydrostatic model, using a standard C grid (Mesinger and Arakawa, 1976) with a hydrostatic-pressure vertical coordinate (Laprise, 1992).

The model runs are initialized right before sunrise at 0600 local time (LT). The initial temperature profile is based on observations from a radiosonde launch prior to a clear night in December 2008 as part of a field study at the Sevilleta National Wildlife Refuge

(SNWR; 34.3 °N, 106.7 °W). The vertical temperature profile has a temperature inversion in the lowest 400 m ($dT/dz = 25 \text{ K km}^{-1}$), and a layer from 400 m to 2000 m that is weakly stable ($dT/dz = 3.1 \text{ K km}^{-1}$). The simulations are initialized with 1 ms^{-1} westerly winds and with microphysics and cumulus parameterizations turned off. The four soil layers in Noah LSM have a thickness of 0.1 m, 0.3 m, 0.6 m and 1 m from top to bottom. The initial temperature of all soil layers is set to be the same as the surface temperature which was 268.15 K. The initial volumetric water content of the four soil layers is 0.05, 0.1, 0.1, and $0.1 \text{ m}^3 \text{ m}^{-3}$ from top to bottom, respectively, which correspond to typical winter conditions in the Northern Chihuahuan Desert (Litvak, personal communication). The sensitivity of the simulations to different atmospheric and soil initializations will be shown in section 3.3. Model simulations were run for 24 hours from 0600 LT for a day in December (21 December, winter solstice) to the following morning at 0600 LT using a time step of 15 sec. The computational domain was located at 30 °N and 0 °E, resulting in sunrise at about 0730 LT and sunset at about 1630 LT on the simulation day. Uniform sandy loam soil is used for both shrubland and grassland in all the simulations. The vegetation cover is set to shrubland in half the domain and to grassland in the other half. To obtain model output representative of the grassland and the shrubland, the output was averaged over 20 grid points in each half of the domain 5 grid points away from the boundary between shrub- and grassland.

Noah LSM assumes default parameters for different vegetation covers including shrubland and grassland. Each land cover is defined by a unique set of vegetation parameters that influence the radiation and energy budgets. In the current study, vegetation parameters, except for vegetation fraction, are based on observations by He et

| LSM Vegetation type | Noah LSM default | | Observation | | Used | |
|----------------------------------|---------------------------|---------------------------|--------------------|--------------------|-----------|-----------|
| | grassland | shrubland | grassland | shrubland | grassland | shrubland |
| Albedo | [0.19, 0.23] ^b | [0.25, 0.30] ^b | 0.209 ^c | 0.204 ^c | 0.2 | 0.2 |
| Emissivity | [0.92, 0.96] ^b | 0.93 | 0.964 ^c | 0.963 ^c | 0.96 | 0.96 |
| Roughness length (m) | [0.10, 0.12] ^b | [0.01, 0.05] ^b | 0.03 | 0.04-0.06 | 0.03 | 0.05 |
| Vegetation fraction ^a | 0.8 | 0.7 | 0.6 | 0.3 | 0.6 | 0.1 |

^avegetation fraction in Noah LSM is the green vegetation fraction or shading factor.

^b those vegetation parameters have seasonal dependencies. The values for December used in the model is indicated in Figure 3.5.

^cwinter values

Table 3.1 Noah LSM default vegetation parameter settings, observations from Sevilleta National Wildlife Refuge in northern Chihuahuan desert, and the vegetation parameters used in this study.

al. (2010) using data from two micrometeorological towers and soundings over adjacent shrubland and grassland sites in the northern Chihuahuan desert, New Mexico. The two observational sites are located in the McKenzie Flats area of the SNWR, within a distance of less than 5 km. Soil type is the same for the shrubland and the grassland site (sandy loam). Dominated by C4 perennial grasses, the average vegetation cover of the grassland site is 60% with 40% bare soil. The C3 shrubland has a 30% vegetation cover with a bare soil fraction of 70%. These estimates of the vegetation cover are based on the analysis of aerial photographs taken during the winter months as shown in Kurc and Small (2004). More information about the soil and atmospheric measurements at the two tower sites can be found in He et al (2010). As shown in Table 3.1, the default parameters of shrubland and grassland differ from the values observed in the field sites at the SNWR. For example, in Noah LSM, the albedo for the shrubland is larger than over the grassland, but our observations show that in the case of the Northern Chihuahuan Desert the albedo over the grassland and the shrubland is almost similar (He et al., 2010). Noah LSM assumes a much larger roughness length in the grassland (0.10-0.12 m, 0.12 m in December) than in the shrubland (0.01-0.05 m, 0.05 m in December) while the

opposite is observed at the SNWR field sites. Therefore, in our simulations, we adjusted the default values of albedo, emissivity and roughness length to reflect the observed values (Table 3.1). The albedo (0.2) and emissivity (0.96) are set to be identical for both shrubland and grassland. The roughness length of shrubland is assigned a larger value (0.05 m) than in the grassland (0.03 m). The sensitivity of the simulations to those three vegetation parameters will be discussed in section 3.2. In our baseline simulation, we used green vegetation fractions of 60% for grassland and 10% for shrubland. The use of a value different from the vegetation cover observed at the shrubland site ($\approx 30\%$) is justified and explained in section 3.2.

3.3 Results and Discussion

3.3.1 Baseline simulation

The simulation captures the observed key features of the temperature differences between shrubland and grassland with higher near-surface air temperature in the shrubland than in the grassland (Figure 3.2). The nighttime air temperature difference increases rapidly around sunset (1600 to 1700 LT) and reaches a maximum value of about 2.7 K around 1800-1900 LT. The averaged air temperature after sunset (1700 to 0600 LT) is about 1.8 K higher in the shrubland than in the grassland. During daytime, the air temperature in the grassland is higher than in the shrubland, which is also qualitatively consistent with the observations (Figure 3.1). The simulated daytime temperature differences are somewhat overestimated which can be explained by the calm initial conditions in the model setup which persisted throughout the simulation period. Increasing the initial wind speed enhances mechanical mixing, thereby decreasing the temperature differences between shrubland and grassland during daytime. The simulated

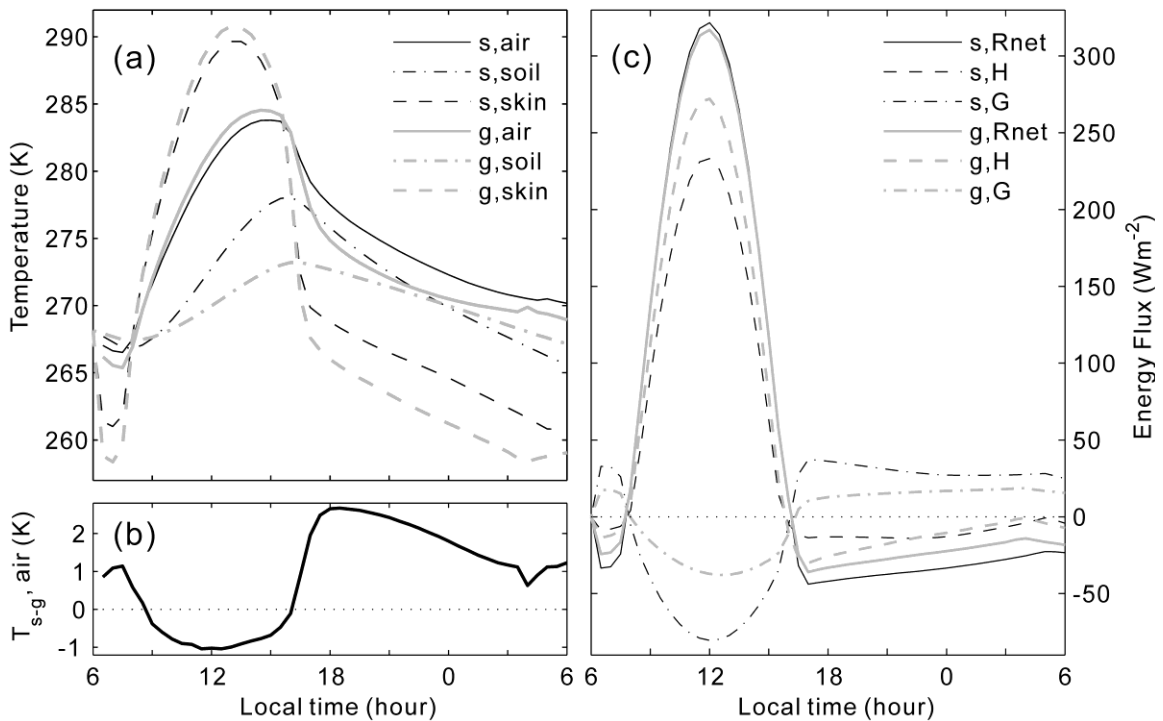


Figure 3.2 Simulated time series of (a) air temperature at 2m height, skin temperature, soil temperature of the 10cm depth layer below ground in the adjacent shrubland ('s') and grassland ('g'); (b) air temperature differences at 2m height between the shrubland and grassland; and (c) the net radiation (Rnet), sensible heat (H) and ground heat fluxes (G) of both land covers.

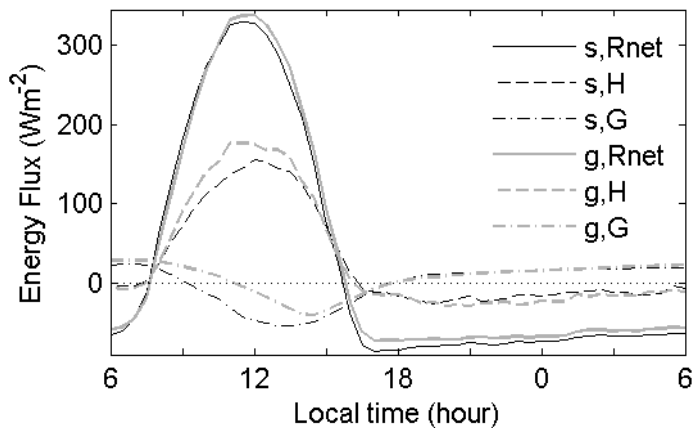


Figure 3.3 Observed time series of net radiation (Rnet), sensible heat (H) and ground heat fluxes (G) over shrubland ('s') and grassland ('g'). Fluxes are the average of 16 selected clear days with small wind speed in the time period from November 2007 to January 2008.

| Energy (in absolute value) | time | Observation | WRF |
|-------------------------------|-------|----------------------|-----------------------|
| Rnet | Day | Little difference~1% | Little difference ~1% |
| | Night | s | s |
| Lup | Night | s | s |
| G | Day | s | s |
| | Night | s | s |
| H | Day | g | g |
| | Bight | g | g |

Table 3.2 Comparison of the observed and simulated energy components in shrubland and grassland during clear winter conditions. “s” indicates that the energy component in absolute value is larger in shrubland than in grassland, while “g” indicates the opposite.

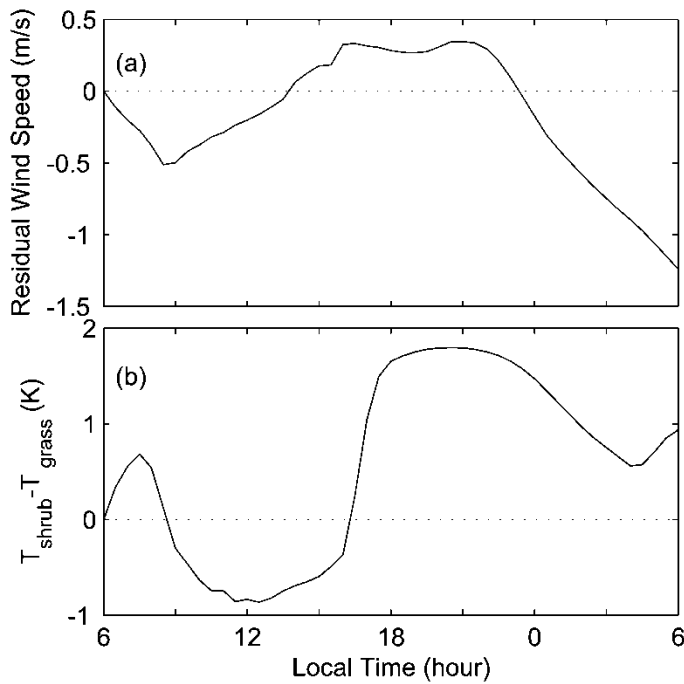


Figure 3.4 (a) Simulated mean residual wind speed in the lowest 50 m and averaged over 11 grid points across the shrubland-grassland boundary. Residual wind speed is defined here as the difference between the simulated wind speed and the ambient geostrophic wind (1m/s, the initial wind speed). Positive values indicate a residual wind component blowing from shrubland to grassland (shrub breeze), while negative values indicate a grass breeze. (b) Simulated mean temperature difference between shrubland and grassland in the lowest 50m.

air temperature, skin temperature and soil temperature were overall in agreement with the observations (data not shown).

The simulated energy components of the adjacent shrubland and grassland (Figure 3.2) are qualitatively consistent with the observations (Figure 3.3, Table 3.2). In particular, the differences in the energy fluxes between the shrubland and the grassland, which He et al. (2010) found to explain the nighttime temperature differences, are well simulated. He et al. (2010) concluded that the larger ground heat fluxes during daytime and the larger nocturnal longwave radiation emitted by the ground in the shrubland play a critical role in explaining the higher nighttime surface temperatures over the shrubland compared to the grassland. In the simulation, the daytime ground heat fluxes in the shrubland are twice as large as those in the grassland, which leads to larger soil heat storage in the shrubland. After sunset, the skin temperature in the shrubland exceeds the skin temperature in the grassland, causing larger upwelling longwave radiation in the shrubland, which contributes to the warmer nocturnal air temperature in the shrubland.

We note that the difference in air temperature between the shrub- and grassland initiated a thermally driven circulation in the simulation with a daytime shrub breeze and a nocturnal grass breeze (Figure 3.4). The intensity of the daytime shrub breeze weakens when the near-ground air temperature over the shrubland becomes higher than over the grassland around sunset. It takes about 5 hours for the warmer air over the shrubland to establish a horizontal pressure gradient in the shallow nocturnal boundary that is strong enough to overcome the shrub breeze. The resulting grass breeze acts to reduce the nighttime temperature differences between the shrubland and grassland.

3.3.2 Sensitivity to vegetation parameters

Different land covers are represented by specific combinations of vegetation parameters in the Noah LSM. Adjusting these parameters to correspond with those observed in the study location affects the simulated land atmosphere exchange and improves model performance (Hogue et al., 2005; Rosero et al., 2010). Therefore, the vegetation parameters were modified and set in agreement with our observations (Table 3.1 and Figure 3.2). The sensitivity of the simulations to changes in these vegetation parameters – namely, the green vegetation fraction, albedo, emissivity and roughness length – was investigated by changing the values of one parameter for both shrubland and grassland while keeping the other parameters the same as in the baseline simulation. In this sensitivity study, the green vegetation fraction was varied from 0.1 to 0.8 with an increment of 0.1 (64 simulations in total); the albedo was varied from 0.19 to 0.3 with an increment of 0.01 (144 simulations in total); the emissivity was varied from 0.92 to 0.94 with an increment of 0.01 (49 simulations in total); and the roughness length was varied from 0.01 m to 0.12 m with an increment of 0.01 m (144 simulations in total). Thus, a total of 401 simulations were performed in this sensitivity study. The analysis focused on the sensitivity of the vegetation parameters to temperature differences averaged from 0000 LT to 0600 LT because shrubs are most sensitive to the freezing-induced xylem cavitation associated with minimum temperatures that usually occur at night and during the winter season (Pockman and Sperry, 1997).

As shown in Figure 3.5, nighttime temperature differences between shrubland and grassland are most sensitive to the green vegetation fraction, while their dependence on the other vegetation parameters is much weaker. By varying green vegetation fraction, albedo, emissivity, and roughness length within the range of values used in this

sensitivity analysis, we obtained maximum changes in temperature differences between shrubland and grassland of 3.4K, 1K, 0.4 K and 0.2 K, respectively. Adjusting the values of the green vegetation fraction and the roughness length to the observed values increases the averaged nighttime temperature difference by 1.0 K and 0.1 K, respectively. Adjusting the albedo and roughness length decreases such temperature difference by 0.3 K and 0.1 K, respectively. Moreover, differences in albedo, emissivity or roughness length alone cannot explain the differences in nighttime temperature observed between the shrubland and the grassland. With the same green vegetation fraction, other vegetation parameters make shrubland always warmer than grassland during the night. However, when the green vegetation fraction of shrubland becomes larger than in grassland, the grassland can even become warmer than the shrubland during night in some cases. Therefore, the green vegetation fraction is the most important vegetation parameter in this case study, which is consistent with the explanation provided by He et al. (2010) for the temperature and energy flux differences observed between shrubland and grassland (He et al. 2010).

In addition to the relative importance of changes in a single vegetation parameter separately from the others as shown in Figure 3.5, we also conducted another sensitivity test to investigate how concurrent changes in multiple vegetation parameters may have an impact on the simulated nighttime temperature. In this sensitivity test, we changed one, two, three and all the four vegetation parameters with all possible combinations from baseline settings to the default values for December in the Noah LSM (Table 3.1, also see the dots and triangles in Figure 3.5). A total of 16 simulations were carried out and the temperature differences between shrubland and grassland averaged from 0000 LT to

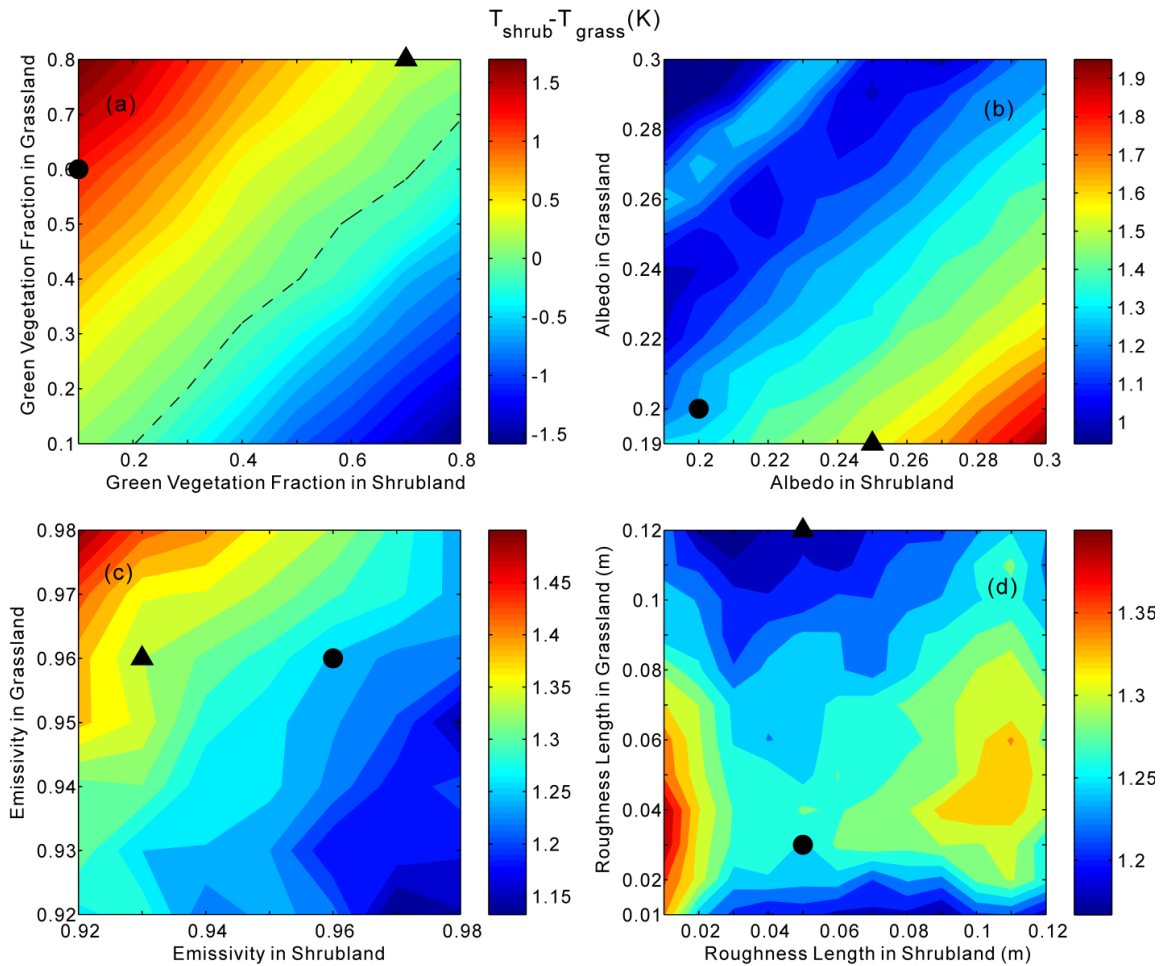


Figure 3.5 Sensitivity of the air temperature differences, averaged from 0000 to 0600 LT, between the shrubland and the grassland to (a) green vegetation fraction, (b) albedo, (c) emissivity and (d) roughness length. Positive values indicate higher air temperatures at 2m above ground in shrubland than in grassland. Zero difference is indicated by the black dashed line. The black triangle corresponds to the default values of the vegetation parameters for December in Noah LSM, and the black dot corresponds to the values of the vegetation parameters used in this study.

0600 LT were analyzed. The effects of changes in multiple vegetation parameters are approximately additive with minimal interactions between the different vegetation parameters (Figure 3.6). For example, changing the green vegetation fraction and albedo to the default values separately, the simulated nighttime temperature differences become

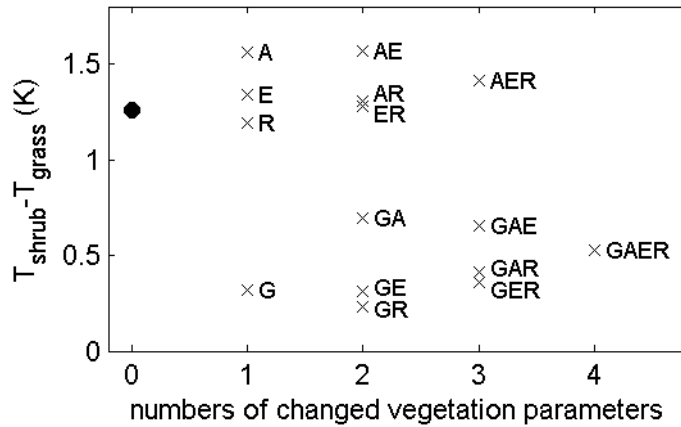


Figure 3.6 Air temperature differences, averaged from 0000 to 0600 LT, between shrubland and grassland for different combinations of changes in vegetation parameters from those used in the baseline simulation (see also black dots in Figure 3.5 and Table 3.1) to those used in default setup of Noah LSM for December (see also triangle markers in Figure 3.5 and Table 3.1). The black dot indicates the temperature difference in the baseline simulation. The changed vegetation parameters are labeled as A for albedo, E for emissivity, R for roughness length, and G for green vegetation fraction. For example, GA indicates the temperature difference between shrubland and grassland in a simulation where the green vegetation factor and albedo are changed from values in the baseline simulation to the default values in Noah LSM.

0.9 K (cooler) and 0.3 K (warmer) relative to the baseline simulation. Changing both the green vegetation fraction and albedo at the same time results in a change of 0.6 K (cooler) relative to the baseline simulation. This sensitivity analysis indicates once again that in this study, the green vegetation fraction is the most important vegetation parameter affecting the simulated nighttime temperature differences.

Because of the key role of the green vegetation fraction in determining the nighttime temperature regime, its values need to be carefully assigned. While previous sensitivity studies that included the vegetation fraction mainly focused on daytime processes such as convective boundary layer growth and convection initiation in different

models (Crawford et al., 2001; James et al., 2009; Kurkowski et al., 2003), this study focuses on nighttime near-surface temperatures. In Noah LSM, the green vegetation fraction can directly affect the near-surface energy exchange by influencing 1) the water fluxes and 2) the thermal diffusivity of top soil layer (Ek et al., 2003). Green vegetation fraction affects water fluxes by determining total plant transpiration, direct soil evaporation, canopy water evaporation and precipitation going into the soil. The latter three components are negligible in the dry winter season on which we focus in this case study. Changes in green vegetation fraction can alter the simulated total plant transpiration and the associated latent heat flux by tens of Wm^{-2} . However, field measurements indicate that during wintertime the latent heat fluxes are very small and usually negligible both in the shrubland and grassland (He et al 2010). Therefore, the coupled Noah LSM and WRF model may easily overestimate the total plant transpiration and therefore the latent heat flux (Hong et al., 2009). As a result of this overestimation, the model simulates unrealistic differences in latent heat flux between shrubland and grassland. These differences affect daytime near-surface energy exchange resulting in a nighttime temperature regime that is different than observed. Thus, we changed the model in such a way that no upward latent heat fluxes occurred in the simulations. After forcing the model to have zero latent heat fluxes, the green vegetation fraction influences the near-surface energy exchange mainly by affecting the top soil thermal diffusivity in our idealized study. In the Noah LSM, an increase in green vegetation fraction increases the insulation of the soil surface by exponentially decreasing the top soil thermal diffusivity (Peters_Lidard et al., 1997; Ek et al., 2003):

$$K_{veg1} = K_{s1} \exp(-\beta_{veg} f_g)$$

where K_{veg1} and K_{s1} are the thermal diffusivities in the top soil layer in vegetated soil and bare soil, respectively, f_g is the green vegetation fraction, and β_{veg} is an empirical coefficient which is set to 2 based on tests with offline Noah LSM (Ek et al., 2003). Larger green vegetation fractions are therefore associated with smaller top soil diffusivity and smaller ground heat fluxes, an effect that is commonly parameterized in LSMs (van den Hurk et al., 2000; Walko et al., 2000). Therefore, in this modified version of the Noah model, the green vegetation fraction does not reflect the actual vegetation cover, but a parameter accounting for canopy effects on the soil thermal properties. Since the soil type is the same in both shrubland and grassland (sandy loam), green vegetation fraction is the only parameter that could reflect the differences in top soil diffusivity. It is plausible that different vegetation types with the same vegetation fraction might have different effects on the soil diffusivity. In the shrubland, plants have branches and leaves that do not insulate the ground surface; the ground surface beneath the canopy is mostly bare and there is very little insulation of the soil surface by plant biomass. Conversely, in the grassland, herbaceous vegetation grows on the ground, thereby sheltering and insulating its surface. Thus, even though – based on photo surveys (Kurc and Small, 2004) – in the shrubland the vegetation cover is 0.3, its top soil diffusivity is close to that of bare soil. To account for this effect of shrub vegetation on soil diffusivity, we set the green vegetation factor parameter to 0.1. We note that changing the green vegetation fraction in shrubland from 0.3 to 0.1 does not affect the general diurnal pattern of temperature differences, but increases the magnitude (by 0.5 K on average from 0000 LT to 0600 LT, see also Figure 3.5a).

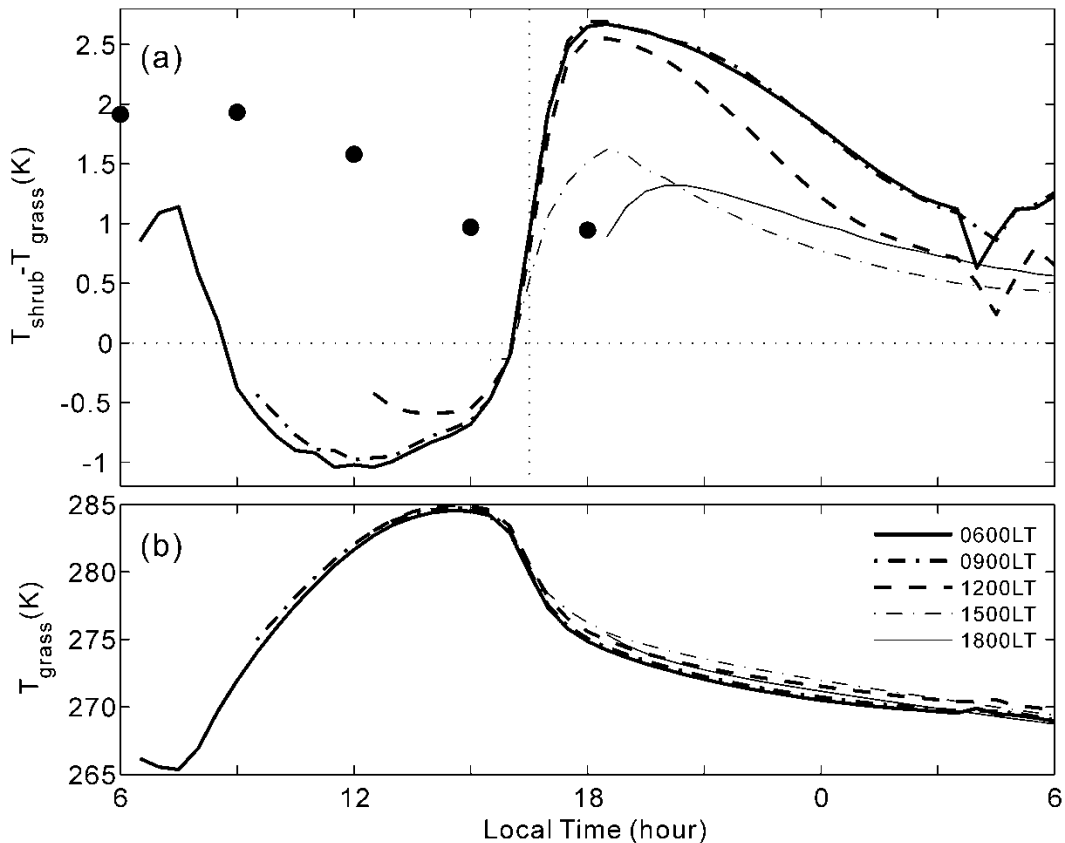


Figure 3.7 (a) Differences in air temperature between shrubland and grassland and (b) the simulated air temperature in grassland for five simulations with different initialization times. The black dots in (a) correspond to mean temperature differences over 12 hours starting from the establishment of higher temperatures in the shrubland than in grassland.

3.3.3 Sensitivity to initialization profiles

The 2-m temperature in a mesoscale model is not only affected by the land surface parameterization scheme but also by other components of the mesoscale model such as the surface layer and the boundary layer parameterization schemes, which, in turn, affect and are affected by the static stability of the boundary layer. We therefore performed several simulations to investigate the sensitivity of the 2-m temperature to the initial temperature profile. We also increased or decreased the surface temperature in the profile without changing the stability to investigate the potential effects of frozen soils on our

simulations (in our initial profile, the surface temperature was just below freezing). Finally, we also investigated the sensitivity of the nighttime temperature differences to the soil moisture content. We found that these factors minimally affected the nighttime temperature differences between shrubland and grassland. An extremely cold surface temperature of 253 K in the initial temperature profile increased the nighttime temperature difference (0000 LT-0600 LT) by 0.1 K compared to the baseline simulation (1.8 K). With a less stable initial temperature profile, temperature differences between the shrubland and grassland show a larger diurnal variability. However, the nighttime temperature differences are almost unaffected. Changes in soil moisture content (by 50% or 200%) directly influence the soil diffusivities, thereby affecting the energy transfer between soil layers, temperature gradients, and the distribution of energy. Those changes, however, do not affect the general pattern or the magnitude of the temperature differences between shrubland and grassland. In fact, the averaged nighttime temperature differences were only on the order of 0.1 K compared to the baseline simulation.

3.3.4 Sensitivity to the daytime warming period

To assess to what extent differences in nocturnal air temperature between the two land covers depend on the occurrence of larger daytime ground heat fluxes in the shrubland, we analyzed the sensitivity of the temperature differences to the initialization time. To this end, the model was initialized at different times, from 0600 LT (before sunrise) to 1800 LT (after sunset) in 3-hourly increments. The temperature profiles of both atmosphere and soil used to initialize the model at 0900 LT, 1200 LT, 1500 LT and 1800 LT were taken from the model output (shrubland portion of the domain) of the simulation initialized at 0600 LT.

Air temperature differences between shrubland and grassland vary with different initialization times, with the earlier initialization times resulting in the largest nighttime temperature differences (Figure 3.7). The simulation initialized at 1800 LT, i.e., after sunset, seems to have larger instantaneous temperature differences than the simulation initialized at 1500 LT. However, temperature differences in the simulation initialized at 1800 LT are established and peak about 2 hours later than the simulations that were initialized earlier, and also start to decrease later. By averaging the same time period starting from the establishment of the temperature difference between shrubland and grassland, the simulation that is initialized at 1800 LT shows the smallest temperature differences (Figure 3.7a). The simulations initialized at 0600 LT and 0900 LT show almost identical nighttime temperature differences, which are almost twice as large as in the simulation initialized at 1800 LT. The simulation initialized at 1200 LT shows a slightly smaller maximum nighttime temperature difference (about 0.1 K) but the temperature differences following the maximum decrease more rapidly throughout the night than in the simulations initialized in the morning. In the early morning, temperature differences in the simulation initialized at 1200 LT reach values that are very similar to those obtained in the simulations initialized in the afternoon.

The dependence of temperature differences on the initialization times can be partly explained by the cumulative solar radiation calculated since the beginning of the simulation. While the cumulative solar radiation is about the same for the simulations initialized at 0600 LT and 0900 LT ($1.18 \times 10^7 \text{ Jm}^{-2}$ and $1.12 \times 10^7 \text{ Jm}^{-2}$, respectively), it is about half that amount for the simulations initialized at 1200 LT ($6.5 \times 10^6 \text{ Jm}^{-2}$), very small at 1500 LT ($1.1 \times 10^6 \text{ Jm}^{-2}$), and zero in simulations initialized at 1800 LT (i.e., after

sunset). This analysis indicates that the amount of solar radiation combined with the insulation differences between the soil surfaces of grassland and shrubland affects the amount of heat going into the soil. The release of this heat at night then affects the nighttime air temperature differences between shrubland and grassland, consistent with the results in He et al. (2010). Although the difference in land surface parameters alone between grassland and shrubland can induce warmer nocturnal conditions in the shrubland, increased soil exposure to solar irradiance and therefore the amount of energy stored in the soil under the shrubland can significantly enhance (double) differences in nighttime air temperature between shrubland and grassland.

3.4 Summary

In this study, we used the mesoscale model WRF coupled with the Noah LSM to simulate the effects of shrub encroachment on nighttime temperature in a shrub-grass transitional area in the Northern Chihuahuan Desert. This area is affected by shrub encroachment, i.e., the replacement of a desert grassland by shrub vegetation. This change in vegetation cover causes an increase in nocturnal temperatures (He et al., 2010; D'Odorico et al, 2010) and a decrease of vegetation exposure to stress and mortality due to freeze-induced xylem cavitation. To investigate the processes underlying this nocturnal warming effect, we set up an idealized 2-D domain across the encroachment front. Using green vegetation fraction, albedo, emissivity and roughness length from field observations we showed that the simulations capture the existence of higher nighttime air temperatures in the shrubland than in the adjacent grassland. Model results showed that the shrubland becomes warmer than grassland around sunset, with an average temperature difference of 1.8 K from sunset to sunrise, which agrees well with the

observations. Differences between the simulated energy components of the adjacent shrubland and grassland are also consistent with the observations. Most importantly, the simulations capture the occurrence of larger diurnal ground heat fluxes and larger nocturnal upwelling longwave radiation in the shrubland than in the grassland, which is consistent with field observations and the mechanism invoked by He et al. (2010) for the explanation of the nighttime temperature differences using a simplified energy balance.

The simulated nighttime temperature differences between shrubland and grassland are not sensitive to the soil moisture content or to the initial temperature profiles in the boundary layer. Simulations in which the green vegetation fraction, albedo, emissivity and roughness length were varied indicate that the green vegetation fraction is the most sensitive parameter affecting nighttime temperature differences between shrubland and grassland. This parameter represents the effects of the canopy on soil surface insulation by changing the top soil diffusivity and therefore the ground heat flux. Thus, because of its impact on the ground heat flux, differences in this parameter between shrubland and grassland are a major contributor to the higher nighttime temperature determined in the shrubland than in adjacent grassland, in agreement with observations (He et al., 2010). Simulations in which the initialization time varied from morning to afternoon show that the storage of heat in the soil during the day influences the magnitude of nighttime temperature differences, which also supports our previous explanation of the higher nighttime temperature in the shrubland than in the grassland (He et al., 2010).

This study successfully simulated the effects of shrub encroachment on nighttime temperature using a mesoscale model. We note, however, that we needed to set plant transpiration equal to zero to be consistent with wintertime field observation. Moreover,

we had to reinterpret the green vegetation fraction as an indicator of soil thermal properties rather than as the actual vegetation cover. In the model, the green vegetation fraction determines the soil diffusivity and evapotranspiration (which is negligible in our case study). Without these adjustments to the model, the simulated latent heat fluxes would be overestimated and provide an unrealistic representation of the surface energy fluxes and nighttime temperature differences between the two vegetation types.

Acknowledgements

This research was supported by NSF-DEB 0743678 and the NSF-DEB 0620482 to the University of Mexico for Long-Term Ecological Research.

CHAPTER 4

CONTRASTING NOCTURNAL TEMPERATURE PROFILES IN ADJACENT SHRUBLAND AND GRASSLAND

4.1 Introduction

The encroachment of woody plants into grass-dominated drylands is a worldwide phenomenon potentially affecting a large portion of the global land surface (Cabral et al., 2003; Lunt et al., 2010; Maestre et al., 2009; Roques et al., 2001; Van Auken, 2000). Shrub encroachment increases the spatial heterogeneity of vegetation cover and nutrients (Schlesinger et al., 1996, Wainwright et al., 2000), affects hydrological processes (Huxman et al., 2005), enhances erosion (Ravi et al., 2007 ; Schlesinger et al., 1999) and decreases rangeland productivity (Geist and Lambin, 2004). The impact of shrub encroachment on the atmosphere and climate has only recently been explored (Beltrán-Przekurat et al., 2008; He et al., 2010). Measurements have found that during winter nights near-surface air temperatures are higher in shrubland than in the adjacent grassland, with a magnitude that is comparable to regional climate change of century scale (He et al., 2014). D’Odorico et al. (2010) hypothesized that the positive feedback between shrub encroachment and nighttime microclimate may favor the establishment of shrubs and therefore enhances shrub encroachment. The higher nighttime temperature in shrubland than in adjacent grassland is caused by a reduction in the vegetation fraction (He et al., 2010), which is a typical change in land surface cover resulting from shrub encroachment in arid environments (e.g., D’Odorico et al., 2012; Turnbull et al., 2010).

The larger bare soil fraction and smaller vegetation fraction allow more soil heating and storage during the day and more heat release from the ground at night, which leads to warmer nighttime conditions in the shrubland. Numerical simulations with an atmospheric model also show higher nighttime surface temperatures in areas characterized by a lower green vegetation fraction (He et al., 2011). The numerical study by He et al. (2011) focused on the surface air temperature without investigating the temperatures of the overlying boundary layer. Having an understanding of the differences in boundary layer structure between the two vegetation covers will provide a more complete picture of the surface-atmosphere interactions associated with the shrub encroachment-microclimate feedback mechanism. It is well known that boundary layer structure can be affected by differences in land cover and vertical energy fluxes (e.g., Pielke et al., 1998, Mahrt, 2000), but a documentation of this effect on the boundary layer structure in an area of shrub encroachment is currently missing. Furthermore, the observed effect can serve as a data set for the evaluation of numerical models that are used in subsequent studies related to shrub encroachment. In this study, we investigate the impact of shrub encroachment on the structure of the nighttime boundary layer using measurements of concurrent temperature profiles in shrubland and grassland. We also evaluate the performance of a single column model version of an atmospheric mesoscale model to simulate the nighttime profiles and investigate the sensitivity of the simulated profiles to planetary boundary layer (PBL) parameterization schemes and vegetation parameters.

4.2 Methods

4.2.1 Study Site and Tethered Sounding Measurements

Field experiments were conducted on the McKenzie Flats area (34.3° N 106.7° W) of the Sevilleta National Wildlife Refuge (SNWR), located in the Northern Chihuahuan desert. The area has been experiencing an abrupt encroachment of creosotebush (*Larrea tridentata*) shrubs into a grassland (Béaz and Collins, 2008; Bhark and Small, 2003). The representative shrubland and grassland locations we chose for the experiments are about 5 km apart with 10m elevation difference. Two field campaigns were performed in December 2008 and November 2011 to measure the concurrent temperature profiles in adjacent shrubland and grassland using tethered balloon systems. The system consists of a GRAW radiosonde (DFM-06) with an accuracy of 0.2C. The altitude was measured by a 20 channel GPS module in the 2008 field campaign and by an additional pressure sensor (accuracy: <1hpa) in the 2011 field campaign to make accurate measurements of the height above ground. In each field campaign, measurements were made from the surface to about 100m above ground during three clear nights with weak winds. Only data collected during the ascents are used in the analyses. We focus on the temperature profiles from the surface to 60 m above the ground which is the altitude reached by most measurements. A total of 24 and 27 concurrent measurements in adjacent shrubland and grassland sites from the 2011 and 2008 field campaigns, respectively, are used in this study. In addition, several radiosonde launches were made in both campaigns obtaining thermodynamic profiles up to about 10 km which are used to initialize the atmospheric mesoscale model.

4.2.2 Model setup

To simulate the temperature profiles, we use the Weather Research and Forecasting (WRF, Skamarock et al. 2008) model version 3.4 coupled with Noah Land Surface Model (LSM, Chen and Dudhia 2001; Ek et al. 2003; Mahrt and Ek 1984). The WRF and Noah LSM combination was used in a previous study to simulate the surface temperature differences and related energy fluxes in shrubland and grassland in SNWR (He et al., 2011). Here, we use a single column (or one-dimensional) configuration with a single vegetation type to focus on the structure of vertical temperature profile that is affected by the underlying land surface properties and boundary layer parameterizations. The model is set with 70 vertical levels (lowest temperature level at 2-3m above ground) extending from the surface to 12 km above ground. We use the same soil moisture initialization, vegetation parameter settings and LSM modifications as in He et al. (2011). In summary, the most important LSM modifications include shutting down the water fluxes because field observations showed negligible latent heat fluxes during wintertime (He et al., 2010) and changing the green vegetation fraction value from 0.8 to 0.6 for grassland and from 0.7 to 0.1 for shrubland with respect to the default parameterizations in Noah LSM. These changes in the green vegetation fraction represent the difference in land surface properties between shrubland and grassland that causes the observed higher nocturnal temperature in shrubland than in grassland (He et al., 2011). In addition, the albedo (0.2) and emissivity (0.96) are set to be the same for both land covers, whereas roughness length is set to 0.03m for grassland and 0.05m for shrubland, which correspond to the field conditions in the Chihuahuan desert (He et al., 2010). The soil moisture is set to $0.05\text{m}^3\text{m}^{-3}$ for the topmost soil layer with a thickness of 0.1 m and to $0.1\text{m}^3\text{m}^{-3}$, for the three soil layers underneath with thicknesses of 0.3m, 0.6m, and 1m,

respectively. The soil temperature is set to the initial temperature at the lowest level in the atmosphere. For an extensive discussion justifying the modified settings, we refer to He et al., (2011).

The model is initialized at 1700 local time (LT), using the temperature profile from a radiosonde that was launched over the grassland on 16 November 2011, with a constant 1 m/s westerly wind profile and 20% relative humidity profile which represents a calm condition and the typical wintertime humidity condition in the SNWR. Three PBL schemes – the Quasi-Normal Scale Elimination (QNSE) scheme (Sukoriansky et al., 2005), the Yonsei University (YSU) scheme (Hong, 2010; Hong et al., 2006) and the University of Washington (UW) scheme (Bretherton and Park, 2009) – are used in this study and their sensitivities are discussed in section 3.4. We also tried other PBL schemes, the MYJ (Mellor-Yamada-Janjic eta) scheme, the ACM2 (Asymmetrical Convective Model version 2) scheme, and the TEMF (Total Energy-Mass Flux) schemes, that are available in WRF but did not simulate the nighttime structure well. Among the three PBL schemes, the YSU scheme is a first order non-local scheme, with specified eddy-diffusivity (K) profile. Both the QNSE and UW schemes use 1.5 order local closure with prognostic turbulence kinetic energy (TKE). The YSU scheme has been updated since WRF version 3.0 to improve the stable boundary layer simulation by allowing more diffusivity. The QNSE scheme uses a novel theory that is designed to improve the stable boundary layer with considerations for internal gravity wave effects and anisotropy for diffusivity. The PBL schemes are paired with specific surface layer schemes in WRF. The YSU boundary layer scheme is paired with the MM5 Monin-Obukhov scheme (Beljaars, 1995; Dyer and Hicks, 1970) and the QNSE

boundary layer scheme is paired with the QNSE surface scheme (Sukoriansky et al., 2005). The UW boundary layer schemes can be paired with two surface layer schemes, and we use the MM5 Monin-Obukhov scheme in this study. For the simulation results in the current study, we use the QNSE scheme since it is developed specifically for the stable boundary layer and has shown improved performance in the lowest part of nocturnal boundary layer (e.g., Kilpeläinen et al., 2012; Mayer et al., 2012; Seaman et al., 2012; Sukoriansky and Galperin, 2008).

4.2.3 Cumulative temperature difference

To quantitatively study the cooling process in the shrubland and grassland, we calculated the cumulative temperature difference (CTD) from the surface to height h ,

$$CTD = -\int_0^h \Delta T dh, \quad \text{where } \Delta T = \Delta T(t, h) = T(t, h) - T_{shrub}(t_0, h), \quad \text{i.e., the temperature}$$

difference at height h between time t and t_0 (the beginning of each night) in the shrubland. The change of CTD ($dCTD/dt$), represents the cumulative cooling rate (CCR) of the layer from surface to height h through time. The choice of the reference temperature profile (i.e., $T_{shrub}(t_0, h)$) will determine the calculated value of CTD, but will not affect the CCR.

The CTD is also calculated from the simulated temperature profiles using temperature differences between the simulated temperature profile at time t and the initialization profile at 1700 LT ($\Delta T = \Delta T(t, h) = T(t, h) - T_{initialization}(t_0, h)$). The CTD is integrated from the surface level to $h=60$ m. An increasing CTD number corresponds to cooling in the lowest 60m above ground, while a decreasing number corresponds to

warming. The CTD has been used in previous studies to investigate nocturnal boundary layer cooling (e.g., De Wekker and Whiteman, 2006).

4.3 Results and Discussion

4.3.1 Observed nocturnal boundary layer profiles

The profiles of temperature differences between shrubland and grassland from all soundings are shown in Figure 4.1. The surface temperature is generally higher in the shrubland than in the adjacent grassland, which is consistent with our previous studies (He et al., 2010; 2011). On average, during the 2011 (2008) campaign, the surface temperature measured in the shrubland is 3.3 C (1.1 C) higher than in the grassland. The temperatures over shrubland and grassland become more similar with height above the surface. In fact, temperature differences between shrubland and grassland mainly exist in the lower 20m of the atmosphere, although in a few cases they extend to more than 60m. During the 2008 and 2011 field campaigns, less than 20% and 40% of the profiles, respectively, exhibit temperature differences between the two land covers larger than 1C above 20m. As a result, the key features of the differences in nocturnal boundary layer temperature between shrubland and grassland can be investigated by focusing on the lower 60 m of the temperature profile.

To demonstrate the differences in temperature structure evolution over shrubland and grassland, we show several temperature profiles during one clear night (16 November 2011) with a mean 3-m wind speed smaller than 2 ms^{-1} as observed at nearby meteorological towers (Figure 4.2). From 1900 to 2300 LT, cooling occurred in both shrubland and grassland, with occasional warming at certain heights as the night proceeded. These warming events are probably due to advection or other processes.

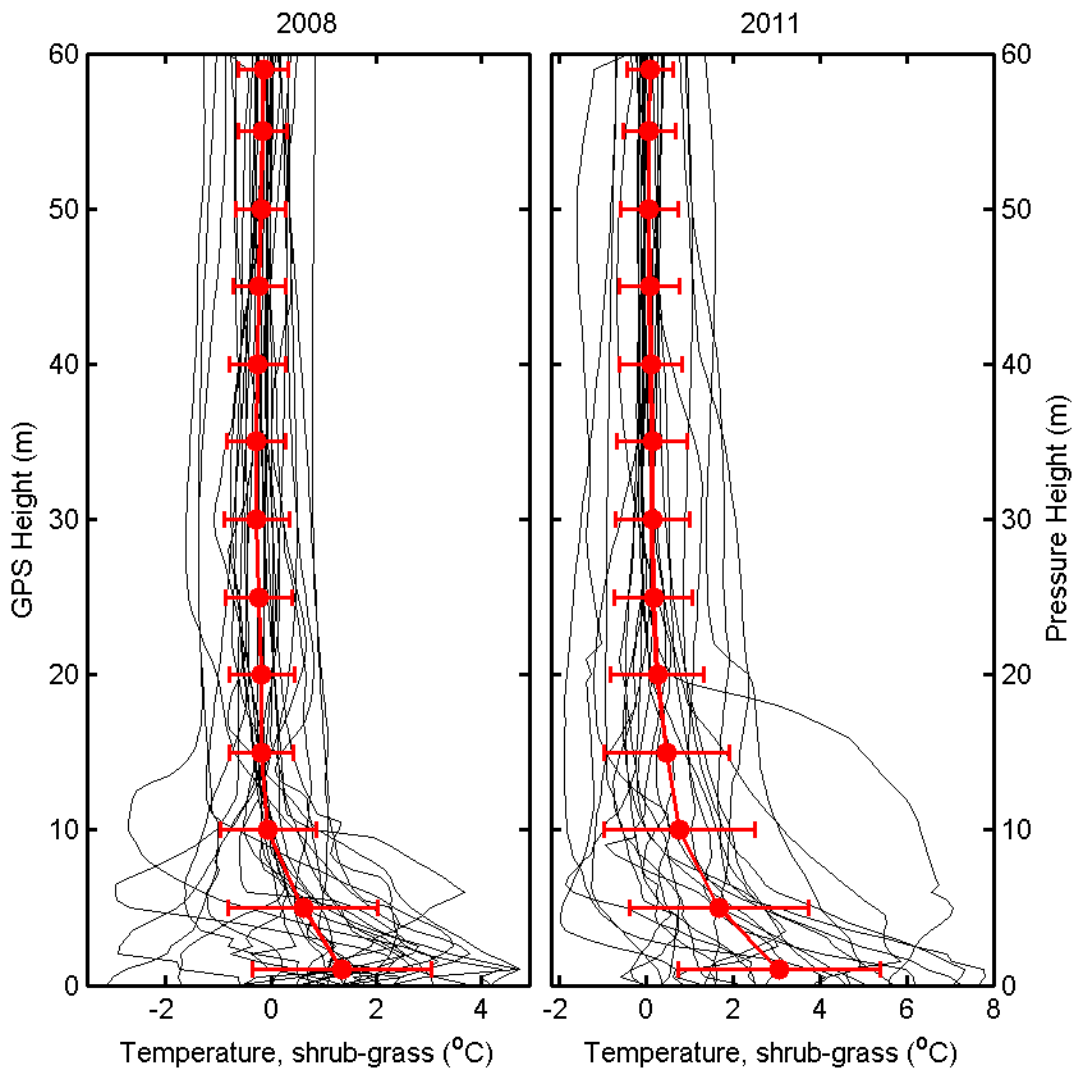


Figure 4.1 Profiles of temperature differences between shrubland and grassland (thin dash-dot lines) observed in 2008 (left) and 2011 (right). Filled circles and error bars show mean and standard deviation of temperatures in 5-m height bins.

Nonetheless, surface temperature was always lower and the surface-based temperature inversion was always stronger in grassland than in shrubland.

The observations provide clear evidence that temperature differences between shrubland and grassland become small above 20m. These temperature differences have also been observed in other cases with different land covers. For example, soundings along a 1 km transect from an open area to a forest area in Sweden show temperature

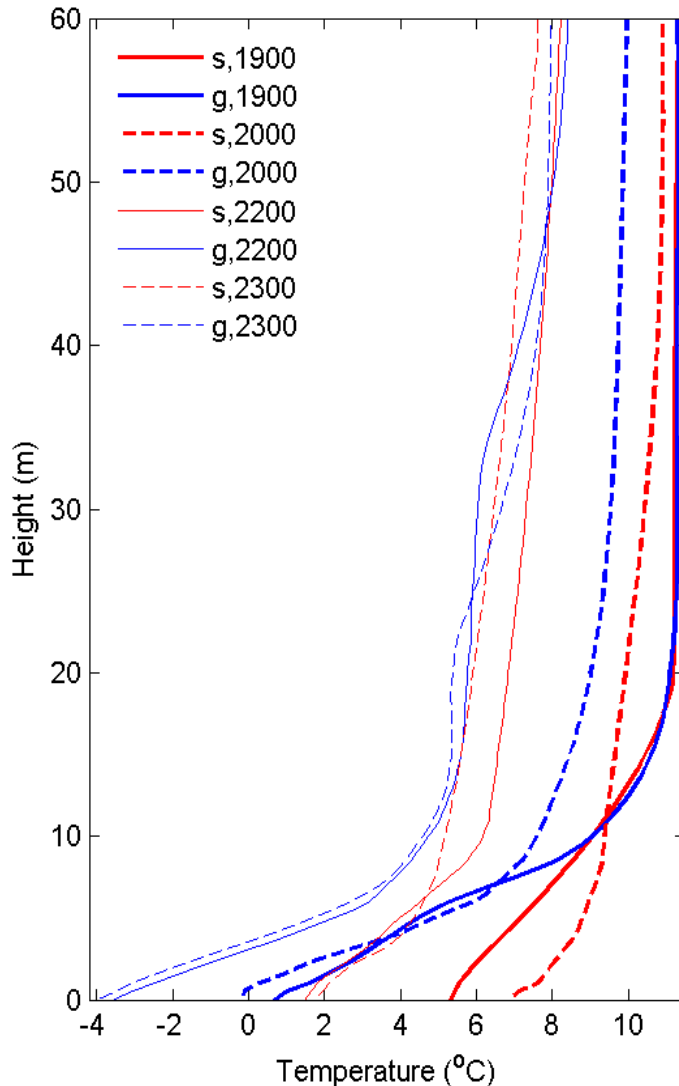


Figure 4.2 Temporal evolution of temperature profiles in adjacent shrubland (“s”) and grassland (“g”) measured in the night of 16 November 2011.

differences up to 40m above ground (about 20m above forest canopy) in a clear calm night (Karlsson, 2000). The height up to which temperature profile differences are observed depends on several factors including the scale of the landscape heterogeneity relative to the boundary layer height, and the fetch (or footprint, or “field of view”).

With respect to the scale of the landscape heterogeneity relative to the boundary layer height, previous investigations have shown that for an impact to occur, the scale of the heterogeneity needs to be at least one to two orders of magnitude larger than the

boundary layer height (e.g., Mahrt, 2000; Raupach and Finnigan, 1995; Shuttleworth, 1988) which equates to a horizontal scale of few kilometers for the nocturnal boundary layer. This size is easily achieved by the scale of landscape of either shrubland or grassland at SNWR. Estimated nocturnal boundary layer heights at 2200 to 0000 LT from available radiosonde data during our experiments ranged from about 100 to 300 m. Temperature differences over grassland and shrubland are therefore confined to about 10-20% of the nocturnal boundary layer height.

The height up to which temperature profile differences are noticeable also depends on the horizontal scale of the fetch. The fetch considers the extent of the source area that impacts the measurement, which varies with stability, surface roughness, observational height (e.g., Hsieh et al., 2000), and also surface heterogeneity (e.g., Göckede et al., 2006). Typically, a reasonable estimate of the fetch is about hundred times the observational height, with a larger fetch for stable condition (Horst and Weil, 1994; Leclerc and Thurtell, 1990). This would mean that the fetch that affects the temperature at about 20m above ground is on the order of a few kilometers, which is comparable to the distance between the shrubland and grassland sites. As a result, it is likely that the source areas of the temperature measured at this level over shrubland and grassland consist of one vegetation cover (either shrubland or grassland depending on the wind direction) so that the temperature difference at and above this level becomes less noticeable. Thus, while the observed near-surface temperature difference is driven by the direct underlying land surface at local scale, at higher levels with increasing wind speeds and larger footprints (e.g. Horst and Weil, 1992; Leclerc and Thurtell, 1990), the influence from the local surface becomes smaller and continues to decrease with height.

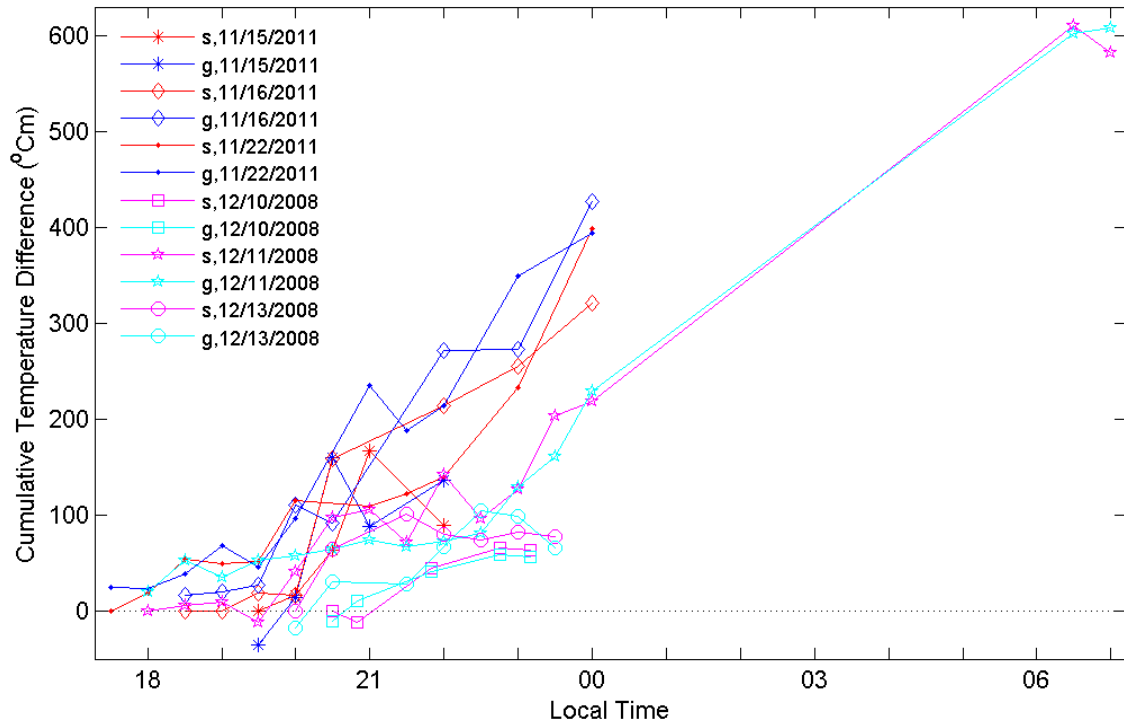


Figure 4.3 Observed cumulative temperature differences (CTD) from surface to 60m in adjacent shrubland (“s”) and grassland (“g”). CTD is calculated relative to the sounding in shrubland at the beginning of each nighttime period (see text).

Changing the locations of the vertical profile measurements may also change the extent of vertical temperature difference. As we move the locations further apart and each location is surrounded by a larger area of grassland or shrubland, the extent of the temperature differences will increase based on our considerations of the fetch. For example, studies of late afternoon soundings in a same irrigated field and surrounded arid landscape have observed temperature differences up to 10-15 m for sounding locations about 200m apart, and up to about 20-30m above ground with locations 450m apart (Hippis and Zehr, 1995; Prueger et al., 1996). On the other hand, possible thermally driven circulations induced by horizontal temperature differences between the shrubland and the grassland (He et al., 2011) can make the horizontal temperature differences in the boundary layer smaller.

CTD calculations are made to study the differences in integrated cooling between the grassland and the shrubland in the lower atmosphere throughout the night (Figure 4.3). On 11 December 2008, measurements were taken for the entire night from right after sunset (1800 LT) to sunrise the following day (0700 LT). While the general trend is always cooling, some warming occurs occasionally during all 6 nights in either the shrubland or the grassland. The CTD is sometimes smaller over the grassland than the shrubland, which indicates that there is actually less cooling over the grassland than over the shrubland in the lowest 60m. 21 out of the 51 available profiles show this feature. However, only 7 concurrent profiles show higher surface temperature in the grassland than in the shrubland. These results confirm that the higher nighttime temperature in the shrubland than in the grassland occurs only in the near surface layer. The measurement on 16 and 22 November 2011 are further used here to study the CCR. Typically, cooling happens faster a few hours after sunset than later in the course of the night, which results in a non-linear CCR throughout the whole night (e.g. De Wekker and Whiteman, 2006; Pielke and Matsui, 2005). For example, the exponential function of CTD can be expressed as $CTD = A - B \exp(-t/\tau)$, where t is the time since the onset of cooling, τ is a fitting parameter which is the time required for the cooling to attain 63.2% of total cooling of the night, and A and B are case specific constants (e.g., De Wekker and Whiteman, 2006). However, the short measurement period in our cases (5.5 and 6.5 hours) compared to 13 to 14 hours of cooling during a winter night, does not provide enough data for a reasonable exponential fitting. Therefore, we use a linear fit to estimate the CCR using $CTD = A + Bt/\tau$ where B is the CCR. In this study, the estimated CCR over shrubland (grassland) is 64 Cm/hr (75 Cm/hr) on 16 November 2011 and 50 Cm/hr

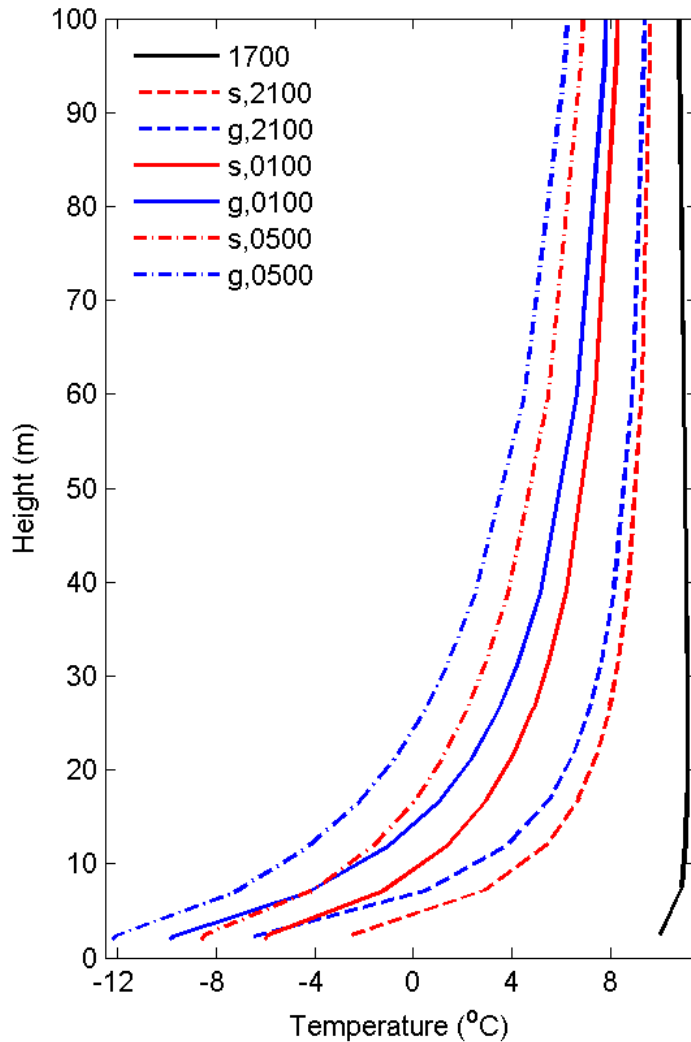


Figure 4.4 The initialization (1700 LT) and simulated temperature profiles over shrubland (“s”) and grassland (“g”) at the different times during the night of 16 November 2011 using the QNSE PBL scheme.

(61 Cm/hr) on 22 November 2011. On both days, the grassland cools faster than the shrubland in the lowest 60m.

4.3.2 Simulated nocturnal boundary layer profiles

WRF is able to simulate the higher surface temperature and weaker near-surface inversion over the shrubland than over the grassland (Figure 4.4). The simulated temperature differences between the two land covers extend to a higher level than in the

observations. One should realize, however, that in the single column model, there is no advection and the temperature profiles are only affected by vertical energy exchange. While temperature differences between grassland and shrubland persist at higher levels, these differences are much smaller than those near the ground. Mean nighttime temperature differences between grassland and shrubland at around 100m (10th vertical level) and 40m (8th level) are only 11% and 25%, respectively, of the temperature differences simulated at the first vertical level (2-3m). These temperature differences are similar for the simulations with the different PBL schemes (the sensitivities will be discussed later). The simulated surface temperature is lower than the observed temperature (compare Figs 2 and 4). This results in a stronger and deeper temperature inversion in the simulations which is another reason why the simulated temperature differences extend up to a larger height than the observed differences. Simulated nighttime temperatures are oftentimes too low related to issues with the decoupling of the surface layer from the boundary layer in stable conditions in numerical modeling (e.g., Derbyshire, 1999). Despite the inherent limitations of the single column model, the simulated temperature differences with largest differences near the ground are in agreement with the observations. Daytime temperature profiles over shrubland and grassland are almost identical in the simulations. Similar results have been reported for different urban settings using idealized numerical modeling in which nocturnal temperature differences were confined to the lowest 100m of the boundary layer (Harman and Belcher, 2006).

The CTD is also calculated from the simulated temperature profiles (Figure 4.5). The CTD in grassland is always larger than in the shrubland with differences increasing

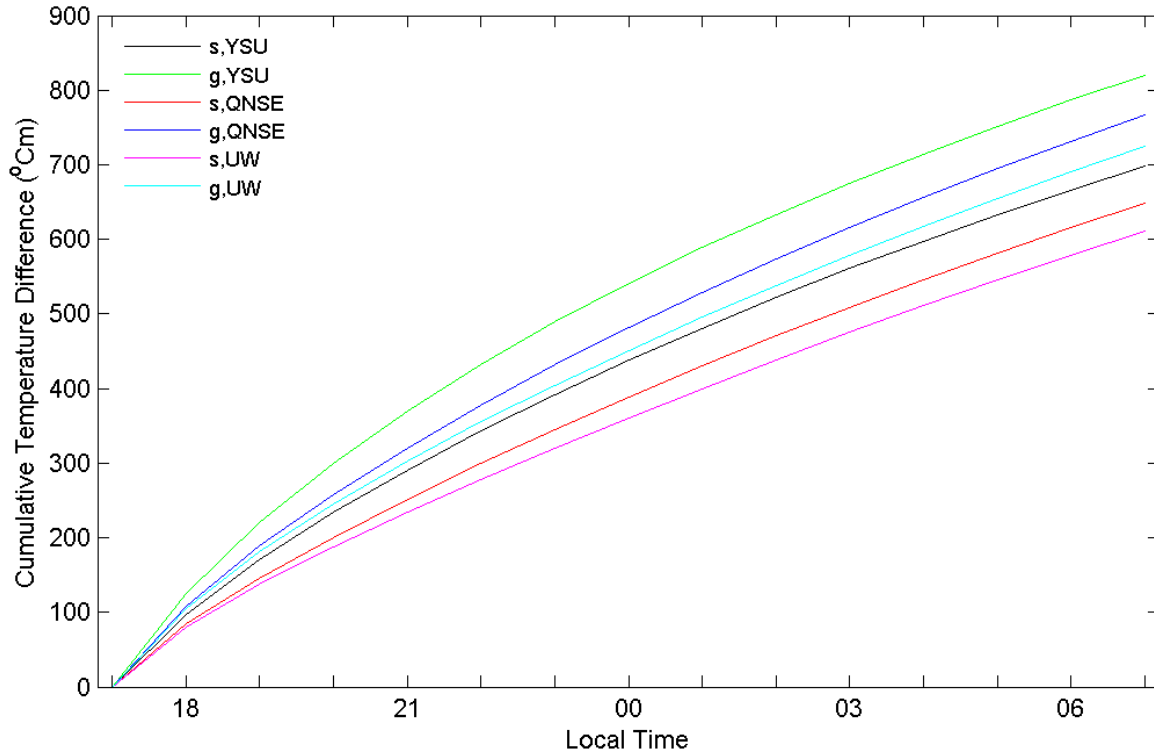


Figure 4.5 Simulated cumulative temperature differences (CTD) from surface to 60m in shrubland (“s”) and grassland (“g”) using three PBL schemes (YSU, QNSE, and UW). CTD is calculated relative to the initial profile at 1700 LT.

up to about 100 Cm by the end of the night. The CCR from 1800 to 0000 LT (about the same time period as for the observational estimates) ranges from 47-51 Cm/hr and 58-69 Cm/hr in shrubland and grassland, respectively. These values agree well with the observed values. The CCR in shrubland and grassland becomes similar after midnight. The difference in CTD between shrubland and grassland increases only by around 20 Cm from 0000 LT to 0600 LT for all PBL schemes. As a result, the difference in CCR between shrubland and grassland is only 3-4 Cm/hr on average after midnight, compared to 11-18 Cm/hr before midnight.

Sensitivity to model configuration

To assess the sensitivity of the simulations to the model configuration, we perform a number of simulations with different settings. We focus on the differences of simulated temperature profiles, CTD, 2m temperature, and energy fluxes between shrubland and grassland. We find that the general pattern and magnitude of simulated surface temperature differences and temperature profiles are not sensitive to the initial temperature profile, humidity profile, wind speed, soil temperature or soil water content, similar to the sensitivity tests using the 2D model (He et al., 2011). The 2m temperature differences between shrubland and grassland during subsequent nights in a simulation that lasts more than 24 hours are larger by about 0.5 to 1.5C, or 14% to 36% in relative magnitude, than the first night depending on the PBL scheme. These differences become smaller with height and are negligible above 40m. Moreover, adding more vertical levels near the ground results in a stronger near-surface inversion in the simulations, but does not affect the simulated temperature profiles qualitatively. The configuration with the larger vertical resolution near the ground is used in the sensitivity simulations discussed next.

Sensitivity to PBL schemes

The selection of PBL scheme and paired surface layer scheme is an important consideration for investigating the evolution of temperature profiles and has in previous studies shown to have an impact on the model performance in different cases and conditions (e.g., Shin and Hong, 2011; Yver et al., 2013). Similar to previous studies, the simulation results is affected by the choice of PBL scheme. For example, using MYJ, ACM2 scheme and TEMP schemes result in either too weak or unrealistically strong

nocturnal inversions, or too large daytime temperature difference between shrubland and grassland. On the other hand, the three PBL schemes used in this study, the QNSE, YSU and UW schemes, represent the temperature profiles in the northern Chihuahuan desert well. We further study the model sensitivity to those three PBL schemes and they only produce slight differences in the simulated temperature differences between shrubland and grassland. For example, the UW scheme simulates higher and the YSU scheme simulates lower nighttime near-surface temperatures than the QNSE scheme. Therefore, compared to the QNSE scheme, the CTD and CCR is larger with the YSU scheme and smaller with the UW scheme (Figure 4.5).

Sensitivity to vegetation parameters

He et al. (2011) studied the sensitivity of the 2m temperature to the vegetation parameters. Here, we focus on the sensitivity of the lowest part of boundary layer using the CTD. We use values for the green vegetation fraction, albedo, emissivity and roughness length that are based on the situation in SNWR, while we use the default values for other vegetation parameters. These four vegetation parameters and specifically the green vegetation fraction, are the important parameters that affect the surface temperature differences between the two land covers (He et al., 2011). Since the albedo and emissivity are the same in shrubland and grassland, the differences between the shrubland and grassland vegetation types come from the different values of the green vegetation fraction, roughness length and some other parameters (i.e., the minimum stomatal resistance and a parameter used in the vapor pressure deficit function). By changing the values of those vegetation parameters, we can essentially change the vegetation cover from shrubland to grassland in the model and investigate the sensitivity

| Settings | Parameters | | | ΔT of lowest 10 levels from 1800 to 0600 LT (°C) | | | | | | ΔT_2 at 0000 LT (°C) | | | ΔCTD at 0000 LT (°Cm) | | |
|----------|------------|----|-------|--|------|-------|------|-------|------|------------------------------|-------|-------|-------------------------------|------|------|
| | gvf | z0 | other | YSU | | QNSE | | UW | | YSU | QNSE | UW | YSU | QNSE | UW |
| S-G | ✓ | ✓ | ✓ | 1.7 | 4.2 | 1.5 | 4.0 | 1.4 | 4.2 | 4.1 | 3.9 | 4.1 | -103 | -93 | -91 |
| I1-G | | ✓ | ✓ | <-.01 | 0.02 | 0.02 | 0.2 | 0.03 | 0.3 | 0 | -0.1 | 0.4 | 0 | 0.9 | -2 |
| I2-G | | | ✓ | <-.01 | 0.02 | <-.01 | 0.03 | <-.01 | 0.04 | 0 | -0.01 | -0.02 | 0 | 0 | 0.08 |

Table 4.1 The mean and maximum absolute differences in temperature ($|\Delta T|$) of the lowest 10 levels (about 100m) from 1800 to 0600 LT, the difference in 2m temperature (ΔT_2) and CTD (ΔCTD) at 0000 LT between a simulation with a particular vegetation setting (S, or I1, or I2) and a simulation with grassland (G). For vegetation parameters, gvf is green vegetation fraction; z0 is roughness length; “other” stands for all parameters other than green vegetation fraction, roughness length, albedo and emissivity. A check mark (“✓”) in the “parameter” boxes indicates that a vegetation parameter was changed relative to the vegetation setting for grassland.

of the simulated temperature differences between shrubland and grassland to the green vegetation fraction and roughness length. Four tests were carried out: shrubland (S); Intermediate state 1 (I1): shrubland with green vegetation fraction of grassland; Intermediate state 2 (I2): shrubland with green vegetation fraction and roughness length of grassland; and grassland (G). The absolute value of the temperature differences ($|\Delta T|$) in the lowest 10 vertical levels, the difference in 2m temperature (ΔT_2) and the CTD (ΔCTD) at 0000 LT, between S, I1, I2 and G are calculated (Table 4.1).

Results suggest that the simulations are almost the same for simulations with vegetation settings I1, I2 and G and are different from a simulation with vegetation setting S (Table 4.1). On average, the temperatures changes (for all $|\Delta T|$, ΔT_2 and ΔCTD) in the nocturnal boundary layer as a result of changing the green vegetation fraction (comparing S-G with I1-G) are two or even more orders of magnitude larger

compared to changing the roughness length and/or other vegetation parameters (I1-G, or I2-G, or comparing I1-G with I2-G). These results suggest that the green vegetation fraction is the most crucial parameter controlling the temperature differences not only at the surface, but also at higher levels above the shrubland and grassland covers. For the nocturnal simulation discussed here, the smaller green vegetation fraction causes a warmer night by allowing a larger energy release from the ground. In addition, the sensitivity to the three different PBL schemes is small. Changing the green vegetation fraction (comparing S-G with I1-G) causes the largest differences in $|\Delta T|$, ΔT_2 and ΔCTD for the YSU scheme, while changing the vegetation parameters other than green vegetation fraction (I1-G and I2-G) causes the largest difference for the UW scheme and the smallest difference for the YSU scheme (for all $|\Delta T|$, ΔT_2 and ΔCTD , Table 4.1).

4.3 Summary and conclusion

Summarizing the findings from our observations and from single column model simulations, along with the knowledge from previous studies, we present how temperature profiles are expected to develop in shrubland and grassland under clear and calm condition. Around sunset, adjacent shrubland and grassland have an almost identical neutral temperature profiles (Figure 4.6A). The grassland cools down faster than the shrubland, which results in a stronger inversion after sunset (Figure 4.6B). As the cooling continues, the height of the stable boundary layer increases. The surface temperature difference between shrubland and grassland persists throughout the night and the grassland maintains a stronger near-surface temperature inversion (Figure 4.6C). Differences in land cover and related land-atmosphere interactions are the driving force leading to differences in air temperature, which mainly influences the near surface

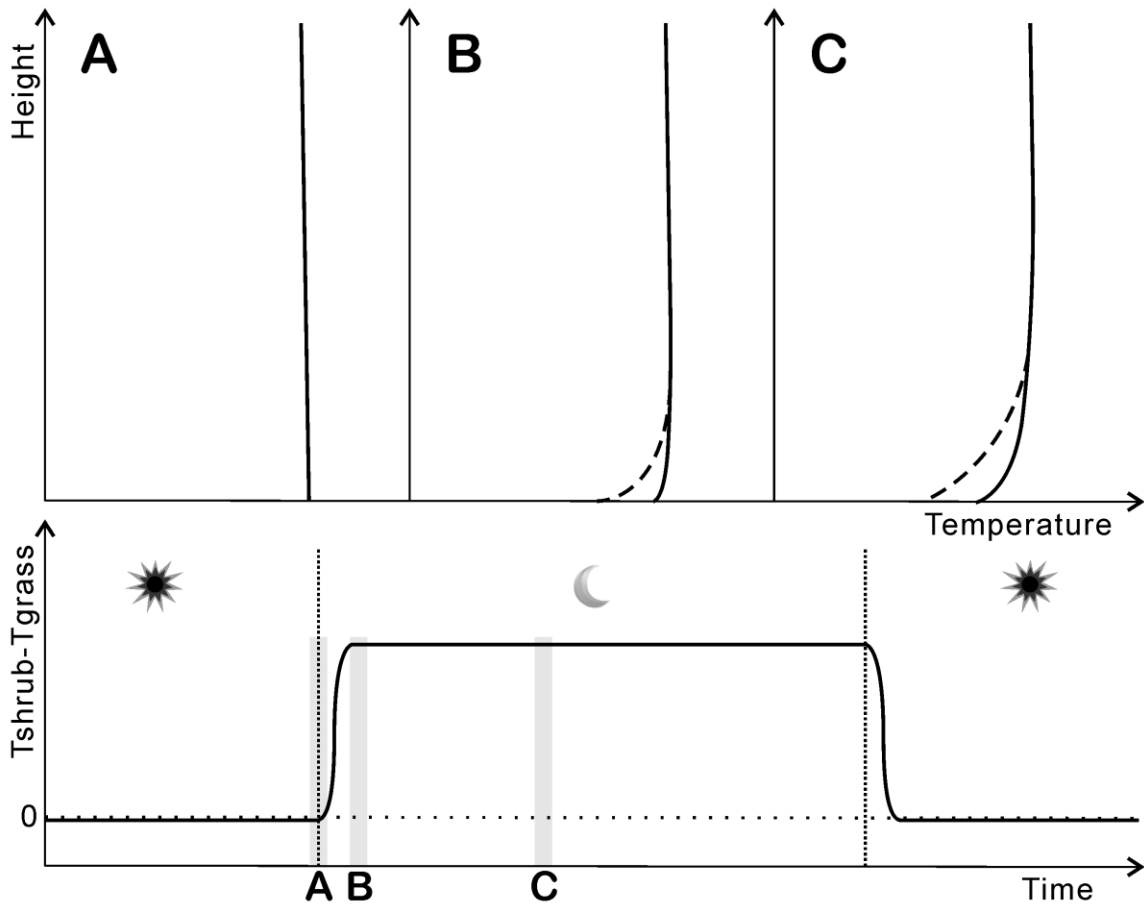


Figure 4.6 Schematic nighttime temperature profiles (upper figure) in shrubland (black line) and grassland (grey line), and near-surface air temperature differences between shrubland and grassland (bottom figure) in clear and calm wind conditions. A is around sunset, B is right after the establishment of the air temperature difference between shrubland and grassland, and C is some time later during the night.

portion of the boundary layer (up to about 20m above ground). The effects of heterogeneities in land surface properties in an area affected by shrub encroachment weaken with height above the surface and temperature differences are negligible above 20 m.

Sensitivity studies with a single column model suggest that the YSU, QNSE and UW PBL schemes can simulate well the difference in nocturnal temperature profiles

between shrubland and grassland. Major features of the temperature difference are not sensitive to the choice of the PBL scheme. The controlling factor in establishing and maintaining the vertical temperature difference between shrubland and grassland is the green vegetation fraction.

The improvements of the simulation of temperature profiles and near-surface temperature that have resulted from the sensitivity studies of PBL schemes in the current study and from two-dimensional investigations in a previous study (He et al., 2011) benefits future three-dimensional numerical studies of areas affected by shrub encroachment using WRF. In a subsequent study, we will use the QNSE PBL scheme with the modified vegetation parameters in three-dimensional WRF simulations to investigate the effects of different vegetation distributions on winter minimum temperature and on the survival probability of juvenile shrubs in SNWR (He et al., submitted).

CHAPTER 5

THE RELATIVE IMPORTANCE OF CLIMATE CHANGE AND SHRUB ENCROACHMENT ON NOCTURNAL WARMING IN THE SOUTHWESTERN U.S.³

5.1 Introduction

Over the past 150 years the southwestern U.S. (as well as many other drylands worldwide) have undergone major changes in vegetation cover resulting from the encroachment of woody plants into desert grasslands (Alan K. Knapp et al., 2008; Van Auken, 2000). This transition has an impact on soil moisture dynamics as well as on the energy exchange between the land surface and the atmosphere (Bhark and Small, 2003; Dugas et al., 1996; Kurc and Small, 2004). The conversion from semiarid grassland to shrubland in the northern Chihuahuan desert shrubland is typically associated with an increase in the bare soil fraction (e.g., D’Odorico et al., 2012) and has (on average) a pronounced nocturnal warming effect of ~2K in wintertime (He et al., 2010). This effect is potentially very important in the winter season when *Larrea tridentata*, a woody species native to North America’s southwestern deserts and one of the two predominant encroaching woody species in the region, remains non-dormant and is thus sensitive to freeze-induced mortality (Medeiros and Pockman, 2011; Pockman and Sperry, 1997). Therefore, a positive feedback between shrub encroachment and winter minimum temperatures may further promote shrub establishment in this region (D’Odorico et al., 2010). Similar feedbacks have been reported for other grassland-to-woodland transitions,

³ In press in International Journal of Climatology: He, Y., D’Odorico, P., De Wekker, S.F.J., 2014. The relative importance of climate change and shrub encroachment on nocturnal warming in the southwestern United States. International Journal of Climatology, in press

where nocturnal warming induced by the encroachment of woody plants favors the survival of cold sensitive trees and shrubs, thereby further enhancing their encroachment (D'Odorico et al., 2013). This feedback process is particularly affected by minimum temperatures because they are directly associated with episodes of freezing induced mortality. The nocturnal warming induced by shrub encroachment in the southwestern U.S. is particularly intense in cold winter nights (D'Odorico et al., 2010). It is still unclear how in this region the warming resulting from the grassland to shrubland conversion compares with the temperature increase induced by large scale drivers of global and regional climate change.

Climate change studies indicate that the global temperatures are expected to keep increasing for the next several decades as a result of fossil fuel emissions as well as abiotic and biotic feedbacks (IPCC, 2007). These warming trends vary geographically with time of the day and season, and are particularly strong for nighttime temperatures. In fact, over the last 50 years nocturnal temperatures have increased twice as much as daytime temperatures (Houghton et al., 2001). Moreover, cold extremes exhibit a more rapid warming (by about 25% over landmass and 30-40% globally) than warm extremes (Kharin et al., 2007). In most of North America, warming is expected to exceed the global mean (IPCC, 2007), especially in the southwestern U.S. (Leung et al., 2004; Seager et al., 2007), which have become warmer and drier more rapidly than the rest of the continental U.S. since the mid-1970s (Williams et al., 2010). These regional climate trends in the deserts of the southwestern U.S. have never been compared to changes in nocturnal microclimate that could result from shrub encroachment. Such a comparison will provide new insights into the importance of the warming induced by changes in

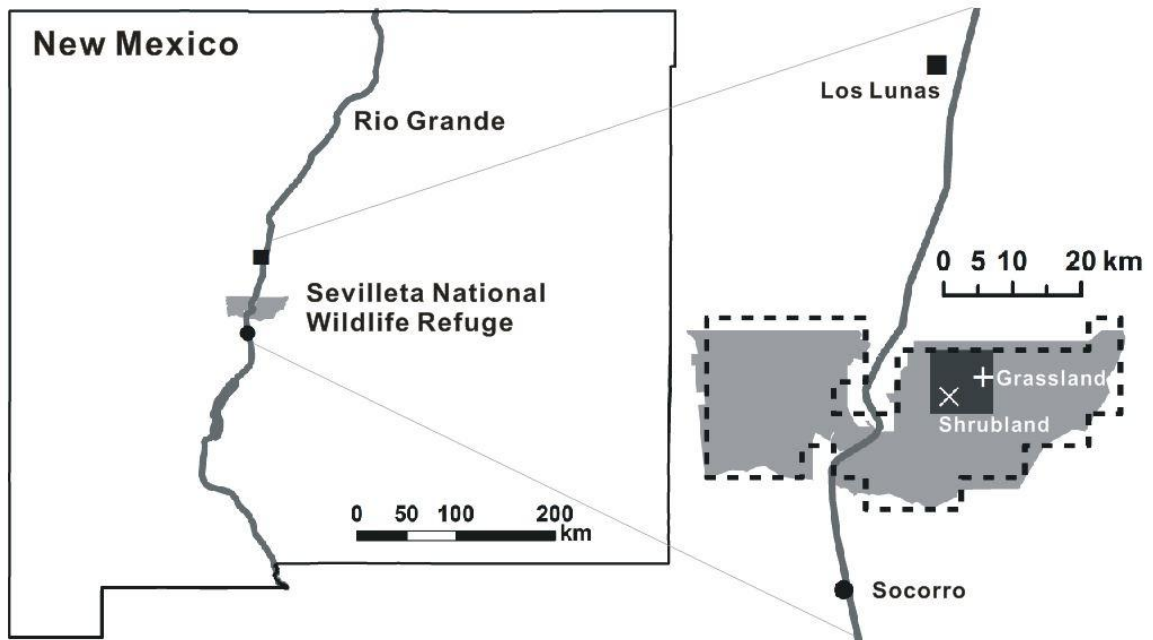


Figure 5.1 Locations of the SNWR (light grey shaded area) in New Mexico, the shrubland (white x symbol) and grassland (white cross symbol) sites at SNWR, and Los Lunas (black square symbol) and Socorro (black circle symbol) USHCN stations located along the Rio Grande (grey line) valley. Also shown are the areas of PRISM grid cells encompassing the McKenzie Flats (dark grey shaded area) and the SNWR (area indicated by the dashed line).

vegetation with respect to the regional effects of climate change. Here we use historical records, regional climate model simulations, and temperature measurements at adjacent grassland and shrubland sites in the northern Chihuahuan desert to compare the nocturnal warming resulting from land cover change with the background temperature trends in the regional climate.

5.2 Methods

The concurrent temperature measurements used in this study were from adjacent shrubland (34.3349° N, 106.7442° W, elevation: 1593m) and grassland (34.3623° N, 106.7019° W, elevation: 1622m) sites in the McKenzie Flats area of the Sevilleta National

Wildlife Refuge (SNWR), located in the northern Chihuahuan desert, New Mexico (Figure 5.1). SNWR has undergone an abrupt change in vegetation cover with an encroaching front of *Larrea tridentata* shrubs into a desert grassland (S. Báez and Collins, 2008; Bhark and Small, 2003). Thus, this area provides an ideal location to monitor the microclimate conditions in adjacent sites with woody and herbaceous vegetation located within a distance of a few kilometers (~5km). Temperature measurements between 2007 and 2010 (at 3m above ground) were obtained from the Ameriflux network (ameriflux.ornl.gov). All data were recorded as thirty minute averages. Only days on which daily minimum temperature observations were available for both the shrubland and grassland sites were used (>90% of all observations).

The longest temperature record for the SNWR is available at the Deep Well station (34.3592° N, 106.7358° W, elevation: 1600m), which is located in the grassland area of the McKenzie Flats. The meteorological tower is operated by the Sevilleta Long Term Ecological Research (LTER, <http://sev.lternet.edu>) and data are available from 1987 onwards. We used the data from December 1989 onwards after the temperature sensor moved to a height of 2.5 m above ground level. A total of 23 winters from 1990 to 2012 were used here to study the local climate warming at SNWR in recent decades.

Long-term historical temperature records in the southwestern U.S. were obtained from the U.S. Historical Climatology Network (USHCN) version 2 serial monthly dataset (Menne et al., 2009). We analyzed the temperature data from Los Lunas (34.7675° N, 106.7611° W, elevation: 1475m) and Socorro (34.0828° N, 106.8831° W, elevation: 1398m) from 1894 onwards, which are the closest USHCN stations to the SNWR (48 km north and 31 km south, respectively) along the Rio Grande valley (Figure 5.1). The USHCN

dataset uses a “pairwise” homogenization algorithm (Menne and Williams, 2010) to effectively minimize the impacts of urbanization and other factors on the historical temperature record (Menne et al., 2010). Nevertheless, the areas (< 1km in radius) around those two stations are mainly covered by non-urban land use types identified on the 2001 National Land Cover Dataset (Homer et al., 2007). Thus, the warming due to urbanization is not expected to affect the analysis of temperature trends based on these two stations from the USHCN.

A gridded climate data set based on station data and the Parameter-elevation Relationships on Independent Slope Model (Daly et al., 2002) available from 1895 onwards, was used to estimate the historical climate warming in the SNWR area for a time period of over one century. PRISM calculates a climate-elevation regression for each DEM (digital elevation model) grid cell and improves the spatial interpolation particularly in complex terrain (Daly et al., 2008). With a resolution of 2.5' for monthly climate data, in New Mexico each PRISM grid cell covers an area of about 21km². In this study, we examined both the area around the encroaching front on the McKenzie Flats (transition between shrubland and grassland, 4 grid cells), and also the entire SNWR (53 grid cells, Figure 5.1).

Future climate change scenarios were based on model simulations from the North American Regional Climate Assessment Program (Mearns et al., 2009, p. 2). NARCCAP provides high spatial resolution (50km×50km) climate simulations for North America for both past (1970s-1990s) and future (2040s-2060s) conditions under the SRES A2 emission scenario (Nakicenovic et al., 2000). A2 is a high emission scenario, which refers to the case of a diverse world with relatively self-reliant economic regions, slow

technological development and large population. NARCCAP uses a number of model combinations based on 4 Atmosphere-Ocean General Circulation Models (AOGCMs) coupled with 6 Regional Climate Models (RCMs). The results from 11 available combinations were processed and analyzed to reduce the bias caused by individual models. We used 4 grid cells closest to the McKenzie Flats, the location of which slightly varies in the different model combinations due to different domain settings and projections. Monthly mean minimum temperature was obtained using the daily minimum temperature output, which was calculated from instantaneous surface temperatures at different time intervals ranging from every 100 seconds to 3 hours from 0600 UTC to 0600 UTC in different model combinations (see the caption of Table 5.1 for details). The monthly minimum temperature data were excluded in this study if 1/3 or more (10 days or more) data were missing within one month (<1% of all winter months).

Because of the sensitivity of *Larrea tridentata* shrubs to freezing temperatures, we focused on winter minimum temperature. The winter of a year is defined as the January and February of that year and December of the previous year. Specifically, we used the average minimum temperature of the coldest month (hereafter referred to as “minimum winter temperature”) in one winter, to study the changes in winter minimum temperature.

5.3 Results

5.3.1 Winter minimum temperature change caused by shrub encroachment

Data recorded at the shrubland and grassland sites from 2007 to 2010 show that the shrubland has a higher minimum temperature than the adjacent grassland throughout the year (Figure 5.2). On average, in 2007-2010 the daily minimum temperature in winter

months in the shrubland was 1.8 K warmer than in the grassland. The daily minimum temperature occurred during nighttime or near dawn in both the shrubland and the grassland during the 12 winter months, except for 5 cases in which daily minimum temperature was observed during daytime. Therefore, such higher daily minimum temperature is closely associated with the nighttime warming in the shrubland. The differences in the minimum winter temperature between shrubland and grassland in the winters of 2008, 2009 and 2010 were 2.5 K, 2.6 K and 0.7 K, respectively.

5.3.2 Historical minimum winter temperature change

The minimum winter temperatures for the grassland site at SNWR and the nearest USHCN stations in central New Mexico are shown in Figure 5.3. General warming trends occurring over the last two decades in the grassland areas at SNWR are consistent with the longer temporal trends in central New Mexico: both Socorro (0.009 K/year) and Los Lunas (0.014 K/year) have been experiencing an increase in winter minimum temperature. Because of the lack of long-term observations in the investigation area, we use PRISM to analyze the historical climate change in the SNWR over a time scale of more than one century. In the McKenzie Flats, the minimum winter temperature shows clearly a warming trend over the past 116 years (Figure 5.3). The estimated increase in the minimum winter temperature in the McKenzie Flats is 0.025 K/year, which is slightly larger than the minimum temperature increase in the whole SNWR (0.013 K/year).

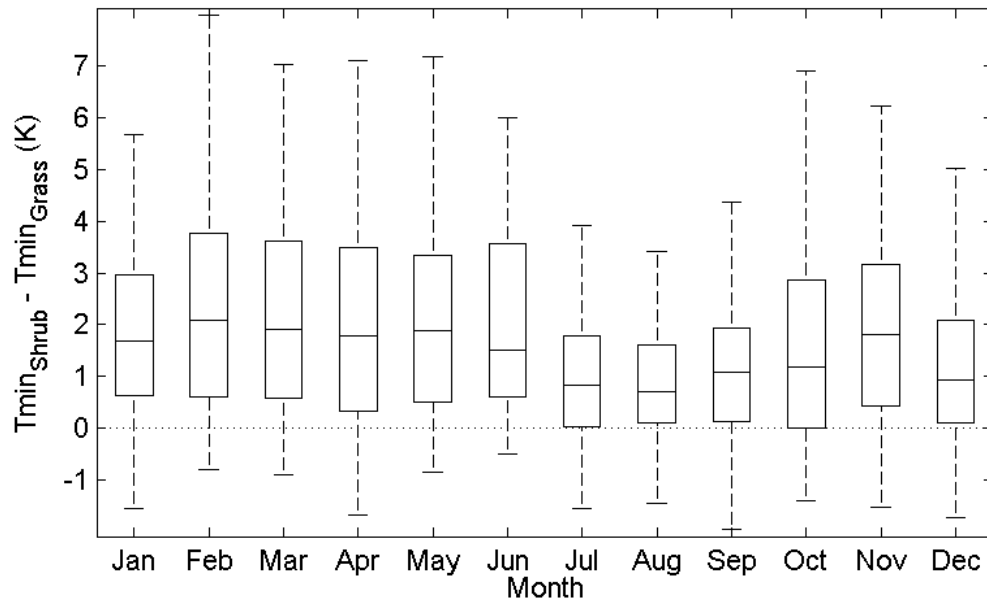


Figure 5.2 box and whisker plot for differences of minimum temperatures between shrubland and grassland for 2007 to 2010.

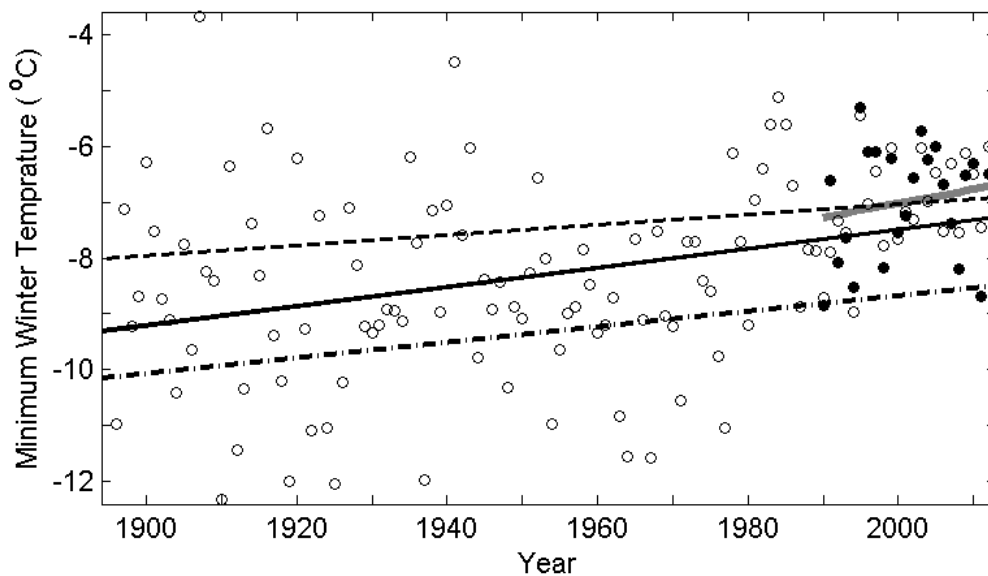


Figure 5.3 Historical minimum winter temperature for the grassland site and McKenzie Flats area at SNWR and at two UHSCN stations in central New Mexico. Shown are the observations from Sevilleta LTER at the deep well station (closed circles and corresponding solid grey trend line, data from 1990 to 2012), PRSIM data for McKenzie Flats (open circles and corresponding solid black trend line, data from 1896 to 2012). Data from the two USHCN stations are shown as trend lines for Los Lunas (dash-dot line) and for Socorro (dashed line, data from 1894-2013).

| Models | AOGCM | CCSM | CGCM3 | GDFL | GDFL | HadCM3 | CCSM | HadCM3 | CGCM3 | GDFL | CCSM | CGCM3 |
|------------------------|-------|------|-------|------|------|--------|------|--------|-------|------|------|-------|
| RCM | CRCM | CRCM | CRCM | ECP2 | HRM3 | HRM3 | MM5I | MM5I | RCM3 | RCM3 | WRFG | WRFG |
| Temperature change (K) | 1.5 | 3.0 | 3.0 | 3.0 | 2.2 | 2.7 | 2.4 | 3.8 | 3.0 | 2.2 | 2.3 | 1.6 |

The full names of the AOGCMs and RCMs are: CCSM (Community Climate System Model version 3), CGCM3 (Canadian Global Climate Model version 3), GDFL (Geophysical Fluid Dynamics Laboratory Climate Model version 2.1), HadCM3 (Hadley Centre Climate Model version 3), CRCM (Canadian Regional Climate Model), ECP2 (Experimental Climate Prediction Center Regional Spectral Model, updated version), HRM3 (Hadley Regional Model 3), MM5I (MM5 – PSU/UCAR Mesoscale Model), RCM3 (Regional Climate Model version 3), and WRFG (Weather Research and Forecasting Model with Grell convective scheme). The daily minimum temperatures are calculated using surface temperatures of every 100 seconds for GDFL/ECP2, every 2 minutes for CCSM/MM5I and HadCM3/MM5I, every 5 minutes for GDFL/HRM3 and HadCM3/HRM3, every 15 minutes for CCSM/CRCM and CGCM3/CRCM, every hour for CCSM/WRFG and CGCM3/WRFG, and every 3 hours for CGCM3/RCM and GDFL/RCM3. Because of missing data, the following months are excluded in the calculation: CGCM3/RCM3: Dec 2068; CCSM/WRFG: Dec 2053; CGCM3/WRFG: Dec 2040, Dec 2045, Dec 2050, Dec 2055, Dec 2060, Dec 2065.

Table 5.1 The average increase in the minimum winter temperature over a 70-year period from current (1969-1999 or 1969-2000, depending on the model combinations) to future (2039-2069 or 2039-2070) using the output of 11 AOGCM and RCM combinations from NARCCAP. These temperature changes are calculated using temperature values obtained as means of the 4 grid points closest to the encroaching front at SNWR.

5.3.3 Future minimum winter temperature change from regional climate simulations

Simulations by all climate model combinations from NARCCAP show an increase in minimum winter temperatures in the future. However, the magnitude of the increase varies among the different model combinations (Table 5.1), ranging from 1.5 to 3.8 K over a time period of 70 years. The median of temperature changes from past to future conditions is very close to the mean value. On average, there is a 2.5 K increase in the minimum winter temperature in the area around SNWR over the same 70 year period (1970s-1990s to 2040s-2060s).

5.4 Discussion

In the SNWR area the long term warming trend in minimum winter temperature is estimated to range between 0.015 and 0.017 K/year in the historical PRISM data (Table 5.2). Using the first and third quartile of 11 NARCCAP model combinations to exclude extreme values, the future warming trend in climate model outputs is slightly higher, varying from 0.031 to 0.043 K/year (Table 5.2). The minimum winter temperature trend at the Deep Well station for the past two decades is stronger than the long-term trend in the PRISM data for the SNWR, which could be associated with the large difference of the time period used in the estimation. In fact, grid point to site comparison indicates that the monthly averaged minimum temperature in winters from PRISM correlates well with the temperature measured at the Deep Well station ($r=0.9135$, $p<0.0001$) and also with the two USHCN stations (Los Lunas: $r=0.8733$, $p<0.0001$; Socorro: $r=0.9134$, $p<0.0001$). Despite the simplicity of the linear regression trend (Karl et al., 2000) and the dependency of such trend on the time period used to fit the regression line (Easterling and

| Temperature Change Induced by Shrub Encroachment | | | | | | |
|--|---------------------------|----------------------------------|------------------------|----------------------------|-----------------------|-----------------------|
| Data Source | Site | Distance (km) | Time Period | Temperature Difference (K) | Warming Rate (K/year) | Corresponding Years† |
| Flux towers | Shrubland minus grassland | 5 | Average of 2008-2010 | 2.0 | | |
| Climate Change | | | | | | |
| | Site/Grids | Spatial Scale (km ²) | Time Period | Start Time | End Time | Warming Rate (K/year) |
| Meteorological tower | Grassland | | | 1990 | 2012 | 0.025 |
| PRISM | Mackenzie Flats | ~85 | | 1896 | 2012 | 0.017 |
| PRISM | SNWR | ~1150 | | 1896 | 2012 | 0.015 |
| NARCCAP | 4 grid points | 10,000 | Average of 1970s-1990s | Average of 2040s-2060s | | 0.031-0.043* |

†: calculated as the observed temperature differences in shrubland and grassland in SNWR divided by the warming rate obtained from historical data or climate modeling.

*: in NARCCAP, the range of warming rate is calculated as the first and third quartile of 11 model combinations.

Table 5.2 Comparison between the increase in minimum winter temperature due to shrub encroachment and the estimated historical and future regional warming trend at the SNWR. The corresponding years indicate the number of years for climate change to cause a warming effect of the same magnitude as the increase in temperature induced by shrub encroachment.

Wehner, 2009) and on the model resolution (Rind, 1988), these estimates compare well to other studies. For example, estimates by the Intergovernmental Panel on Climate Change (IPCC, 2007) suggest a 0.03 to 0.035 K/year increase over the 21st century in winter temperatures for the southwestern U.S under the A1B scenario. An increase of 0.028 to 0.043 K/year in monthly minimum temperature for January, February and March was reported for the western U.S. by (Barnett et al., 2008) over the 2nd half of 20th century, while the average global predicted trend is 0.054 K/year over land for the 21st century in the A2 scenario (Kharin et al., 2007).

In addition to the mean winter minimum temperature, the occurrence of extreme cold events is another factor that is closely associated with the survival and productivity of shrubs due to freezing intolerance. In 2007-2010, the grassland site in SNWR recorded only 3 days with temperature lower than -15 °C, a critical value at which the juveniles of *larrea tridentata* start experiencing mortality, based on laboratory cold treatment experiments (Medeiros and Pockman, 2011). In contrast, such extreme cold events did not occur in the shrubland during the same time period. Moreover, at SNWR, 89% of the winter days in 2007-2010 had temperatures below freezing (i.e., <0 °C) in the grassland, compared to 80% in the shrubland. At the Deep Well Station, the occurrence of both freezing and extreme cold events showed large fluctuations from year to year without a clear tendency. For the recent 23 years, the number of days when daily minimum temperature dropped below -15 °C varied between 0 to 5 days per winter, while the percentage of winter days that experienced freezing temperatures varied between 72% and 96%. Although the impacts of climate change on freezing and extreme cold events

are not evident, shrub encroachment does show a role in decreasing the occurrence of both events in the SNWR.

The NARCCAP simulations use a high emission scenario, A2, and therefore may overestimate the warming trend. The NARCCAP regional climate model simulations are only driven by fossil fuel emission without accounting for the effects of land use change. Thus, these simulations may underestimate temperature trends in the regions impacted by shrub encroachment and the associated warming effect. The NARCCAP outputs used in this study consist of 4 grid cells, each covering a 2,500 km² area, which is much larger than the PRISM data also used in this study. Therefore, the mountainous regions east and west of the Rio Grande valley could affect the land surface properties of each grid cell. For example, the altitude of the grid cells used in the analysis ranges from 1706m to 2169m while altitudes at McKenzie Flats range from 1550 to 1650m. Therefore, NARCCAP results represent the overall regional climate change trend in central New Mexico, rather than the condition of the area close to shrub encroachment front.

The impact of shrub encroachment on regional climate entails an increase in minimum winter temperatures of about 2K, which is comparable to the changes in temperature associated with regional climate warming over a time period of about one century, based on historical trends and model predictions of climate warming for the 21st century in the SNWR area (Table 5.2). This effect of shrub-induced warming could have important implications for the process of shrub encroachment. As climate warming is one of the many interactive drivers of shrub encroachment in the southwestern U.S. (Archer, 1990), the nighttime warming caused by the presence of shrubs could also contribute to the shift from grass to shrub dominance. In addition, since the effect of shrub-induced

warming has the same magnitude as the background climate warming trends measured at decade-to-century time scales, it should be accounted for in a regional assessment of (nocturnal) climate warming. While many other cases of warming caused by vegetation cover change, such as the tundra-woodland transition (Chapin et al., 2005) and deforestation (Lewis and Wang, 1998) , have been extensively investigated, this study addresses an often overlooked case of land cover change (i.e., shrub encroachment in hot drylands) that has seldom been investigated in the context of its effects on local climate.

Some areas of the southwestern US are also affected by other changes in land cover conditions that are known for having an impact on the local climate. Most notably, urbanization in the Los Angeles, Tucson, Phoenix, and Albuquerque areas has been reported to induce a warmer microclimate (e.g., Roth et al., 1989; Baker et al., 2002; Hawkins et al., 2004; Imhoff et al., 2010), known as “urban heat island effect”. The intensity of urban heat islands in general depend on a number of factors such as seasonality and city size (Memon et al., 2008; Oke, 1982), but in hot arid and semi-arid areas it is overall similar in magnitude (Hsu, 1984; Jauregui, 1997; Streutker, 2003) to the effect of shrub encroachment. This shift in vegetation cover, however, affects a much more extended region of millions of hectares in southwestern North America (Van Auken, 2000) and therefore plays a more important role in shaping the local climate.

Acknowledgements

This research was supported by National Science Foundation (Grant no: NSF-DEB-0743678 and NSF-DEB-0620482). The temperature data from the study site were collected and made publicly available by the Sevilleta LTER. The authors thank Scott

Collins (University of New Mexico) and the Sevilleta LTER for making this work possible.

CHAPTER 6

THE ROLE OF VEGETATION-MICROCLIMATE FEEDBACK IN PROMOTING SHRUB ENCROACHMENT IN THE NORTHERN CHIHUAHUAN DESERT

6.1 Introduction

Shrub encroachment is a land cover change that is affecting many regions of the world under a variety of climates, soils and geographic conditions (Ravi et al. 2009). It entails an often abrupt transition from grassland to shrubland vegetation that has been observed over the last 100-150 years (Van Auken 2000). Changes in vegetation cover are known to alter the near-surface energy fluxes with important impacts on weather and climate (e.g. Pielke et al. 1998). In the northern Chihuahuan desert, shrub encroachment has been found to modify water vapor fluxes and soil moisture dynamics (Bhark and Small 2003; Kurc and Small 2007, 2004) and nocturnal air temperatures (D'Odorico et al. 2010). Grassland conversion to creosotebush (*Larrea tridentata*) shrubland, enhances the diurnal soil heating and the nocturnal longwave radiation from the ground. These processes lead to an average nighttime air temperature that is 2K higher in the shrubland than in the adjacent grassland (He et al. 2010). Since *Larrea tridentata* shrubs are cold sensitive (Medeiros and Pockman 2011; Pockman and Sperry 1997), a positive feedback between shrub encroachment and winter minimum temperature may exist in this desert, and may sustain further shrub encroachment (D'Odorico et al. 2010). Similar feedbacks have been reported to promote the transition from grassland to wood land in other

ecosystems such as Arctic tundra and high-altitude alpine regions (D'Odorico et al. 2013). The role of this feedback in the spatiotemporal dynamics of shrub expansion in desert landscapes, however, remains poorly investigated.

Two way interactions and feedbacks between vegetation cover and climate have been studied intensively through process-based coupled atmosphere-vegetation models. These models simulate the land-atmosphere interactions for different land covers and therefore are widely used to assess the impact of vegetation cover on climate (e.g., Bonan 1998; Ek et al. 2003). For example, simulations by “manually” changing the vegetation cover have explained the ongoing expansion of shrubs into the Arctic tundra, and have shown how this change in vegetation cover is expected to enhance Arctic warming through decreased albedo (Bonan et al. 1992; Foley et al. 1994) and enhanced transpiration (Swann et al. 2010). On the other hand, dynamic vegetation models, which account for different plant functional types and their fast and/or slow response to the environment, are often used to determine vegetation distribution under different climate conditions (e.g., Bonan et al. 2003). For instance, Zeng et al. (2008) simulated shrub distribution in arid and semi-arid regions worldwide. Tietjen et al. (2010) developed a coupled water and vegetation dynamic model to investigate the response of grasses and shrubs to the changing climate in African drylands. A more comprehensive way to study vegetation-climate feedback is by coupling climate models with dynamic vegetation models. Both asynchronous coupling and full coupling (also known as integrated synchronous coupling) have been developed; the former iteratively updates one model when the other reaches an equilibrium state (e.g., Claussen 1997), and the latter couples

the two models at every time step so that the transient response can also be simulated (e.g., Doherty et al. 2000; Foley et al. 1998).

In the case of shrub encroachment in northern Chihuahuan desert, only few studies have addressed the interactions between vegetation and near surface temperature. Kurc and Small (2004; 2007) investigated the effect of shrub and grass vegetation the surface energy and water fluxes. Pockman and Sperry (1997), Martínez-Vilalta and Pockman (2002) and Medeiros and Pockman (2011) carried out a series of cold lab treatment experiments to test the response and damage of juvenile creosotebush to low temperature. Hayden (1998) and Carre (2005) reported observations of differences in minimum temperature between shrubland and grassland sites. D'Odorico et al. (2010) proposed a vegetation-microclimate feedback mechanism associated with shrub-induced warming. He et al. (2010) studied the winter nocturnal warming in shrubland and analyzed the differences in surface properties and energy fluxes in shrubland and grassland sites to explain the mechanism underlying the nocturnal warming of the shrubland microclimate. Warmer nocturnal conditions are found in the shrubland in the lowest 20m above ground (He and De Wekker submitted). Such a shrub-induced warming is of great importance since it is comparable to the effects of regional climate warming at the century scale (He et al. 2014). These nighttime temperature difference and related land surface process were explained for a two-dimensional configuration of the grassland-shrubland transition using an atmospheric mesoscale model coupled with a land surface model (He et al. 2011). D'Odorico et al. 2013 used a conceptual model to show the possible emergence of bistability and abrupt state shift in ecosystem dynamics induced by vegetation-microclimate. However, to date, it is unclear whether and how the

conversion from grassland to shrubland favors further shrub encroachment through the vegetation-microclimate feedback. A representation of vegetation-atmosphere interactions in a three-dimensional process-based model is needed to further our understanding of the role played by this feedback in sustaining the transition from grass to shrub dominance and the location of the grassland-shrubland boundary under current climate conditions.

This study assesses the interactions between shrub encroachment and winter nighttime temperature with a spatially-explicit three-dimensional coupled atmosphere-land surface mesoscale model and investigates how the vegetation-microclimate feedback may promote further shrub encroachment. To this end, we use multiple scenarios of shrubland and grassland distribution. The simulated winter minimum temperatures associated with these different land cover scenarios are then used with cold stress indices based on plant physiological experiments to determine the spatial distribution of cold stress and the mortality probability of juvenile shrubs. By analyzing the change of cold stress with respect to different vegetation distributions, the role of vegetation cover in the survival of juvenile shrubs through the vegetation-microclimate feedback is evaluated and a suitable pattern of maximum shrub expansion is determined.

6.2 Methods

6.2.1 Numerical model setup

In this study, we use the Weather Research and Forecasting (Skamarock et al. 2008) model coupled with the Noah Land Surface Model (LSM, Chen and Dudhia 2001; Ek et al. 2003; Mahrt and Ek 1984). This model combination has been widely used and has been shown to reliably simulate land-surface interaction in various locations,

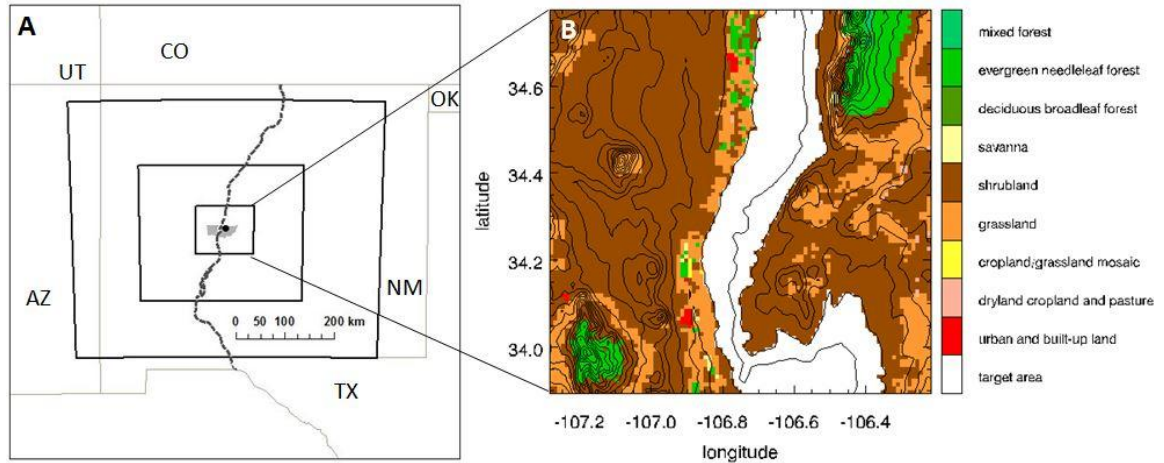


Figure 6.1 Domain setting (A), and vegetation distribution and isoheights within the 3rd (innermost) domain (B). The three domains (black solid thick lines) are centered on the McKenzie flat area within the SNWR (light grey area). The Rio Grande in NM (dashed line) and the location of the Deep Well station in the grassland (black dot) are also shown. NM and the neighboring states are labeled and state boundaries are shown in light grey lines. In the zoomed-in figure (B), the white polygon is the target area used to investigate different vegetation distributions. The vegetation cover in the rest of the domain is from default settings based on USGS maps. The isoheights are shown with 100m interval, ranging from 1300m to 3100m.

especially with modified parameterizations based on local conditions (e.g., Barlage et al. 2010; Hines and Bromwich 2008; Hong et al. 2009). Previous studies have successfully simulated the land atmosphere interactions in the shrubland and grassland, and explained the temperature difference observed over these two land covers both at the surface and in the lowest part of boundary layer (He et al. 2011; He and De Wekker submitted).

The model is set up with three nested domains, centered on the McKenzie Flats area within the Sevilleta National Wildlife Refuge (SNWR) in central New Mexico (Figure 6.1), which has been undergoing an abrupt transition from desert grassland to creosote dominated shrubland (Bhark & Small 2003, B éz & Collins 2008). Two-way nesting is used in the simulations. From the outermost) to the innermost domain, there are

59, 93 and 99 grid cells with horizontal scales of 9km, 3km and 1km, respectively. Such a high resolution in the innermost domain allows for the potential movement of the shrub encroachment front (which is expected to occur at decadal time scales) to be spatially resolved. The 65 vertical levels in the model extend to about 15km altitude with the lowest grid points located at about 5m above ground. There are 4 soil layers with thicknesses of 0.1m, 0.3m, 0.6m and 1m (starting from the top). The initial and boundary conditions are driven by 3-hourly North American Regional Reanalysis (Mesinger et al. 2006) data with a horizontal resolution of 32 km.

Following (He et al. 2011; He and De Wekker submitted), the effects of vegetation cover on water fluxes (e.g., transpiration, evaporation, and infiltration), and soil properties (e.g., soil insulation) are treated separately. The green vegetation fraction parameter that affects the soil properties is taken equal to 0.6 for the grassland and 0.1 for the shrubland. These values represent the land surface properties of shrubland and grassland that cause the observed temperature difference between the two land covers (He et al. 2011). The default setting is used for the green vegetation fraction that affects water fluxes. This default setting is derived from satellite data and does not change with changes in vegetation cover. We set the same emissivity for shrubland and grassland and use a value (0.96) in agreement with previous measurements (He et al., 2010). Albedo is taken from satellite-based maps and does not change between the two vegetation types. The following physics options are used in the model: the Rapid Radiative Transfer Model scheme for longwave radiation (Mlawer et al. 1997), the Dudhia scheme for shortwave radiation (Dudhia 1989), the WSM 6-class Graupel scheme for microphysics (Hong and Lim 2006), the Kain-Fritsch (KF- Eta) scheme for cumulus (Kain and Fritsch 1993,

1990), the Quasi-Normal Scale Elimination (Sukoriansky et al. 2006, 2005) scheme planetary boundary layer scheme and the Eddy Diffusivity\Mass Flux (EDMF, Pergaud et al. 2009) option for convective conditions.

Some additional modifications are made to better simulate the conditions in the SNWR. For example, the initial soil moisture is changed to half the default value (which is provided by NARR) for all levels to produce a soil moisture condition that is close to field measurements throughout the simulation time period. Based on measurements made by a portable photosynthesis system (LiCor6400) in November 2011, the minimum stomatal resistance is set to be 999 sm^{-1} for grassland, while its default value (300 sm^{-1}) is kept for shrubland. This modification, along with the smaller soil moisture content, reduces both the diurnal variability and the difference in latent heat between shrubland and grassland, and leads to better agreement with field observations (He et al. 2010).

In this study we use two winter cases: the winter of 2010-2011 and the winter of 2011-2012. For each winter, the simulation is initialized on November 1, at 00 UTC and terminated on March 1 of the following year, at 12 UTC. We consider the first 10 days of the simulation as a spin-up time when the energy fluxes are not stabilized. The results of the spin-up time are not included in the analysis. The winter of 2010-2011 is an extreme cold winter, with record low temperatures since the deployment of the first long term meteorological tower in SNWR in 1987. The temperature reached as low as -30 C in the grassland and dieback of creosotebush was observed (Bettinelli et al. 2013). The winter of 2011-2012 was an “average” winter, in which the mean temperature from November 11 to the end of February at the Deep Well station (for more details on the station, see Figure 6.1 and section 6.2.3) was 2.8 C , the same as the 23-year long term mean for the

| vegetation distribution scenario | numbers of grids setting | | simulation winter case | | description |
|--|-----------------------------|-----------------------|---------------------------|---------------|---|
| | grassland | shrubland | 2010- 2011 | 2011- 2012 | |
| SV_G | 99 | 0 | X | X | single vegetation cover with grassland |
| SV_S | 0 | 99 | X | X | single vegetation cover with shrubland |
| | grassland in north | shrubland in south | | | |
| GS_S10 | 59 | 40 | X | | shrubland-grassland boundary located at 10 grids south from current condition |
| GS_CURR | 49 | 50 | X | | combination of shrubland and grassland that mostly close to current condition |
| GS_N5 | 44 | 55 | X | | shrubland-grassland boundary moving 5 grids north from current condition |
| GS_N10 | 39 | 60 | X | | shrubland-grassland boundary moving 10 grids north from current condition |
| GS_N20 | 29 | 70 | X | | shrubland-grassland boundary moving 20 grids north from current condition |
| GS_N25 | 24 | 75 | X | | shrubland-grassland boundary moving 25 grids north from current condition |

Table 6.1 The vegetation distribution scenarios used in this study.

same averaging time period. Several radiosonde measurements were taken at the SNWR during November 2011 and used to validate the model (see He and De Wekker, submitted).

6.2.2 Experiment design: Vegetation distribution scenarios

Because of the lack of accurate vegetation maps for the SNWR, we use different vegetation distribution scenarios and simulate their effects on winter minimum temperature. Here we focus on the area east of the Rio Grande with elevation range from 1500-1700m above mean sea level (Figure 6.1B), where creosote shrubs and grasses are typically found. We evaluate suitable distributions of shrubs and grasses based on the north-south distribution of minimum temperature fields and the cold stress to juvenile shrubs.

First, to examine the overall effects of shrubland and grassland cover, we perform simulations with only grass and only shrub cover within the target area (Table 6.1). Thus

the whole target area is set to either grassland (SV_G) or shrubland (SV_S). We use the reanalysis data from both winters to drive these single vegetation cover scenarios and investigate the different exposure of juvenile shrubs to cold stress in “average” and extreme cold winter conditions.

Additionally, simulations with six different vegetation distributions with shrubland in the south and grassland in the north are carried out, to assess how the vegetation cover distribution affects further shrub encroachment through vegetation-microclimate feedbacks (Table 6.1). The scenario with 49 grid cells of grassland in the north and 50 grid cells of shrubland in the south (GS_CURR) is the one that most closely represents to the current location of the shrub encroachment front in the McKenzie Flats. We consider four scenarios of further shrub encroachment, namely with 5 grid cells north (GS_N5), 10 grid cells north (GS_N10), 20 grid cells north (GS_N20), and 25 grid cells north (GS_N25) of the current location of the ecotone. We also simulate the case of an encroaching front that is moved 10 grid cells south from the current condition (GS_S10).

6.2.3 Model validation data

We evaluate the model output using station data from the McKenzie Flats in the SNWR. Basic meteorological variables, such as temperature and wind, are from meteorological towers in a grassland site (Deep Well station, 34.358 °N, 106.689 °W, elevation: 1601m) and an ecotone site (Five Points station, 34.334 °N, 106.728 °W, elevation: 1614m). Moreover, the model output is evaluated using energy fluxes (winter of 2007-2008) and soil moisture records (2008) from two flux towers located in the grassland (34.360 °N, 106.700 °W, elevation: 1598m) and shrubland (34.335 °N, 106.745 °W, elevation: 1608m). In addition, four radiosonde measurements taken at a

grassland site (34.359°N 106.688°W, 1601m), and three radiosonde measurements taken at a shrubland site (34.339°N 106.742°W, 1601m) during three clear nights in November 2011, are used to evaluate the vertical profiles of the model output. We note that the focus of the model evaluation is on the differences in the soil and meteorological variables between different vegetation covers rather than on their absolute values.

6.2.4 Mortality probability of creosotebush juveniles and cold stress indices

To determine the suitability of microclimate conditions to the establishment and growth of creosote bush, we use mortality probability values based on cold lab treatment experiments by Medeiros and Pockman (2011), who measured the percentage of juvenile plants surviving low temperature treatments under drought condition. These experiments showed total mortality of juvenile shrubs at -24 C, 66% mortality at -19 C, while -15 C is the lowest minimum temperature treatment that did not cause shrub mortality. Linear interpolation is used to estimate the mortality probability of juvenile shrub as a function of the minimum treatment temperature, following D’Odorico et al. (2010). Since the minimum temperature treatment was maintained for 2.5 hours in the lab experiment, we determine shrub mortality based on 2 hour minimum temperature values ($T_{\min 2}$) from the simulation, which is the minimum simulated temperature that lasts for at least two hours. To calculate $T_{\min 2}$, we first consider the lowest mean temperature in any continuous two hour intervals (in the simulation) within one day, and then use the higher temperature among those two hour intervals as the 2 hour minimum temperature. The mortality probability $MP(T_{\min 2})$ is then calculated and further interpreted as a cold stress index to measure the cold damage in juvenile shrubs. A few other indices are used to express freezing stress in creosote bush.

We first assume that there is no cumulative effect of cold damage from low temperature events occurring in the same winter. This leads to an index that describes the shrub mortality probability during one winter season $MP(T_{\min 2})$ in the coldest night which we call the “Peak Mortality Probability”: $PMP = MP(T_{\min 2_winter})$.

To account for the cumulative effect of cold damage caused by every cold night in a certain winter season, we calculate the “Cumulative Mortality Probability” (CMP) as follows: after the first cold night (night 1), the percentage of surviving juvenile shrubs is $1 - MP(T_{\min 2_day1})$. Assuming that all these cold events are independent, the probability that juvenile shrubs survive the second cold night (night 2) is $(1 - MP(T_{\min 2_day1})) \times (1 - MP(T_{\min 2_day2}))$. Thus, considering all the cold nights occurring throughout the winter, the survival probability can be expressed as the product (Π) of the survival probability for a sequence of cold nights: $\Pi(1 - MP(T_{\min 2_daily}))$, while CMP is $CMP = 1 - \Pi(1 - MP(T_{\min 2_daily}))$.

Finally, we define a “Total Stress Index” (TSI) that assumes the existence of an additive effect of cold events on plant stress: $TSI = \sum MP(T_{\min 2_daily})$. TSI can be zero or any positive number.

In the study, we used all three indices to provide a more comprehensive assessment of cold stress in juvenile shrubs. Total mortality is assumed to occur if PMP or CMP are larger than 99.9%.

| Meteorological Tower Observation | | | | |
|----------------------------------|-----------|-------|-------------|------|
| Location | Deep Well | | Five Points | |
| Vegetation cover | grassland | | ecotone | |
| Mean Minimum | 2010-2011 | -7.4* | -5.2 | |
| Temperature (°C) | 2011-2012 | -5 | -3.6 | |
| Simulation | | | | |
| Location of grid cell | Deep Well | | Five Points | |
| Vegetation cover setting | SV_G | SV_S | SV_G | SV_S |
| Mean Minimum | 2010-2011 | -8 | -5.9 | -8.8 |
| Temperature (°C) | 2011-2012 | -5.8 | -3.8 | -6.2 |

*: There are 14 days with partially missing data that excluded in the analysis.

Table 6.2 Comparison between simulated mean winter daily minimum temperature in the grid points corresponding to the location of the Deep Well and the Five Points stations, and the observed mean daily minimum temperature in these two stations.

6.3 Results and discussion

6.3.1 Minimum temperatures with single vegetation cover

The minimum temperature in the McKenzie Flats is well simulated by the model (Table 6.2), despite the discrepancies existing in the spatial scales between grid cells and point measurements at the field sites. On average, there is a small cold bias in the simulation, though in the extreme cold events the simulated temperature is higher than the observation. For example, the record low temperature in winter of 2010-2011 was -29.9°C at the Deep Well station (shrubland) and -26.6°C at the Five Points station (grassland), while the simulated lowest temperature in McKenzie flat area is -27.0°C with grassland cover, and -22.4°C with shrubland cover. A small warm bias is not unusual in model simulations of extreme cold events e.g., Dulière et al. 2011; Kostopoulou et al. 2009; García-Díez et al. 2013) and the scale mismatch between grid cells and station measurements affects the comparison with field data, particularly when the focus is on

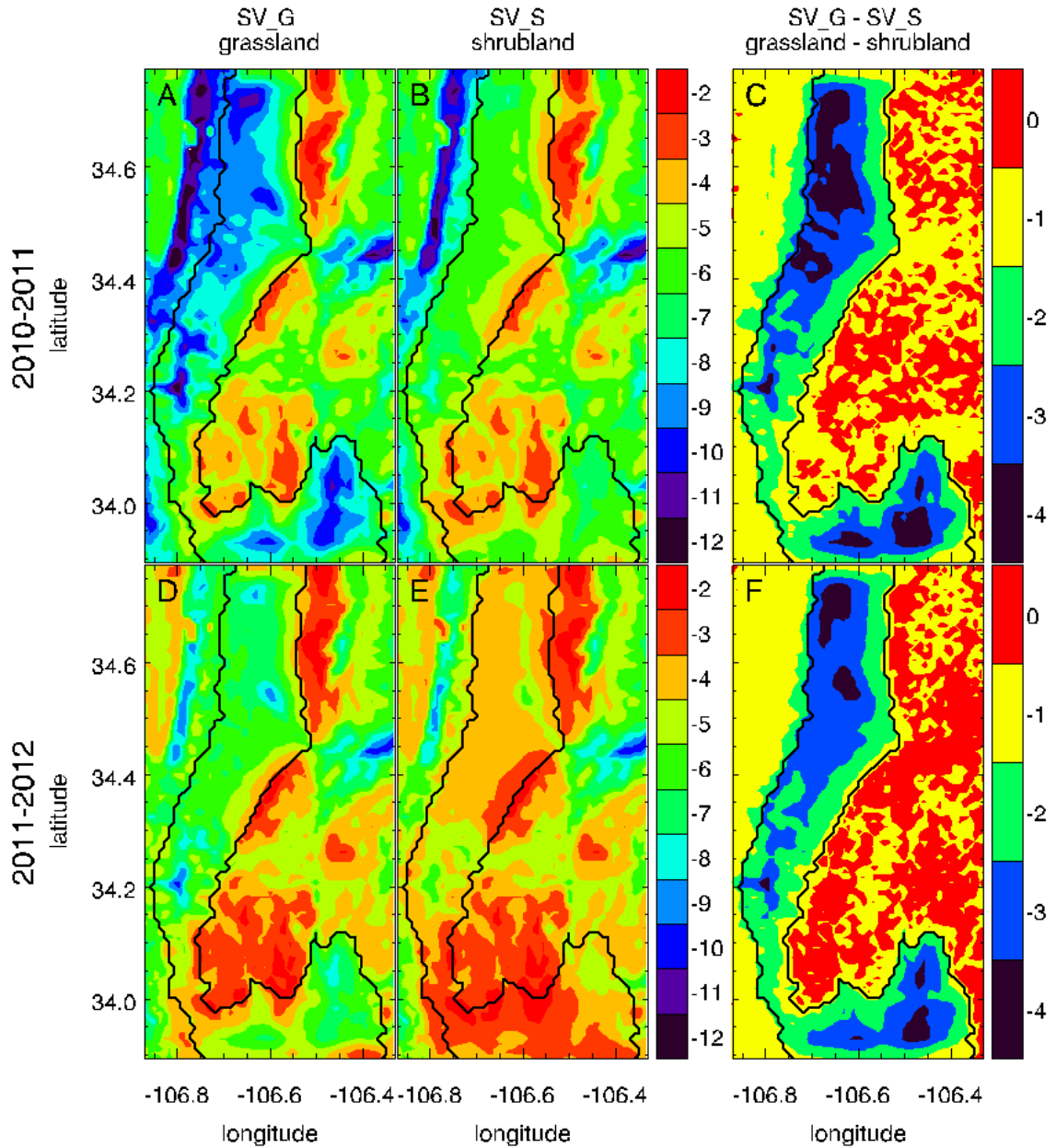


Figure 6.2 Mean daily minimum temperature in winter 2010-2011 (A, B and C) and winter 2011-2012 (D, E and F) obtained from simulations with the target area (enclosed by the black solid line) covered by grassland SV_G (A and D), shrubland SV_S (B and E) vegetation, and the difference between grassland and shrubland vegetation setting SV_G-SV_S (C and F).

small temporal scales, such as those of extreme events (e.g., Zhang et al. 2011). Nonetheless, the temperature difference between the cases with shrubland and grassland

covers is well simulated throughout the winter. Besides the near-surface air temperature, we also evaluated the simulations with available tower and radiosonde observations of the wind field and the thermodynamic structure in the lower atmosphere, and observations of the energy fluxes, soil temperature and soil moisture. Simulations agreed well with these observations (not shown) as was also shown in some of our other related mesoscale modeling work (He et al., 2011; He and De Wekker, submitted).

The mean daily minimum temperatures obtained from simulations with complete grassland and shrubland covers are shown in Figure 6.2. The shrubland is always warmer than the grassland in both winters. The temperature difference between the two vegetation settings is 2-4 K in most of the target area. In the extreme cold winter the mean daily minimum temperature is always at least 2K lower than in the “average” winter case with the same vegetation cover. However, the areas that show relatively large or small temperature difference between simulations with the two vegetation covers are almost the same for both winters (Figure 6.2). Along the east edge of the target area, such a temperature difference is generally smaller. We attribute this to the influences from the grid cells outside the target area to their neighbors inside the target area through advection and horizontal energy transfer. As the conditions, including the vegetation, outside the target area are set to be non-varying in all simulations, the temperature of the grid cells near the border is relatively less affected upon the changing vegetation cover inside the target area. This effect is especially strong along the east edge given the prevailing nocturnal wind from the mountains at the east side. The very similar effect may be also the cause of the relatively small temperature difference seen at the area located between 33.95°N and 34.15°N which is the narrowest part of the target area

(Figure 6.2). Due to its small width in west-to-east direction (6-7 grid cells in width), most of the cells enclosed in this area are affected by the outside cells. In addition, this area has sandy clay loam soils, which have a different thermal diffusivity coefficient than the other soils in the 3rd domain.

6.3.2 Cold mortality to juvenile shrub with single vegetation cover

To relate the simulated minimum temperature to the survival and mortality of juvenile shrubs, we calculated all three cold stress indices for the grassland and shrubland cover cases in both winters (Figure 6.3). Generally, the grassland cover has a microclimate with stronger cold stress for juvenile shrubs than the shrubland. As expected, the cold stress is much stronger in the extreme cold winter than in the normal winter. In both winters, the largest cold stress differences occur in the area north of 34.15°N. As discussed in section 6.3.2, the target area between 33.95°N and 34.15°N exhibits only small or no differences in cold stress indices between the two vegetation covers. In the extreme cold winter, the southern part of the target area experiences a relatively strong difference in cold stress with the two vegetation covers, while these differences are much smaller in the “average” winter. Additionally, the locations where different cold stress exists are not consistent for these two winters. Similar patterns can be found in the difference in mean daily minimum temperature between grassland and shrubland covers (Figure 6.2).

We will focus on the region that in both winters exhibits distinct cold stress conditions for juvenile shrubs depending on whether they grow in a grassland or a shrubland. This region, which is in the northern part (> 34.15°N) of the target area (except for the eastern edge), is also where the current shrub encroaching front (about 34.34°N) is

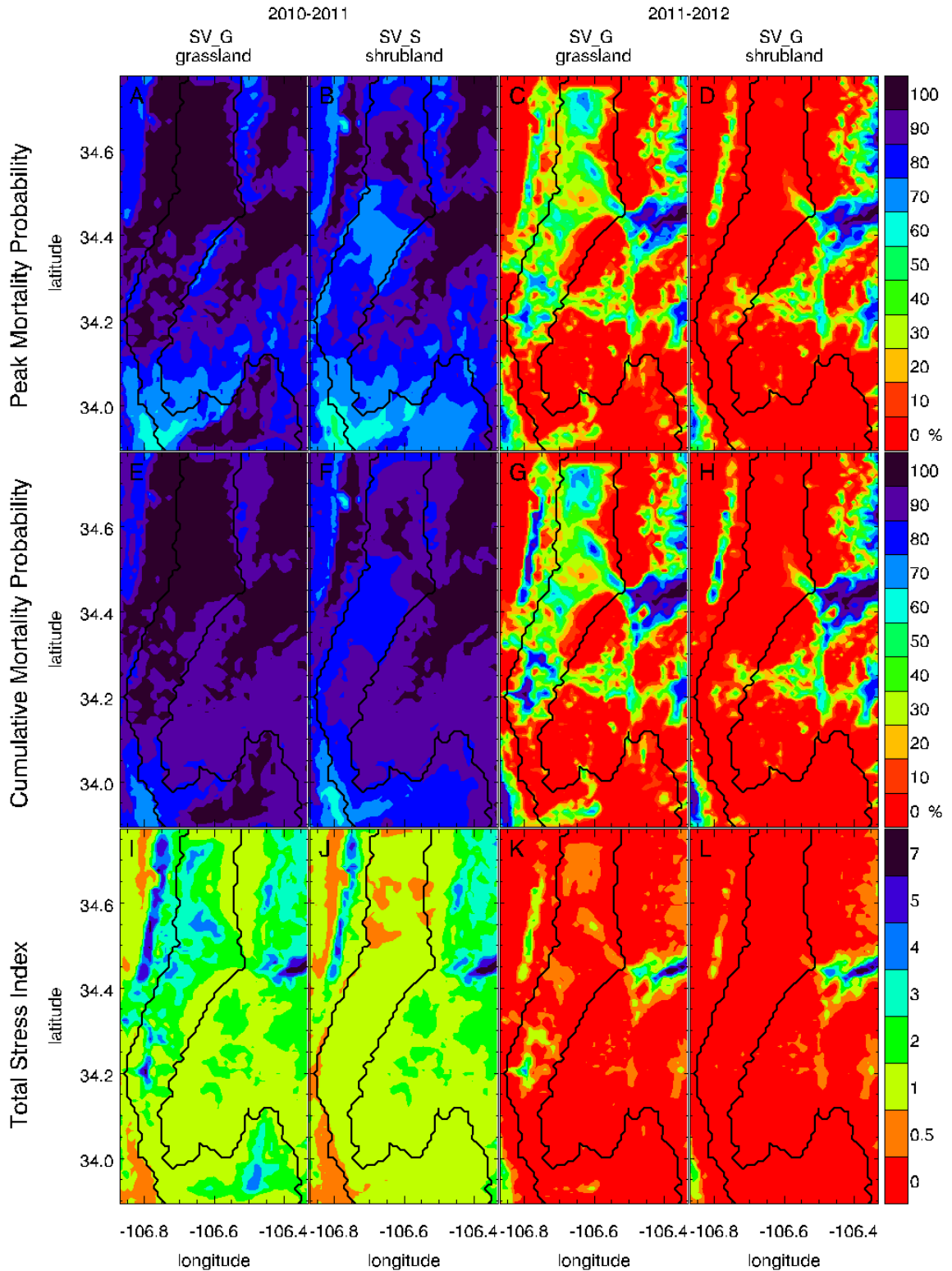


Figure 6.3 The simulated peak mortality probability (PMP, first row, A, B, C and D), cumulative mortality probability (CMP, second row, E, F, G and H), and total stress index (TSI, third row, I, J, K, L) calculated for winter 2010-2011 (first and second column, A, B,

E, F, I and J) and winter 2011-2012 (third and fourth column, C, D, G, H, K and L) with grassland cover SV_G (first and third column, A, C, E, G, I and K) and shrubland cover SV_S (second and fourth column, B, D, F, H, J, and L) in the target area that enclosed by the thick solid line.

located.

Among the three cold stress indices, we mainly use PMP and CMP to assess the possible mortality of juvenile shrubs, and use TSI as an additional criterion to analyze areas with very large cold stress. During the “average” winter around the current encroachment front, there is almost no cold stress for juvenile shrubs when the target area is a shrubland, while moderate cold stress (30% to 50% in PMP and CMP) occurs in the case of grassland. Thus, conditions are more favorable for the survival and growth of juvenile shrubs in the shrubland than the grassland. In the extreme cold winter, juvenile shrubs in the area around the current encroachment front will experience almost total mortality (90% to 100% in PMP and CMP) with grassland cover. The potential mortality probability is still high for juvenile shrubs with shrubland cover (70% in PMP and 80% in CMP), but lower than in the case with grassland cover. Thus, more juvenile shrubs are likely to survive in the shrubland than in the grassland after extreme cold winters. In summary, juvenile shrubs located around the current encroachment front have always better survival probability with shrubland than with grassland cover.

In the extreme cold winter, the area north of 34.4 N has 100% juvenile mortality probability (for both PMP and CMP) with the grassland cover. While with shrubland cover the mortality probability is also very high, it does not reach total mortality in most part of the region. Although the patterns of PMP and CMP appear to be similar with the

two vegetation covers in the region, the actual cold stress may be much more intense in the grassland since the TSI in the grassland is much larger (by >1) than in the shrubland. Additionally, several locations within the area have a TSI >3 , indicating the occurrence of multiple extreme cold nights and a high likelihood of complete mortality of juvenile shrubs. These values of the cold indices correspond to a critical zone for juvenile shrubs, in which they cannot survive with grassland cover, but may partly survive if the landscape is covered by shrubland vegetation. The grassland-shrubland vegetation existing in such a critical zone is an example of a bi-stable ecosystem induced by positive vegetation-microclimate feedbacks (D'Odorico et al. 2013). The bi-stable system can be either a stable shrubland in which juvenile shrubs can establish and survive, or a stable grassland in which grasses survive but juvenile shrubs cannot establish.

Simulations with the target area covered by shrubland vegetation show that in the extreme cold winter there is an area with total mortality (evaluated both in terms of PMP and CMP). Thus, in this area, juvenile shrubs may experience die-back even when growing in a shrubland. The area could be associated with a possible northern limit of shrub encroachment, analyzed and discussed in detail in section 6.3.3.

We need to emphasize that all of the three cold stress indices are diagnostic indicators and none of them can serve as a predictor, due to the discrepancy between laboratory tests used to evaluate the cold tolerance of juvenile shrubs (Medeiros and Pockman, 2010) and field situations as well as the gaps existing between field conditions and model simulations. Even in the laboratory, the proportion of juvenile shrubs that survived after cold treatment, is different from the proportion of juveniles retaining leaves, and the experimental results strongly depend on soil moisture (Medeiros and Pockman

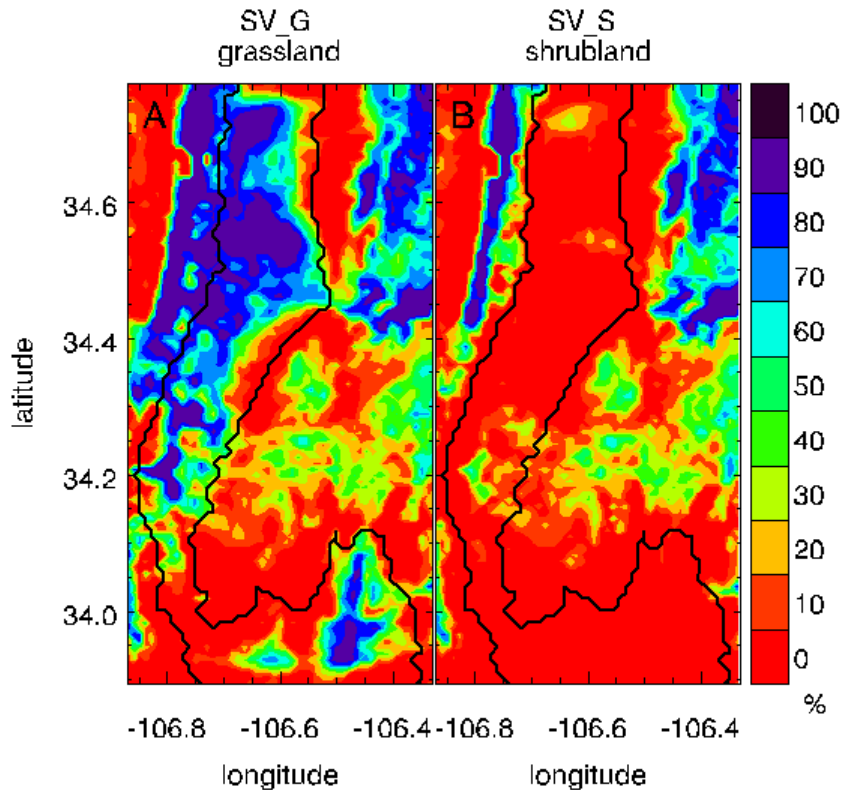


Figure 6.4 The simulated cumulative mortality probability (CMP) of winter 2010-2011 without the three extreme cold days (and nights) calculated with grassland cover SV_G (A) and shrubland cover SV_S (B) in the target area that enclosed by the thick solid line.

2011). Moreover, it is not clear how adult shrubs respond to low temperature because lab based physiological studies concentrated on juveniles. Nevertheless, by utilizing these diagnostic indices, we have been able to simulate and investigate differences in cold stress emerging with different vegetation covers.

In the extreme cold winter, the record low temperature was measured on 2/3/2011. If we exclude the three days (2/2/2011-2/4/2011) that are closely associated with this lowest recorded temperature, the three cold stress indices calculated for winter 2010-2011 exhibit a pattern similar to those in the winter of 2011-2012 (CMP is shown as an example in Figure 6.4). However, all the cold stress indices remain higher in the winter of 2010-2011 than in 2011-2012, especially with grassland cover. In particular, in

most of the critical zone, the CMP is larger than 80% if the landscape is covered by a grassland, which suggests that the intense cold damage to juvenile shrubs in grassland could potentially also occur in a non-extreme winter, thereby limiting shrub encroachment. The similar patterns of the cold stress indices of the winter 2010-2011 excluding the three extreme cold days (Figure 6.4) and the winter 2011-2012 (Figure 6.3G, H) suggest that the “average” winter case represents a common pattern of cold stress differences between shrubland and grassland.

6.3.3 Cold stress to juvenile shrub with combination of shrubland and grassland covers

Because of the diagnostic nature of the cold stress indices, different vegetation distribution scenarios (Table 6.1) are used here to test the feedback between shrub encroachment and winter minimum temperature. We consider the case with shrubland vegetation in the south and grassland in the north, separated by an ecotone or encroachment front. Under current conditions, it is reasonable to expect that shrubs will further encroach into the grassland favored by a number of drivers such as increasing CO₂ concentration (e.g., Polley et al. 1992), shift of rainfall regime (e.g., Brown et al. 1997), and fire management (e.g. Archer et al. 1995). Here we investigate how shrub expansion may be sustained by the feedback of vegetation with its microclimate (D’Odorico et al., 2010). Seedling establishment and the growth of pioneer juvenile shrubs beyond the shrubland-grassland boundary would lead to the formation of a pioneer shrub community north of the original front. Based on the analysis from section 6.3.2, the cold stress in normal winters would not cause detrimental damage to the pioneer juveniles. However, during extreme cold winters, the survival of pioneer juveniles in the

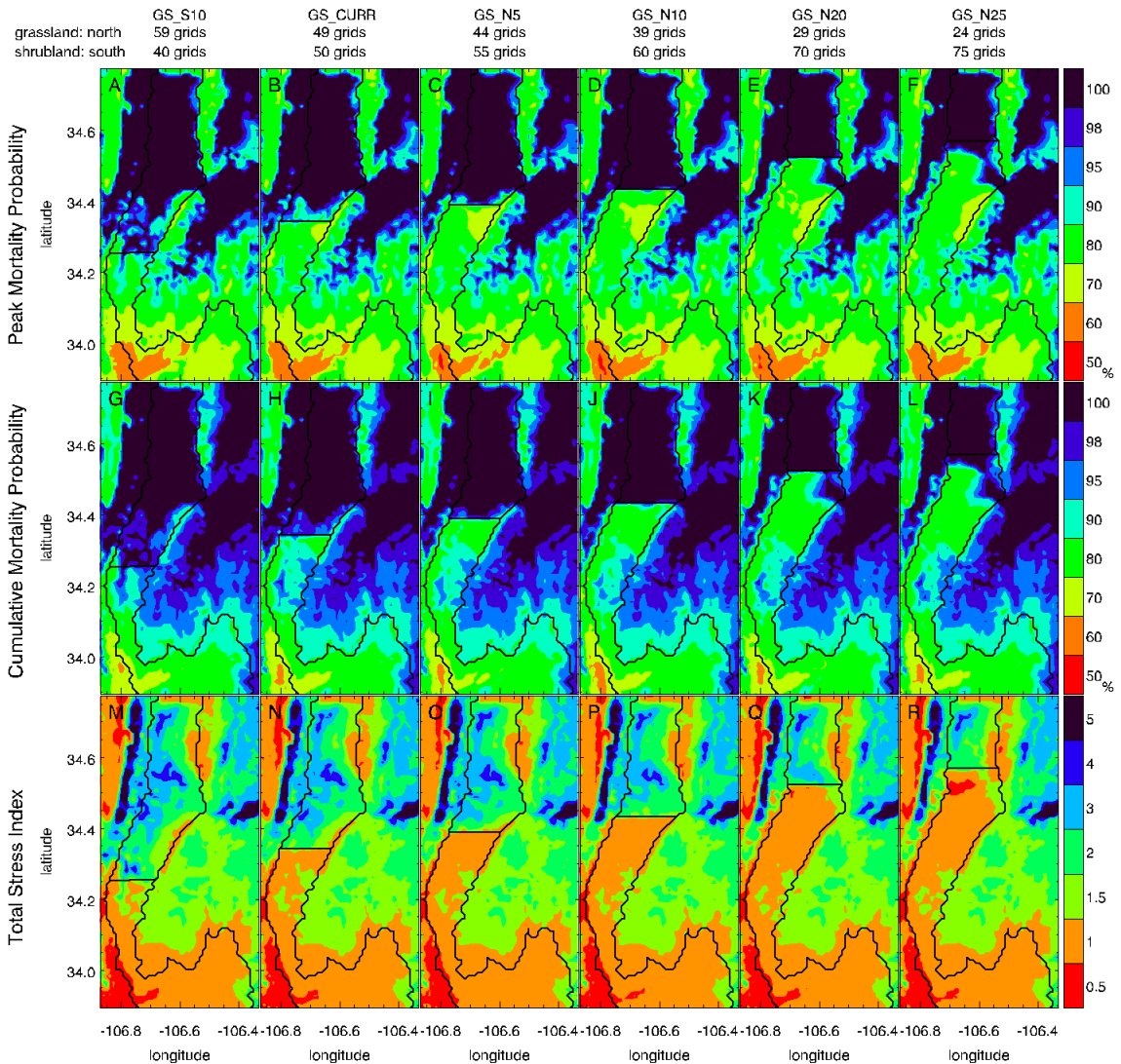


Figure 6.5 The simulated peak mortality probability (PMP, first row, A, B, C, D, E and F), cumulative mortality probability (CMP, second row, G, H, I, J, K and L), and total stress index (TSI, third row, M, N, O, P, Q and R) for winter 2010-2011 using different vegetation distributions with grassland in the north and shrubland in the southern in the target area (enclosed by the black solid line). The west to east straight black solid line within the target indicates the shrubland-grassland boundary. The following positions of this boundary are considered: GS_S10 (first column, A, G and M); GS_CURR (first column, B, H and N); GS_N5 (first column, C, I and O); GS_N10 (first column, D, J and P); GS_N20 (first column, E, K and Q); GS_N25 (first column, F, L and R).

grassland becomes uncertain. Therefore, we consider different configurations of the

encroachment front and evaluate whether the interaction between vegetation and microclimate would allow for a successful establishment of pioneer juveniles.

As in the case of single vegetation cover scenarios, we use CMP and PMP to assess the survival conditions for juvenile shrubs (Figure 6.5). For the GS_S10 and GS_CURR scenarios, pioneer juveniles have a good chance to survive in the grassland during the extreme cold winter. With further shrub encroachment (GS_N5), pioneer juveniles have a good chance to survive in the grassland if they are close to the shrubland-grassland boundary. As the encroachment front moves further north, the pioneer juveniles in the case of GS_N10 and GS_N20 cannot survive throughout the extreme winter if they are surrounded by grasses. In the northernmost shrub distribution scenario considered in this study (GS_N25), juvenile shrubs cannot even survive at the northern end of the shrubland during extreme cold winter. This result indicates a potential northern limit of shrub encroachment under current climate conditions because shrubs at the northern end of the shrubland cannot provide (through the vegetation-microclimate feedback) an environment that is warm enough for the survival of juvenile shrubs in extreme cold winters. We find that such a potential northern limit for shrub expansion under current climate conditions is about 35.4N. This line also corresponds to conditions of 100% mortality probability (based both on PMP and CMP) in simulations with single shrubland cover (SV_S, Figure 6.3).

Although the patterns of PMP and CMP around the shrubland-grassland boundary vary from case to case, the characteristics of the TSI are relatively consistent in all the scenarios. The encroachment fronts spatially correspond to a TSI isoline of 1.5 (Figure 6.5). In all vegetation distribution scenarios most of the area with shrubland cover has a

TSI smaller than 1.5 while the TSI of most of the area with grassland cover is greater than 1.5.

The vegetation distribution scenarios used in this study are based on reasonable assumptions of how vegetation cover may change, a common approach used in model-based studies (e.g., Swann et al. 2010). Although historical photography has provided evidence of shrub encroachment in SNWR, the shrub expansion rate has not been determined. Based on historical records of shrub encroachment available for other areas of the Chihuahuan desert (Gibbens et al. 2005), the scenarios considered here are not unreasonable for changes in vegetation cover that are expected to occur at decadal to century time scales. In addition, we note that the vegetation scenarios along with the diagnostic indices are used here as an alternative to vegetation dynamic models. To date there are no models of shrub encroachment in desert landscapes that include the effect of the vegetation- microclimate feedback. Nonetheless, this simplified approach investigates the sole effect of vegetation-microclimate feedback, without the need to account for various factors (e.g., fire, winter and summer precipitation, D’Odorico et al. 2006; Muldavin et al. 2007) governing the productivity of shrubs and grasses.

The results using split shrubland and grassland distributions suggest that juvenile shrubs always have better survival chances if surrounded by a shrub community (Figure 6.5). At a certain point of its northward migration the shrubland cannot expand further north because pioneer juveniles may not be able to survive throughout the extreme cold winter. Therefore, we can conclude that the establishment of a shrub community is important for the survival of juvenile shrubs during extreme cold winters because shrubs are cold sensitive but create a warmer environment through the vegetation-microclimate

feedback. Such a feedback may favor further shrub encroachment. There is however, a northern limit for juvenile shrub expansion; beyond that limit, shrub juveniles are likely to encounter total mortality in extreme cold winters even when they are surrounded by shrubland vegetation. This fact is further supported by the observation that the SNWR is one of the northernmost and coldest places where creosotebush is currently found (Pockman and Sperry 1997).

6.4 Summary

We used the atmospheric mesoscale model WRF and diagnostic indices to simulate the winter minimum temperature and the resulting cold stress occurrences in juvenile shrubs with different grassland and/or shrubland vegetation cover scenarios in the northern Chihuahuan desert. The model is able to simulate the difference in minimum temperature between the two land covers, while the related energy fluxes agree with the observations. The mean winter minimum temperature is about 2-4 K higher with shrubland than with grassland cover. By relating the minimum temperature to cold stress of juvenile shrubs we showed that the survival of juvenile shrubs is always enhanced by shrubland cover through a vegetation-microclimate feedback. Thus, the feedback may allow juvenile shrubs to avoid mortality in some parts of the region even in the extreme cold winters. Therefore, a critical zone may exist in which the grassland-shrubland system exhibits bi-stability. In other words, this zone would be stable either as a grassland or as a shrubland. In fact, in this zone juvenile shrubs may survive with shrubland cover but cannot survive with microclimate conditions created by a grassland cover. Additionally, by using combined shrubland and grassland distributions, we test the role of vegetation cover on a potential further encroachment of shrubs. Different

vegetation scenarios show that the establishment of a shrub community is important for the survival of juvenile shrubs during extreme cold winters by elevating the temperature and reducing cold stress. The vegetation-microclimate feedback could favor further shrub encroachment with a northward migration of the grassland-and-shrubland front until encroachment reaches a northern limit, beyond which creosote juveniles would not survive even if surrounded by adult shrubs. Such a northern limit is where the warming induced by the shrubland cover cannot provide an environment that is warm enough to avoid juvenile mortality in extreme cold winters. Our study demonstrates how shrub encroachment can potentially be enhanced by the effects of positive vegetation-microclimate feedbacks.

CHAPTER 7

SUMMARY AND CONCLUSION

Shrub encroachment, a worldwide ecological phenomenon that is associated with changes in vegetation cover from herbaceous to woody composition, usually causes land degradation and loss of ecosystem services in arid and semi-arid areas. The relative abrupt shrubland-to-grassland transition, both in time and in space, suggests that positive feedbacks may be involved in the ecosystem dynamics. A number of environmental and anthropogenic drivers and feedbacks have been proposed in an effort to explain the rapid encroachment of shrub species. However, the interaction and feedback processes between shrub encroachment in hot drylands and microclimate remain poorly understood.

The research presented in this dissertation addresses the interaction and feedback processes between shrub encroachment and microclimate, with the focus on creosotebush encroachment in the northern Chihuahuan desert in the southwest U.S. Average nighttime air temperature is about 2 K warmer over the shrubland than over the adjacent grassland, with a more prominent nighttime warming effect during cold calm winter nights. Due to the cold intolerance of the shrub species, a positive feedback between shrub encroachment and nighttime temperature may exist, which could introduce bi-stability to the shrubland-grassland system and contribute to the abrupt shift in alternative stable states (i.e., transition from grassland to shrubland).

The physical mechanisms underlying shrub-induced nocturnal warming are investigated analyzing the observed energy fluxes and using a process-based one dimensional model. Because of the larger fraction of bare soil in the shrubland than in the grassland, more energy flows into the ground in the shrubland than in the grassland

during daytime. This energy is then released at night mainly as longwave radiation, which causes the difference in the nighttime air temperatures between the two land covers. Thus, the elevated nighttime temperature is associated with the modification of the land surface property by shrub encroachment. Although the patched pattern of shrubs and the resulting large fraction of bare soil causes the temperature difference between shrubland and grassland, such a temperature difference does not exist at the patch scale, but only at the landscape scale. Shrub-induced nocturnal warming and the responsible energy fluxes are simulated well by idealized two-dimensional simulations using a mesoscale model with adjusted vegetation parameters that are in agreement with the observed parameters. Sensitivity tests using a number of vegetation parameters indicate that the green vegetation fraction is the key factor causing the higher nocturnal temperature in shrubland than in grassland, mainly by its effects on soil surface insulation, soil thermal diffusivity, and therefore on ground heat fluxes.

Concurrent measurements of temperature profiles in the nocturnal boundary layer in adjacent shrubland and grassland show that the temperature difference between the two vegetation covers mainly exist within the lowest 20m above ground. In calm clear conditions, the lowest part of the boundary layer in grassland cools faster, resulting in a much stronger temperature inversion over grassland than over shrubland. Such a vertical temperature difference between shrubland and grassland is established shortly after sunset and is then maintained throughout the night. Sensitivity simulations using a single column model with a variety of boundary layer parameterization schemes and vegetation parameter settings suggest that the boundary layer structure is most sensitive to changes in green vegetation fraction.

The relative importance of shrub-induced warming compared to regional climate warming is also examined. Using historical observations and future climate model outputs, the estimated regional increase in minimum winter temperature ranges from 1 to 4 K per century. Since the winter minimum temperatures are observed to be ~2 K higher in shrubland than in the adjacent grassland, the warming resulting from shrub encroachment is comparable to a change in regional climate over a time scale of one century. This comparable warming suggests that shrub encroachment has an overall important effect on the regional climate.

The role of the vegetation-microclimate feedback in promoting further shrub encroachment is investigated using an atmospheric mesoscale model and diagnostic indices. The winter minimum temperature and the resulting cold stress occurrences in juvenile shrubs are simulated with different grassland and/or shrubland vegetation cover scenarios. Results show that the vegetation-microclimate feedback elevates the minimum temperature by 2-4 K on average, which may allow juvenile shrubs to avoid mortality in some parts of the region even in the extreme cold winters. As a result, a critical zone with bi-stability of either stable grassland or stable shrubland may exist, where the juvenile shrubs may survive with the warmer microclimate condition created by the shrubland cover but cannot survive with grassland cover. The vegetation-microclimate feedback also makes the establishment of a shrub community important for the survival of juvenile shrubs during extreme cold winters due to the reduced cold stress. The northward migration of shrubland could be favored by the feedback until the encroachment front reaches a northern limit, beyond which juvenile shrubs would not survive even under the elevated nocturnal temperature of shrubland cover. It is demonstrated how the effects of

the positive vegetation-microclimate feedback could potentially enhance shrub encroachment.

To summarize, this study highlights the ability of shrub encroachment to modify the microclimate near the ground by increasing the nocturnal temperature, and the role of the shrub-induced warming in sustaining current juvenile shrubs and/or enhancing further shrub encroachment. This novel vegetation-microclimate feedback mechanism contributes to the comprehensive understanding of the effects, the drivers and the ecosystem dynamics of shrub encroachment in hot drylands. The positive feedback is more important in the northern migration of shrubland where the cold stress could be a limiting factor. The feedback also has potential implications for the response of shrub encroachment to global or regional climate change. Highlights of the findings of this dissertation include:

- Shrubland is observed to have a higher nighttime temperature, by 2 K on average, than adjacent grassland in the northern Chihuahuan desert in the southwestern U.S.
- Due to the cold intolerance of creosotebush, a positive feedback between shrub encroachment and nighttime temperature may exist.
- The nighttime warming is caused by an increase in soil fraction in the zone affected by shrub encroachment, which enhances diurnal soil heating and nocturnal release of longwave radiation.
- The temperature difference between shrubland and grassland mainly exists in the lowest 20m.

- The shrub-induced warming has an overall important effect because it is comparable to regional climate change of a time scale of about one century.
- Numerical model simulations suggest that the survival of juvenile shrubs could be favored by the elevated temperature and the reduced cold stress created by the shrubland cover. Therefore, the positive vegetation-microclimate feedback may potentially promote further shrub encroachment.

This dissertation uses both observational and modeling approaches to investigate the interactions between the encroachment of creosotebush and the nocturnal temperature in the northern Chihuahuan desert, which lead to a detailed understanding of the vegetation-microclimate feedback process that facilitates the local grassland-to-shrubland transition. As the shrub encroachment is a widely distributed phenomenon, it will be very interesting to expand such studies to other ecosystems. Since the increase in bare soil fraction is a common consequence of shrub encroachment in drylands, in principle, the encroachment of other shrub species may affect the microclimate in a similar way. If such a shrub-induced microclimate warming is indeed a widely existing phenomenon, shrub encroachment spreading a large area can possibly play an important role in changing the regional climate. Additionally, how the modified microclimate condition affects the plant physiology and whether or not a feedback can be induced under different vegetation and climate conditions will be outstanding future research topics. On the other hand, no matter how widely the vegetation-microclimate feedback may apply, it is worthwhile to be incorporated in the coupled climate and vegetation dynamic model. The development of the coupled climate/vegetation model, of course, requires a comprehensive knowledge of the feedback. Such model will then greatly

contribute to the understanding and possible prediction of the extent of the shrub encroachment as well as the changes in regional climate with respect to the vegetation-microclimate feedback.

REFERENCES

- Alward, R. D., J. K. Detling, and D. G. Milchunas (1999), Grassland Vegetation Changes and Nocturnal Global Warming, *Science*, 283(5399), 229–231, doi:10.1126/science.283.5399.229.
- Anderies, J. M., M. A. Janssen, and B. H. Walker (2002), Grazing management, resilience, and the dynamics of a fire-driven rangeland system, *Ecosystems*, 5(1), 23–44, doi:10.1007/s10021-001-0053-9.
- Archer, S. (1989), Have southern Texas savannas been converted to woodlands in recent history?, *Am. Nat.*, 134(4), 545–561.
- Archer, S. (1990), Development and Stability of Grass/Woody Mosaics in a Subtropical Savanna Parkland, Texas, U. S. A., *J. Biogeogr.*, 17(4/5), 453–462, doi:10.2307/2845377.
- Archer, S. (1994), Woody plant encroachment into southwestern grasslands and savannas: rates, patterns and proximate causes., in *Ecological implications of livestock herbivory in the west*, pp. 13–68, Society for Range Management.
- Archer, S., D. S. Schimel, and E. A. Holland (1995), Mechanisms of shrubland expansion: land use, climate or CO₂?, *Clim. Change*, 29(1), 91–99, doi:10.1007/BF01091640.
- Archer, S., C. Scifres, C. R. Bassham, and R. Maggio (1988), Autogenic succession in a subtropical savanna: conversion of grassland to thorn woodland, *Ecol. Monogr.*, 58(2), 111–127, doi:10.2307/1942463.

- Bachelet, D., R. P. Neilson, J. M. Lenihan, and R. J. Drapek (2001), Climate Change Effects on Vegetation Distribution and Carbon Budget in the United States, *Ecosystems*, 4(3), 164–185, doi:10.1007/s10021-001-0002-7.
- Béaz, S., and S. L. Collins (2008), Shrub Invasion Decreases Diversity and Alters Community Stability in Northern Chihuahuan Desert Plant Communities, *PLoS ONE*, 3(6), e2332, doi:10.1371/journal.pone.0002332.
- Baker, L. A., A. J. Brazel, N. Selover, C. Martin, N. McIntyre, F. R. Steiner, A. Nelson, and L. Musacchio (2002), Urbanization and warming of Phoenix (Arizona, USA): Impacts, feedbacks and mitigation, *Urban Ecosyst.*, 6(3), 183–203, doi:10.1023/A:1026101528700.
- Balling, R. (1988), The climatic impact of a Sonoran vegetation discontinuity, *Clim. Change*, 13(1), doi:10.1007/BF00140163. [online] Available from: <http://www.springerlink.com/content/u1r0n74378j828p1/> (Accessed 18 May 2011)
- Balling, R. C., J. M. Klopatek, M. L. Hildebrandt, C. K. Moritz, and C. J. Watts (1998), Impacts of land degradation on historical temperature records from the Sonoran Desert, *Clim. Change*, 40(3), 669–681.
- Barlage, M., F. Chen, M. Tewari, K. Ikeda, D. Gochis, J. Dudhia, R. Rasmussen, B. Livneh, M. Ek, and K. Mitchell (2010), Noah land surface model modifications to improve snowpack prediction in the Colorado Rocky Mountains, *J. Geophys. Res. Atmospheres*, 115(D22), doi:10.1029/2009JD013470.
- Barnett, T. P. et al. (2008), Human-Induced Changes in the Hydrology of the Western United States, *Science*, 319(5866), 1080–1083, doi:10.1126/science.1152538.

- Beljaars, A. C. M. (1995), The parametrization of surface fluxes in large-scale models under free convection, *Q. J. R. Meteorol. Soc.*, *121*(522), 255–270, doi:10.1002/qj.49712152203.
- Beltrán-Przekurat, A., R. A. Pielke Sr., D. P. C. Peters, K. A. Snyder, and A. Rango (2008), Modeling the effects of historical vegetation change on near-surface atmosphere in the northern Chihuahuan Desert, *J. Arid Environ.*, *72*(10), 1897–1910, doi:10.1016/j.jaridenv.2008.05.012.
- Bettinelli, J., K. W. Wright, and D. L. Marshall (2013), How does an extreme cold event affect the bee community in a Creosote shrubland?, 98th Annual Ecological Society of America Meeting, Minneapolis, MN.
- Bhark, E. W., and E. E. Small (2003), Association between Plant Canopies and the Spatial Patterns of Infiltration in Shrubland and Grassland of the Chihuahuan Desert, New Mexico, *Ecosystems*, *6*(2), 185–196, doi:10.1007/s10021-002-0210-9.
- Bonan, G. B. (1997), Effects of land use on the climate of the United States, *Clim. Change*, *37*(3), 449–486.
- Bonan, G. B. (1998), The Land Surface Climatology of the NCAR Land Surface Model Coupled to the NCAR Community Climate Model*, *J. Clim.*, *11*(6), 1307–1326, doi:10.1175/1520-0442(1998)011<1307:TLSCOT>2.0.CO;2.
- Bonan, G. B. (1999), FROST FOLLOWED THE PLOW: IMPACTS OF DEFORESTATION ON THE CLIMATE OF THE UNITED STATES, *Ecol. Appl.*, *9*(4), 1305–1315, doi:10.1890/1051-0761(1999)009[1305:FFTPIO]2.0.CO;2.

- Bonan, G. B. (2002), *Ecological climatology: concepts and applications*, Cambridge University Press.
- Bonan, G. B., S. Levis, S. Sitch, M. Vertenstein, and K. W. Oleson (2003), A dynamic global vegetation model for use with climate models: concepts and description of simulated vegetation dynamics, *Glob. Change Biol.*, 9(11), 1543–1566, doi:10.1046/j.1365-2486.2003.00681.x.
- Bonan, G. B., D. Pollard, and S. L. Thompson (1992), Effects of boreal forest vegetation on global climate, *Nature*, 359(6397), 716–718, doi:10.1038/359716a0.
- Breshears, D. D. et al. (2005), Regional vegetation die-off in response to global-change-type drought, *Proc. Natl. Acad. Sci.*, 102(42), 15144–15148, doi:10.1073/pnas.0505734102.
- Bretherton, C. S., and S. Park (2009), A New Moist Turbulence Parameterization in the Community Atmosphere Model, *J. Clim.*, 22(12), 3422–3448, doi:10.1175/2008JCLI2556.1.
- Brisson, J., and J. F. Reynolds (1994), The Effect of Neighbors on Root Distribution in a Creosotebush (*Larrea Tridentata*) Population, *Ecology*, 75(6), 1693–1702, doi:10.2307/1939629.
- Brown, J. H., T. J. Valone, and C. G. Curtin (1997), Reorganization of an arid ecosystem in response to recent climate change, *Proc. Natl. Acad. Sci.*, 94(18), 9729–9733.
- Bryant, N. A., L. F. Johnson, A. J. Brazel, R. C. Balling, C. F. Hutchinson, and L. R. Beck (1990), Measuring the effect of overgrazing in the Sonoran Desert, *Clim. Change*, 17(2-3), 243–264, doi:10.1007/BF00138370.

- Buffington, L. C., and C. H. Herbel (1965), Vegetational changes on a semidesert grassland range from 1858 to 1963, *Ecol. Monogr.*, 35(2), 139, doi:10.2307/1948415.
- Businger, J. A., J. C. Wyngaard, Y. Izumi, and E. F. Bradley (1971), Flux-Profile Relationships in the Atmospheric Surface Layer, *J. Atmospheric Sci.*, 28(2), 181–189, doi:10.1175/1520-0469(1971)028<0181:FPRITA>2.0.CO;2.
- Cabral, A. C., J. M. Miguel, A. J. Rescia, M. F. Schmitz, and F. D. Pineda (2003), Shrub encroachment in Argentinean savannas, *J. Veg. Sci.*, 14(2), 145–152, doi:10.1111/j.1654-1103.2003.tb02139.x.
- Campbell, G. S., and J. M. Norman (1998), *An Introduction to Environmental Biophysics: 2nd edition*, Springer.
- Carre, D. E. (2005), Influences of hydrocarbon emissions by *Larrea tridentata* on the thermal structure of the lower atmospheric boundary layer, University of Virginia, Charlottesville, Virginia.
- Chapin, F. S. et al. (2005), Role of land-surface changes in Arctic summer warming, *Science*, 310(5748), 657–660, doi:10.1126/science.1117368.
- Charney, J. G. (1975), Dynamics of deserts and drought in the Sahel, *Q. J. R. Meteorol. Soc.*, 101(428), 193–202, doi:10.1002/qj.49710142802.
- Charney, J., W. J. Quirk, S. Chow, and J. Kornfield (1977), A Comparative Study of the Effects of Albedo Change on Drought in Semi-Arid Regions, *J. Atmospheric Sci.*, 34(9), 1366–1385, doi:10.1175/1520-0469(1977)034<1366:ACSOTE>2.0.CO;2.
- Chen, F., and J. Dudhia (2001), Coupling an Advanced Land Surface-Hydrology Model with the Penn State-NCAR MM5 Modeling System. Part I: Model

- Implementation and Sensitivity, *Mon. Weather Rev.*, *129*(4), 569–585,
doi:10.1175/1520-0493(2001)129<0569:CAALSH>2.0.CO;2.
- Chen, F., K. Mitchell, J. Schaake, Y. Xue, H.-L. Pan, V. Koren, Q. Y. Duan, M. Ek, and
A. Betts (1996), Modeling of land surface evaporation by four schemes and
comparison with FIFE observations, *J. Geophys. Res.*, *101*(D3), PP. 7251–7268,
doi:199610.1029/95JD02165.
- Claussen, M. (1997), Modeling bio-geophysical feedback in the African and Indian
monsoon region, *Clim. Dyn.*, *13*(4), 247–257, doi:10.1007/s003820050164.
- Collins, W. D. et al. (2006), The Community Climate System Model Version 3
(CCSM3), *J. Clim.*, *19*(11), 2122–2143, doi:10.1175/JCLI3761.1.
- Cook, B. I., G. B. Bonan, S. Levis, and H. E. Epstein (2008), Rapid vegetation responses
and feedbacks amplify climate model response to snow cover changes, *Clim.
Dyn.*, *30*(4), 391–406, doi:10.1007/s00382-007-0296-z.
- Crawford, T. M., D. J. Stensrud, F. Mora, J. W. Merchant, and P. J. Wetzel (2001), Value
of Incorporating Satellite-Derived Land Cover Data in MM5/PLACE for
Simulating Surface Temperatures, *J. Hydrometeorol.*, *2*(5), 453–468,
doi:10.1175/1525-7541(2001)002<0453:VOISDL>2.0.CO;2.
- D’Odorico, P., J. D. Fuentes, W. T. Pockman, S. L. Collins, Y. He, J. S. Medeiros, S. De
Wekker, and M. E. Litvak (2010), Positive feedback between microclimate and
shrub encroachment in the northern Chihuahuan desert, *Ecosphere*, *1*(6), art17,
doi:10.1890/ES10-00073.1.

- D'Odorico, P., Y. He, S. Collins, S. F. J. De Wekker, V. Engel, and J. D. Fuentes (2013), Vegetation–microclimate feedbacks in woodland–grassland ecotones, *Glob. Ecol. Biogeogr.*, 22(4), 364–379, doi:10.1111/geb.12000.
- D'Odorico, P., F. Laio, and L. Ridolfi (2006), A probabilistic analysis of fire-induced tree-grass coexistence in savannas., *Am. Nat.*, 167(3), E79.
- D'Odorico, P., G. S. Okin, and B. T. Bestelmeyer (2012), A synthetic review of feedbacks and drivers of shrub encroachment in arid grasslands, *Ecohydrology*, 5(5), 520–530, doi:10.1002/eco.259.
- Daly, C., W. P. Gibson, G. H. Taylor, G. L. Johnson, and P. Pasteris (2002), A knowledge-based approach to the statistical mapping of climate, *Clim. Res.*, 22(2), 99–113.
- Daly, C., M. Halbleib, J. I. Smith, W. P. Gibson, M. K. Doggett, G. H. Taylor, J. Curtis, and P. P. Pasteris (2008), Physiographically sensitive mapping of climatological temperature and precipitation across the conterminous United States, *Int. J. Climatol.*, 28(15), 2031–2064, doi:10.1002/joc.1688.
- Derbyshire, S. H. (1999), Boundary-Layer Decoupling over Cold Surfaces as a Physical Boundary-Instability, *Bound.-Layer Meteorol.*, 90(2), 297–325, doi:10.1023/A:1001710014316.
- De Wekker, S. F. J., and C. D. Whiteman (2006), On the Time Scale of Nocturnal Boundary Layer Cooling in Valleys and Basins and over Plains, *J. Appl. Meteorol. Climatol.*, 45(6), 813–820, doi:10.1175/JAM2378.1.

- Doherty, R., J. Kutzbach, J. Foley, and D. Pollard (2000), Fully coupled climate/dynamical vegetation model simulations over Northern Africa during the mid-Holocene, *Clim. Dyn.*, *16*(8), 561–573, doi:10.1007/s003820000065.
- Dudhia, J. (1989), Numerical Study of Convection Observed during the Winter Monsoon Experiment Using a Mesoscale Two-Dimensional Model, *J. Atmospheric Sci.*, *46*(20), 3077–3107, doi:10.1175/1520-0469(1989)046<3077:NSOCOD>2.0.CO;2.
- Dugas, W. A., R. A. Hicks, and R. P. Gibbens (1996), Structure and function of C3 and C4 Chihuahuan Desert plant communities. Energy balance components, *J. Arid Environ.*, *34*(1), 63–79, doi:10.1016/0190-5676(96)00093-3.
- Dulière, V., Y. Zhang, and E. P. Salathé (2011), Extreme Precipitation and Temperature over the U.S. Pacific Northwest: A Comparison between Observations, Reanalysis Data, and Regional Models^{*}, *J. Clim.*, *24*(7), 1950–1964, doi:10.1175/2010JCLI3224.1.
- Dullinger, S., T. Dirnböck, and G. Grabherr (2004), Modelling climate change-driven treeline shifts: relative effects of temperature increase, dispersal and invasibility, *J. Ecol.*, *92*(2), 241–252, doi:10.1111/j.0022-0477.2004.00872.x.
- Dyer, A. J. (1974), A review of flux-profile relationships, *Bound.-Layer Meteorol.*, *7*(3), 363–372, doi:10.1007/BF00240838.
- Dyer, A. J., and B. B. Hicks (1970), Flux-gradient relationships in the constant flux layer, *Q. J. R. Meteorol. Soc.*, *96*(410), 715–721, doi:10.1002/qj.49709641012.
- Easterling, D. R., and M. F. Wehner (2009), Is the climate warming or cooling?, *Geophys. Res. Lett.*, *36*(8), doi:10.1029/2009GL037810.

- Ek, M. B., K. E. Mitchell, Y. Lin, E. Rogers, P. Grunmann, V. Koren, G. Gayno, and J. D. Tarpley (2003), Implementation of Noah land surface model advances in the National Centers for Environmental Prediction operational mesoscale Eta model, *J. Geophys. Res.*, *108*, 16 PP., doi:200310.1029/2002JD003296.
- Eldridge, D. J., M. A. Bowker, F. T. Maestre, E. Roger, J. F. Reynolds, and W. G. Whitford (2011), Impacts of shrub encroachment on ecosystem structure and functioning: towards a global synthesis, *Ecol. Lett.*, *14*(7), 709–722, doi:10.1111/j.1461-0248.2011.01630.x.
- Eltahir, E. A. B., and R. L. Bras (1996), Precipitation recycling, *Rev. Geophys.*, *34*(3), 367–378, doi:10.1029/96RG01927.
- Epstein, H. E., J. Beringer, W. A. Gould, A. H. Lloyd, C. D. Thompson, F. S. Chapin III, G. J. Michaelson, C. L. Ping, T. S. Rupp, and D. A. Walker (2004), The nature of spatial transitions in the Arctic, *J. Biogeogr.*, *31*(12), 1917–1933, doi:10.1111/j.1365-2699.2004.01140.x.
- Felker, P., P. R. Clark, P. Nash, J. F. Osborn, and G. H. Cannell (1982), Screening *Prosopis* (Mesquite) for Cold Tolerance, *For. Sci.*, *28*(3), 556–562.
- Foley, J. A. et al. (2005), Global Consequences of Land Use, *Science*, *309*(5734), 570–574, doi:10.1126/science.1111772.
- Foley, J. A., M. H. Costa, C. Delire, N. Ramankutty, and P. Snyder (2003), Green surprise? How terrestrial ecosystems could affect earth's climate, *Front. Ecol. Environ.*, *1*(1), 38–44, doi:10.1890/1540-9295(2003)001[0038:GSHTEC]2.0.CO;2.

- Foley, J. A., J. E. Kutzbach, M. T. Coe, and S. Levis (1994), Feedbacks between climate and boreal forests during the Holocene epoch, *Publ. Online 01 Sept. 1994*
Doi101038371052a0, 371(6492), 52–54, doi:10.1038/371052a0.
- Foley, J. A., S. Levis, I. C. Prentice, D. Pollard, and S. L. Thompson (1998), Coupling dynamic models of climate and vegetation, *Glob. Change Biol.*, 4(5), 561–579, doi:10.1046/j.1365-2486.1998.t01-1-00168.x.
- Fraedrich, K., A. Kleidon, and F. Lunkeit (1999), A Green Planet versus a Desert World: Estimating the Effect of Vegetation Extremes on the Atmosphere, *J. Clim.*, 12(10), 3156–3163, doi:10.1175/1520-0442(1999)012<3156:AGPVAD>2.0.CO;2.
- García-Díez, M., J. Fernández, L. Fita, and C. Yaguez (2013), Seasonal dependence of WRF model biases and sensitivity to PBL schemes over Europe, *Q. J. R. Meteorol. Soc.*, 139(671), 501–514, doi:10.1002/qj.1976.
- Geiger, R. (1965), *The climate near the ground*, Harvard University Press, Cambridge, Mass.
- Geist, H. J., and E. F. Lambin (2004), Dynamic Causal Patterns of Desertification, *BioScience*, 54(9), 817, doi:10.1641/0006-3568(2004)054[0817:DCPOD]2.0.CO;2.
- Gibbens, R. P., and J. M. Lenz (2001), Root systems of some Chihuahuan Desert plants, *J. Arid Environ.*, 49(2), 221–263, doi:10.1006/jare.2000.0784.
- Gibbens, R. P., R. P. McNeely, K. M. Havstad, R. F. Beck, and B. Nolen (2005), Vegetation changes in the Jornada Basin from 1858 to 1998, *J. Arid Environ.*, 61(4), 651–668, doi:10.1016/j.jaridenv.2004.10.001.

- Gillette, D. A., and A. M. Pitchford (2004), Sand flux in the northern Chihuahuan desert, New Mexico, USA, and the influence of mesquite-dominated landscapes, *J. Geophys. Res. Earth Surf.*, 109(F4), F04003, doi:10.1029/2003JF000031.
- Göckede, M., T. Markkanen, C. B. Hasager, and T. Foken (2006), Update of a Footprint-Based Approach for the Characterisation of Complex Measurement Sites, *Bound.-Layer Meteorol.*, 118(3), 635–655, doi:10.1007/s10546-005-6435-3.
- Goslee, S. C., K. M. Havstad, D. P. C. Peters, A. Rango, and W. H. Schlesinger (2003), High-resolution images reveal rate and pattern of shrub encroachment over six decades in New Mexico, U.S.A., *J. Arid Environ.*, 54(4), 755–767, doi:10.1006/jare.2002.1103.
- Gosz, J. R., D. I. Moore, G. A. Shore, H. D. Grover, W. Rison, and C. Rison (1995), Lightning Estimates of Precipitation Location and Quantity on the Sevilleta Lter, New Mexico, *Ecol. Appl.*, 5(4), 1141–1150, doi:10.2307/2269361.
- Grover, H. D., and H. B. Musick (1990), Shrubland encroachment in southern New Mexico, U.S.A.: An analysis of desertification processes in the American southwest, *Clim. Change*, 17(2-3), 305–330, doi:10.1007/BF00138373.
- Harman, I. N., and S. E. Belcher (2006), The surface energy balance and boundary layer over urban street canyons, *Q. J. R. Meteorol. Soc.*, 132(621), 2749–2768, doi:10.1256/qj.05.185.
- Hawkins, T. W., A. J. Brazel, W. L. Stefanov, W. Bigler, and E. M. Saffell (2004), The Role of Rural Variability in Urban Heat Island Determination for Phoenix, Arizona, *J. Appl. Meteorol.*, 43(3), 476–486, doi:10.1175/1520-0450(2004)043<0476:TRORVI>2.0.CO;2.

- Hayden, B. P. (1998), Ecosystem feedbacks on climate at the landscape scale, *Philos. Trans. R. Soc. Lond. B. Biol. Sci.*, 353(1365), 5–18, doi:10.1098/rstb.1998.0186.
- He, Y., P. D’Odorico, and S. F. J. De Wekker (submitted), The role of vegetation-microclimate feedback in promoting shrub encroachment in the northern Chihuahuan desert
- He, Y., P. D’Odorico, and S. F. J. De Wekker (2014), The relative importance of climate change and shrub encroachment on nocturnal warming in the southwestern United States, *Int. J. Climatol.*, doi:10.1002/joc.3992.
- He, Y., P. D’Odorico, S. F. J. De Wekker, J. D. Fuentes, and M. Litvak (2010), On the impact of shrub encroachment on microclimate conditions in the northern Chihuahuan desert, *J. Geophys. Res.*, 115, 10 PP., doi:201010.1029/2009JD013529.
- He, Y., and S. F. J. De Wekker (submitted), Contrasting nocturnal temperature profiles in adjacent shrubland and grassland
- He, Y., S. F. J. De Wekker, J. D. Fuentes, and P. D’Odorico (2011), Coupled land-atmosphere modeling of the effects of shrub encroachment on nighttime temperatures, *Agric. For. Meteorol.*, 151, 1690–1697.
- Hibbard, K. A., S. Archer, D. S. Schimel, and D. W. Valentine (2001), Biogeochemical changes accompanying woody plant encroachment in a subtropical savanna, *Ecology*, 82(7), 1999–2011, doi:10.1890/0012-9658(2001)082[1999:BCAWPE]2.0.CO;2.
- Hines, K. M., and D. H. Bromwich (2008), Development and Testing of Polar Weather Research and Forecasting (WRF) Model. Part I: Greenland Ice Sheet

- Meteorology*, *Mon. Weather Rev.*, 136(6), 1971–1989,
doi:10.1175/2007MWR2112.1.
- Hipps, L. E., and D. F. Zehr (1995), Determination of evaporation from integrated profiles of humidity and temperature over an inhomogeneous surface, *Bound.-Layer Meteorol.*, 75(3), 287–299, doi:10.1007/BF00712698.
- Hogue, T. S., L. Bastidas, H. Gupta, S. Sorooshian, K. Mitchell, and W. Emmerich (2005), Evaluation and Transferability of the Noah Land Surface Model in Semiarid Environments, *J. Hydrometeorol.*, 6(1), 68–84, doi:10.1175/JHM-402.1.
- Homer, C., J. Dewitz, J. Fry, M. Coan, N. Hossain, C. Larson, N. Herold, A. Mckerrow, J. Vandriel, and J. Wickham (2007), Completion of the 2001 National Land Cover Database for the Conterminous United States, *Photogramm. Eng. Remote Sens.*, 73(4), 337–341.
- Hong, S., V. Lakshmi, E. E. Small, F. Chen, M. Tewari, and K. W. Manning (2009), Effects of vegetation and soil moisture on the simulated land surface processes from the coupled WRF/Noah model, *J. Geophys. Res.*, 114, 13 PP.,
doi:200910.1029/2008JD011249.
- Hong, S.-Y. (2010), A new stable boundary-layer mixing scheme and its impact on the simulated East Asian summer monsoon, *Q. J. R. Meteorol. Soc.*, 136(651), 1481–1496, doi:10.1002/qj.665.
- Hong, S.-Y., and J.-O. J. Lim (2006), The WRF single-moment 6-class microphysics scheme (WSM6), *J. Korean Meteorol. Soc.*, 42, 129–151.

- Hong, S.-Y., Y. Noh, and J. Dudhia (2006), A New Vertical Diffusion Package with an Explicit Treatment of Entrainment Processes, *Mon. Weather Rev.*, 134(9), 2318–2341, doi:10.1175/MWR3199.1.
- Horst, T. W., and J. C. Weil (1992), Footprint estimation for scalar flux measurements in the atmospheric surface layer, *Bound.-Layer Meteorol.*, 59(3), 279–296, doi:10.1007/BF00119817.
- Horst, T. W., and J. C. Weil (1994), How Far is Far Enough?: The Fetch Requirements for Micrometeorological Measurement of Surface Fluxes, *J. Atmospheric Ocean. Technol.*, 11(4), 1018–1025, doi:10.1175/1520-0426(1994)011<1018:HFIFET>2.0.CO;2.
- Houghton, J. T., Y. Ding, D. J. Griggs, M. Noguer, P. J. van der Linden, X. Dai, K. Maskell, and C. A. Johnson (2001), *Climate change 2001: the scientific basis*, Cambridge University Press Cambridge, UK.
- Hsieh, C.-I., G. Katul, and T. Chi (2000), An approximate analytical model for footprint estimation of scalar fluxes in thermally stratified atmospheric flows, *Adv. Water Resour.*, 23(7), 765–772, doi:10.1016/S0309-1708(99)00042-1.
- Hsu, S. (1984), Variation of an urban heat island in Phoenix, *Prof. Geogr.*, 36(2), 196–200, doi:10.1111/j.0033-0124.1984.00196.x.
- Huenneke, L. F., J. P. Anderson, M. Remmenga, and W. H. Schlesinger (2002), Desertification alters patterns of aboveground net primary production in Chihuahuan ecosystems, *Glob. Change Biol.*, 8(3), 247–264, doi:10.1046/j.1365-2486.2002.00473.x.

- Van den Hurk, B. J. J. M., P. Viterbo, A. C. M. Beljaars, and A. K. Betts (2000), *Offline Validation of the ERA40 Surface Scheme*, European Centre for Medium-Range Weather Forecasts.
- Huxman, T. E., B. P. Wilcox, D. D. Breshears, R. L. Scott, K. A. Snyder, E. E. Small, K. Hultine, W. T. Pockman, and R. B. Jackson (2005), Ecohydrological implications of woody plant encroachment, *Ecology*, 86(2), 308–319, doi:10.1890/03-0583.
- Imhoff, M. L., P. Zhang, R. E. Wolfe, and L. Bounoua (2010), Remote sensing of the urban heat island effect across biomes in the continental USA, *Remote Sens. Environ.*, 114(3), 504–513, doi:10.1016/j.rse.2009.10.008.
- IPCC (2007), *Climate Change 2007: The Physical Science Basis, Contribution of Working Group I to the Fourth Assessment Report of the Intergovernmental Panel on Climate Change*, edited by S. Solomon, D. Qin, M. Manning, R. Alley, T. Berntsen, N. Bindoff, Z. Chen, A. Chidthaisong, J. Gregory, and G. Hegerl, Cambridge University Press, Cambridge.
- James, K. A., D. J. Stensrud, and N. Yussouf (2009), Value of Real-Time Vegetation Fraction to Forecasts of Severe Convection in High-Resolution Models, *Weather Forecast.*, 24(1), 187–210, doi:10.1175/2008WAF2007097.1.
- Janjic, Z. I. (1996), The surface layer in the NCEP Eta Model, pp. 19–23, American Meteorological Society, Norfolk, VA.
- Janjic, Z. I. (2002), Nonsingular implementation of the Mellor–Yamada level 2.5 scheme in the NCEP Meso model, *NCEP Note 437*, 61 pp.
- Jauregui, E. (1997), Heat island development in Mexico City, *Atmos. Environ.*, 31(22), 3821–3831, doi:10.1016/S1352-2310(97)00136-2.

- Kain, J. S., and J. M. Fritsch (1990), A One-Dimensional Entraining/Detraining Plume Model and Its Application in Convective Parameterization, *J. Atmospheric Sci.*, 47(23), 2784–2802, doi:10.1175/1520-0469(1990)047<2784:AODEPM>2.0.CO;2.
- Kain, J. S., and J. M. Fritsch (1993), Convective parameterization for mesoscale models: The Kain-Fritsch scheme, *Represent. Cumulus Convect. Numer. Models Meteorol. Monogr.*, 24, 165–170.
- Karl, T. R., R. W. Knight, and B. Baker (2000), The record breaking global temperatures of 1997 and 1998: Evidence for an increase in the rate of global warming?, *Geophys. Res. Lett.*, 27(5), 719–722, doi:10.1029/1999GL010877.
- Karlsson, I. M. (2000), Nocturnal Air Temperature Variations between Forest and Open Areas, *J. Appl. Meteorol.*, 39(6), 851–862, doi:10.1175/1520-0450(2000)039<0851:NATVBF>2.0.CO;2.
- Kharin, V. V., F. W. Zwiers, X. Zhang, and G. C. Hegerl (2007), Changes in Temperature and Precipitation Extremes in the IPCC Ensemble of Global Coupled Model Simulations, *J. Clim.*, 20(8), 1419–1444, doi:10.1175/JCLI4066.1.
- Kiehl, J. T., J. J. Hack, G. B. Bonan, B. A. Boville, D. L. Williamson, and P. J. Rasch (1998), The National Center for Atmospheric Research Community Climate Model: CCM3*, *J. Clim.*, 11(6), 1131–1149, doi:10.1175/1520-0442(1998)011<1131:TNCFAR>2.0.CO;2.
- Kilpeläinen, T., T. Vihma, M. Manninen, A. Sjöblom, E. Jakobson, T. Palo, and M. Maturilli (2012), Modelling the vertical structure of the atmospheric boundary

- layer over Arctic fjords in Svalbard, *Q. J. R. Meteorol. Soc.*, *138*(668), 1867–1883, doi:10.1002/qj.1914.
- Knapp, A. K. et al. (2008a), Shrub encroachment in North American grasslands: shifts in growth form dominance rapidly alters control of ecosystem carbon inputs, *Glob. Change Biol.*, *14*(3), 615–623, doi:10.1111/j.1365-2486.2007.01512.x.
- Knapp, A. K., J. K. McCarron, A. M. Silletti, G. A. Hoch, J. C. Heisler, M. S. Lett, J. M. Blair, J. M. Briggs, and M. D. Smith (2008b), Ecological Consequences of the Replacement of Native Grassland by *Juniperus virginiana* and Other Woody Plants, in *Western North American Juniperus Communities*, vol. 196, edited by O. W. Auken, pp. 156–169, Springer New York, New York, NY.
- Körner, C. (1998), A re-assessment of high elevation treeline positions and their explanation, *Oecologia*, *115*(4), 445–459, doi:10.1007/s004420050540.
- Kostopoulou, E., K. Tolika, I. Tegoulas, C. Giannakopoulos, S. Somot, C. Anagnostopoulou, and P. Maheras (2009), Evaluation of a regional climate model using in situ temperature observations over the Balkan Peninsula, *Tellus A*, *61*(3), 357–370, doi:10.1111/j.1600-0870.2009.00389.x.
- Kurc, S. A., and E. E. Small (2004), Dynamics of evapotranspiration in semiarid grassland and shrubland ecosystems during the summer monsoon season, central New Mexico, *Water Resour. Res.*, *40*, 15 PP., doi:200410.1029/2004WR003068.
- Kurc, S. A., and E. E. Small (2007), Soil moisture variations and ecosystem-scale fluxes of water and carbon in semiarid grassland and shrubland, *Water Resour. Res.*, *43*, 13 PP., doi:200710.1029/2006WR005011.

- Kurkowski, N. P., D. J. Stensrud, and M. E. Baldwin (2003), Assessment of Implementing Satellite-Derived Land Cover Data in the Eta Model, *Weather Forecast.*, *18*(3), 404–416, doi:10.1175/1520-0434(2003)18<404:AOISDL>2.0.CO;2.
- Laliberte, A. S., A. Rango, K. M. Havstad, J. F. Paris, R. F. Beck, R. McNeely, and A. L. Gonzalez (2004), Object-oriented image analysis for mapping shrub encroachment from 1937 to 2003 in southern New Mexico, *Remote Sens. Environ.*, *93*(1-2), 198–210, doi:16/j.rse.2004.07.011.
- Van Langevelde, F. et al. (2003), Effects of fire and herbivory on the stability of savanna ecosystems, *Ecology*, *84*(2), 337–350.
- Laprise, R. (1992), The Euler Equations of Motion with Hydrostatic Pressure as an Independent Variable, *Mon. Weather Rev.*, *120*(1), 197–207, doi:10.1175/1520-0493(1992)120<0197:TEEOMW>2.0.CO;2.
- Leclerc, M. Y., and G. W. Thurtell (1990), Footprint prediction of scalar fluxes using a Markovian analysis, *Bound.-Layer Meteorol.*, *52*(3), 247–258, doi:10.1007/BF00122089.
- LeMone, M. A., F. Chen, J. G. Alfieri, M. Tewari, B. Geerts, Q. Miao, R. L. Grossman, and R. L. Coulter (2007), Influence of land cover and soil moisture on the horizontal distribution of sensible and latent heat fluxes in southeast Kansas during IHOP_2002 and CASES-97, *J. Hydrometeorol.*, *8*(1), 68–87.
- Leung, L. R., Y. Qian, X. Bian, W. M. Washington, J. Han, and J. O. Roads (2004), Mid-Century Ensemble Regional Climate Change Scenarios for the Western United

States, *Clim. Change*, 62(1), 75–113,

doi:10.1023/B:CLIM.0000013692.50640.55.

Lewis, T. J., and K. Wang (1998), Geothermal evidence for deforestation induced warming: Implications for the Climatic impact of land development, *Geophys. Res. Lett.*, 25(4), 535–538, doi:10.1029/98GL00181.

Lunt, I. D., L. M. Winsemius, S. P. McDonald, J. W. Morgan, and R. L. Dehaan (2010), How widespread is woody plant encroachment in temperate Australia? Changes in woody vegetation cover in lowland woodland and coastal ecosystems in Victoria from 1989 to 2005, *J. Biogeogr.*, 37(4), 722–732, doi:10.1111/j.1365-2699.2009.02255.x.

Maestre, F. T. et al. (2009), Shrub encroachment can reverse desertification in semi-arid Mediterranean grasslands, *Ecol. Lett.*, 12(9), 930–941, doi:10.1111/j.1461-0248.2009.01352.x.

Mahrt, L. (1998), Stratified Atmospheric Boundary Layers and Breakdown of Models, *Theor. Comput. Fluid Dyn.*, 11(3-4), 263–279, doi:10.1007/s001620050093.

Mahrt, L. (2000), Surface Heterogeneity and Vertical Structure of the Boundary Layer, *Bound.-Layer Meteorol.*, 96(1), 33–62, doi:10.1023/A:1002482332477.

Mahrt, L., and M. Ek (1984), The Influence of Atmospheric Stability on Potential Evaporation., *J. Appl. Meteorol.*, 23, 222–234.

Mahrt, L., and H. Pan (1984), A two-layer model of soil hydrology, *Bound.-Layer Meteorol.*, 29(1), 1–20, doi:10.1007/BF00119116.

- Martano, P. (2000), Estimation of Surface Roughness Length and Displacement Height from Single-Level Sonic Anemometer Data, *J. Appl. Meteorol.*, 39(5), 708–715, doi:10.1175/1520-0450(2000)039<0708:EOSRLA>2.0.CO;2.
- Martínez-Vilalta, J., and W. T. Pockman (2002), The vulnerability to freezing-induced xylem cavitation of *Larrea tridentata* (Zygophyllaceae) in the Chihuahuan desert, *Am. J. Bot.*, 89(12), 1916–1924, doi:10.3732/ajb.89.12.1916.
- Mayer, S., M. O. Jonassen, A. Sandvik, and J. Reuder (2012), Profiling the Arctic Stable Boundary Layer in Advent Valley, Svalbard: Measurements and Simulations, *Bound.-Layer Meteorol.*, 143(3), 507–526, doi:10.1007/s10546-012-9709-6.
- Mearns, L. O., W. Gutowski, R. Jones, R. Leung, S. McGinnis, A. Nunes, and Y. Qian (2009), A Regional Climate Change Assessment Program for North America, *Eos*, 90(36), P. 311, doi:200910.1029/2009EO360002.
- Medeiros, J. S., and W. T. Pockman (2011), Drought increases freezing tolerance of both leaves and xylem of *Larrea tridentata*, *Plant Cell Environ.*, 34(1), 43–51, doi:10.1111/j.1365-3040.2010.02224.x.
- Memon, R. A., D. Y. C. Leung, and C. LIU (2008), A review on the generation, determination and mitigation of Urban Heat Island, *J. Environ. Sci.*, 20(1), 120–128, doi:10.1016/S1001-0742(08)60019-4.
- Menne, M. J., and C. N. Williams (2010), Homogenization of Temperature Series via Pairwise Comparisons, *J. Clim.*, 22, 1700–1717.
- Menne, M. J., C. N. Williams, and M. A. Palecki (2010), On the reliability of the U.S. surface temperature record, *J. Geophys. Res.*, 115, 9 PP., doi:201010.1029/2009JD013094.

- Menne, M. J., C. N. Williams, and R. S. Vose (2009), The U.S. Historical Climatology Network Monthly Temperature Data, Version 2, *Bull. Am. Meteorol. Soc.*, *90*, 993–1007.
- Mesinger, F. et al. (2006), North American Regional Reanalysis., *Bull. Am. Meteorol. Soc.*, *87*, 343–360.
- Mesinger, F., and A. Arakawa (1976), *Numerical methods used in atmospheric models*. GARP Publ. 17, 64 pp. Available from WMO, Case Postale 2300, CH-1211 Geneva2, Switzerland.
- Mlawer, E. J., S. J. Taubman, P. D. Brown, M. J. Iacono, and S. A. Clough (1997), Radiative transfer for inhomogeneous atmospheres: RRTM, a validated correlated-k model for the longwave, *J. Geophys. Res. Atmospheres*, *102*(D14), 16663–16682, doi:10.1029/97JD00237.
- Muldavin, E. H., D. I. Moore, S. L. Collins, K. R. Wetherill, and D. C. Lightfoot (2007), Aboveground net primary production dynamics in a northern Chihuahuan Desert ecosystem, *Oecologia*, *155*(1), 123–132, doi:10.1007/s00442-007-0880-2.
- Nakicenovic, N. et al. (2000), *Special report on emissions scenarios: a special report of Working Group III of the Intergovernmental Panel on Climate Change*, Pacific Northwest National Laboratory, Richland, WA (US), Environmental Molecular Sciences Laboratory (US).
- Noy-Meir, I. (1975), Stability of grazing systems: an application of predator-prey graphs, *J. Ecol.*, *63*(2), 459–481, doi:10.2307/2258730.
- Oke, T. R. (1982), The energetic basis of the urban heat island, *Q. J. R. Meteorol. Soc.*, *108*(455), 1–24, doi:10.1002/qj.49710845502.

- Okin, G. S., P. D'Odorico, and S. R. Archer (2009), Impact of feedbacks on Chihuahuan desert grasslands: Transience and metastability, *J. Geophys. Res.*, *114*, 8 PP., doi:200910.1029/2008JG000833.
- Pacala, S. W. et al. (2001), Consistent Land- and Atmosphere-Based U.S. Carbon Sink Estimates, *Science*, *292*(5525), 2316–2320, doi:10.1126/science.1057320.
- Pergaud, J., V. Masson, S. Malardel, and F. Couvreux (2009), A Parameterization of Dry Thermals and Shallow Cumuli for Mesoscale Numerical Weather Prediction, *Bound.-Layer Meteorol.*, *132*(1), 83–106, doi:10.1007/s10546-009-9388-0.
- Pielke, R. A. P., and T. Matsui (2005), Should light wind and windy nights have the same temperature trends at individual levels even if the boundary layer averaged heat content change is the same?, *Geophys. Res. Lett.*, *32*(21), L21813, doi:10.1029/2005GL024407.
- Pielke, R. A., Sr, R. Avissar, M. Raupach, A. J. Dolman, X. Zeng, and A. S. Denning (1998), Interactions between the atmosphere and terrestrial ecosystems: influence on weather and climate, *Glob. Change Biol.*, *4*(5), 461–475, doi:10.1046/j.1365-2486.1998.t01-1-00176.x.
- Pockman, W. T., and J. S. Sperry (1997), Freezing-induced xylem cavitation and the northern limit of *Larrea tridentata*, *Oecologia*, *109*(1), 19–27, doi:10.1007/s004420050053.
- Polley, H. W. (1997), Implications of Rising Atmospheric Carbon Dioxide Concentration for Rangelands, *J. Range Manag.*, *50*(6), 562–577.

- Polley, H. W., H. B. Johnson, and H. S. Mayeux (1992), Carbon Dioxide and Water Fluxes of C3 Annuals and C3 and C4 Perennials at Subambient CO₂ Concentrations, *Funct. Ecol.*, 6(6), 693–703, doi:10.2307/2389966.
- Prueger, J. H., L. E. Hipps, and D. I. Cooper (1996), Evaporation and the development of the local boundary layer over an irrigated surface in an arid region, *Agric. For. Meteorol.*, 78(3–4), 223–237, doi:10.1016/0168-1923(95)02234-1.
- Raupach, M. R., and J. J. Finnigan (1995), Scale issues in boundary-layer meteorology: Surface energy balances in heterogeneous terrain, *Hydrol. Process.*, 9(5-6), 589–612, doi:10.1002/hyp.3360090509.
- Ravi, S., P. D’Odorico, L. Wang, C. S. White, G. S. Okin, S. A. Macko, and S. L. Collins (2009), Post-fire resource redistribution in desert grasslands: a possible negative feedback on land degradation, *Ecosystems*, 12(3), 434–444, doi:10.1007/s10021-009-9233-9.
- Ravi, S., P. D’Odorico, T. M. Zobeck, T. M. Over, and S. L. Collins (2007), Feedbacks between fires and wind erosion in heterogeneous arid lands, *J. Geophys. Res. Biogeosciences*, 112(G4), n/a–n/a, doi:10.1029/2007JG000474.
- Reynolds, J. F., R. A. Virginia, P. R. Kemp, A. G. de Soyza, and D. C. Tremmel (1999), Impact of drought on desert shrubs: effects of seasonality and degree of resource island development, *Ecol. Monogr.*, 69(1), 69–106, doi:10.1890/0012-9615(1999)069[0069:IODODS]2.0.CO;2.
- Rind, D. (1988), Dependence of Warm and Cold Climate Depiction on Climate Model Resolution, *J. Clim.*, 1(10), 965–997, doi:10.1175/1520-0442(1988)001<0965:DOWACC>2.0.CO;2.

- Roques, K. G., T. G. O'Connor, and A. R. Watkinson (2001), Dynamics of shrub encroachment in an African savanna: relative influences of fire, herbivory, rainfall and density dependence, *J. Appl. Ecol.*, 38(2), 268–280, doi:10.1046/j.1365-2664.2001.00567.x.
- Rosenfeld, D., Y. Rudich, and R. Lahav (2001), Desert dust suppressing precipitation: A possible desertification feedback loop, *Proc. Natl. Acad. Sci.*, 98(11), 5975–5980, doi:10.1073/pnas.101122798.
- Rosero, E., Z.-L. Yang, T. Wagener, L. E. Gulden, S. Yatheendradas, and G.-Y. Niu (2010), Quantifying parameter sensitivity, interaction, and transferability in hydrologically enhanced versions of the Noah land surface model over transition zones during the warm season, *J. Geophys. Res. Atmospheres*, 115(D3), D03106, doi:10.1029/2009JD012035.
- Rotenberg, E., and D. Yakir (2010), Contribution of Semi-Arid Forests to the Climate System, *Science*, 327(5964), 451–454, doi:10.1126/science.1179998.
- Roth, M., T. R. Oke, and W. J. Emery (1989), Satellite-derived urban heat islands from three coastal cities and the utilization of such data in urban climatology, *Int. J. Remote Sens.*, 10(11), 1699–1720, doi:10.1080/01431168908904002.
- Schlesinger, W. H., A. D. Abrahams, A. J. Parsons, and J. Wainwright (1999), Nutrient losses in runoff from grassland and shrubland habitats in Southern New Mexico: I. rainfall simulation experiments, *Biogeochemistry*, 45(1), 21–34, doi:10.1007/BF00992871.

- Schlesinger, W. H., J. A. Raikes, A. E. Hartley, and A. F. Cross (1996), On the Spatial Pattern of Soil Nutrients in Desert Ecosystems, *Ecology*, 77(2), 364–374, doi:10.2307/2265615.
- Schlesinger, W. H., J. F. Reynolds, G. L. Cunningham, L. F. Huenneke, W. M. Jarrell, R. A. Virginia, and W. G. Whitford (1990), Biological feedbacks in global desertification, *Science*, 247(4946), 1043 –1048, doi:10.1126/science.247.4946.1043.
- Scott, R. L., T. E. Huxman, D. G. Williams, and D. C. Goodrich (2006), Ecohydrological impacts of woody-plant encroachment: seasonal patterns of water and carbon dioxide exchange within a semiarid riparian environment, *Glob. Change Biol.*, 12(2), 311–324, doi:10.1111/j.1365-2486.2005.01093.x.
- Seager, R. et al. (2007), Model Projections of an Imminent Transition to a More Arid Climate in Southwestern North America, *Science*, 316(5828), 1181 –1184, doi:10.1126/science.1139601.
- Seaman, N. L., B. J. Gaudet, D. R. Stauffer, L. Mahrt, S. J. Richardson, J. R. Zielonka, and J. C. Wyngaard (2012), Numerical Prediction of Submesoscale Flow in the Nocturnal Stable Boundary Layer over Complex Terrain, *Mon. Weather Rev.*, 140(3), 956–977, doi:10.1175/MWR-D-11-00061.1.
- Shin, H. H., and S.-Y. Hong (2011), Intercomparison of Planetary Boundary-Layer Parametrizations in the WRF Model for a Single Day from CASES-99, *Bound.-Layer Meteorol.*, 139(2), 261–281, doi:10.1007/s10546-010-9583-z.
- Shukla, J., C. Nobre, and P. Sellers (1990), Amazon Deforestation and Climate Change, *Science*, 247(4948), 1322–1325, doi:10.1126/science.247.4948.1322.

- Shuttleworth, W. J. (1988), Macrohydrology — The new challenge for process hydrology, *J. Hydrol.*, 100(1–3), 31–56, doi:10.1016/0022-1694(88)90180-1.
- Skamarock, W. C., J. B. Klemp, J. Dudhia, D. O. Gill, D. M. Barker, M. G. Duda, X. Y. Huang, W. Wang, and J. G. Powers (2008), A description of the Advanced Research WRF version 3. NCAR Technical Note 475, *Boulder Natl. Cent. Atmospheric Res.*, 133.
- Small, E. E., and S. A. Kurc (2003), Tight coupling between soil moisture and the surface radiation budget in semiarid environments: Implications for land-atmosphere interactions, *Water Resour. Res.*, 39, 14 PP., doi:200310.1029/2002WR001297.
- Solomon, S., G.-K. Plattner, R. Knutti, and P. Friedlingstein (2009), Irreversible climate change due to carbon dioxide emissions, *Proc. Natl. Acad. Sci.*, 106(6), 1704 – 1709, doi:10.1073/pnas.0812721106.
- Stephenson, N. L. (1990), Climatic Control of Vegetation Distribution: The Role of the Water Balance, *Am. Nat.*, 135(5), 649–670.
- Streutker, D. R. (2003), Satellite-measured growth of the urban heat island of Houston, Texas, *Remote Sens. Environ.*, 85(3), 282–289, doi:10.1016/S0034-4257(03)00007-5.
- Stull, R. B. (1988), *An Introduction to Boundary Layer Meteorology*, Springer.
- Sukoriansky, S., and B. Galperin (2008), Anisotropic turbulence and internal waves in stably stratified flows (QNSE theory), *Phys. Scr.*, 2008(T132), 014036, doi:10.1088/0031-8949/2008/T132/014036.

- Sukoriansky, S., B. Galperin, and V. Perov (2005), Application of a New Spectral Theory of Stably Stratified Turbulence to the Atmospheric Boundary Layer over Sea Ice, *Bound.-Layer Meteorol.*, 117(2), 231–257, doi:10.1007/s10546-004-6848-4.
- Sukoriansky, S., B. Galperin, and V. Perov (2006), A quasi-normal scale elimination model of turbulence and its application to stably stratified flows, *Nonlin Process. Geophys*, 13(1), 9–22, doi:10.5194/npg-13-9-2006.
- Swann, A. L., I. Y. Fung, S. Levis, G. B. Bonan, and S. C. Doney (2010), Changes in Arctic vegetation amplify high-latitude warming through the greenhouse effect, *Proc. Natl. Acad. Sci.*, 107(4), 1295–1300, doi:10.1073/pnas.0913846107.
- Tietjen, B., F. Jeltsch, E. Zehe, N. Classen, A. Groengroeft, K. Schifffers, and J. Oldeland (2010), Effects of climate change on the coupled dynamics of water and vegetation in drylands, *Ecohydrology*, 3(2), 226–237, doi:10.1002/eco.70.
- Turnbull, L., J. Wainwright, R. Brazier, and R. Bol (2010), Biotic and Abiotic Changes in Ecosystem Structure over a Shrub-Encroachment Gradient in the Southwestern USA, *Ecosystems*, 13(8), 1239–1255, doi:10.1007/s10021-010-9384-8.
- Van Auken, O. W. (2000), Shrub invasions of North American semiarid grasslands, *Annu. Rev. Ecol. Syst.*, 31(1), 197–215, doi:10.1146/annurev.ecolsys.31.1.197.
- Van Auken, O. W. (2009), Causes and consequences of woody plant encroachment into western North American grasslands, *J. Environ. Manage.*, 90(10), 2931–2942, doi:10.1016/j.jenvman.2009.04.023.
- Villegas, J. C., D. D. Breshears, C. B. Zou, and P. D. Royer (2010), Seasonally pulsed heterogeneity in microclimate: phenology and cover effects along deciduous

grassland–forest continuum, *Vadose Zone J.*, 9(3), 537–547,
doi:10.2136/vzj2009.0032.

Walker, B. H., D. Ludwig, C. S. Holling, and R. M. Peterman (1981), Stability of semi-arid savanna grazing systems, *J. Ecol.*, 69(2), 473–498, doi:10.2307/2259679.

Walko, R. L., L.E. Band, J. Baron , T.G.F. Kittel, R. Lammers, T.J. Lee, D. Ojima, R.A. Pielke, C. Taylor, C. Tague, C.J. Tremback, P.L. Vidale, (2000), Coupled Atmosphere–Biophysics–Hydrology Models for Environmental Modeling, *J. Appl. Meteorol.*, 39(6), 931–944, doi:10.1175/1520-0450(2000)039<0931:CABHMF>2.0.CO;2.

Wesely, M. L., and B. B. Hicks (1977), Some Factors that Affect the Deposition Rates of Sulfur Dioxide and Similar Gases on Vegetation, *J. Air Pollut. Control Assoc.*, 27(11), 1110–1116, doi:10.1080/00022470.1977.10470534.

Westoby, M., B. Walker, and I. Noy-Meir (1989), Range management on the basis of a model which does not seek to establish equilibrium, *J. Arid Environ.*, 17(2), 235–239.

Whiteman, C. D., X. Bian, and J. L. Sutherland (1999), Wintertime Surface Wind Patterns in the Colorado River Valley, *J. Appl. Meteorol.*, 38(8), 1118–1130, doi:10.1175/1520-0450(1999)038<1118:WSWPIT>2.0.CO;2.

Williams, A. P., C. D. Allen, C. I. Millar, T. W. Swetnam, J. Michaelsen, C. J. Still, and S. W. Leavitt (2010), Forest Responses to Increasing Aridity and Warmth in the Southwestern United States, *Proc. Natl. Acad. Sci.*, 107(50), 21289–21294, doi:10.1073/pnas.0914211107.

- Wilson, J. B., and A. D. Q. Agnew (1992), Positive-feedback switches in plant communities, *Adv. Ecol. Res.*, 23, 263–336.
- Xue, Y. (1996), The Impact of Desertification in the Mongolian and the Inner Mongolian Grassland on the Regional Climate, *J. Clim.*, 9(9), 2173–2189, doi:10.1175/1520-0442(1996)009<2173:TIODIT>2.0.CO;2.
- Xue, Y., and J. Shukla (1993), The Influence of Land Surface Properties on Sahel Climate. Part 1: Desertification, *J. Clim.*, 6(12), 2232–2245, doi:10.1175/1520-0442(1993)006<2232:TIOISP>2.0.CO;2.
- Yver, C. E., H. D. Graven, D. D. Lucas, P. J. Cameron-Smith, R. F. Keeling, and R. F. Weiss (2013), Evaluating transport in the WRF model along the California coast, *Atmos Chem Phys*, 13(4), 1837–1852, doi:10.5194/acp-13-1837-2013.
- Zeng, X., X. Zeng, and M. Barlage (2008), Growing temperate shrubs over arid and semiarid regions in the Community Land Model–Dynamic Global Vegetation Model, *Glob. Biogeochem. Cycles*, 22(3), GB3003, doi:10.1029/2007GB003014.
- Zhang, X., L. Alexander, G. C. Hegerl, P. Jones, A. K. Tank, T. C. Peterson, B. Trewin, and F. W. Zwiers (2011), Indices for monitoring changes in extremes based on daily temperature and precipitation data, *Wiley Interdiscip. Rev. Clim. Change*, 2(6), 851–870, doi:10.1002/wcc.147.